

**Effects of Initial Microbial Density on Disinfection Efficiency
in a Continuous Flow System and Validation of
Disinfection Batch Kinetics in a Continuous Flow System**

A Thesis

Submitted to the Faculty

of

Drexel University

by

Lijie Li

in partial fulfillment of the

requirements for the degree

of

Doctor of Philosophy

February 2004

© Copyright 2004
Lijie Li. All Rights Reserved

Dedications

To My Parents

And

To My Husband

Acknowledgements

I express my sincere gratitude to my advisor, Dr. Charles N. Haas. This work would not have been made possible without his knowledgeable guidance and generous support. I deeply appreciate Dr. Haas for all the support and encouragement he has been given to me during my graduate study and research in Drexel University.

I thank my committee members that have served on my candidacy and final thesis defense: Dr. Weiling Huang, Dr. Mehrdad Lordgooei, Dr. Joseph Martin, Dr. Rajakkannu Mutharasan, and Dr. Susan Kilham. I thank each for their invaluable advices and help.

I am grateful to my fellow researchers Tim Bartrand, Dr. Dennis Greene, Dr. Baris Kaymak, and Jason Marie, for their encouragement and friendship. My appreciation also goes to the former SESEP faculty, students and staff for their great help at various times. They all made my experience at Drexel University a memorable one.

I can not express my appreciation enough to my parents Zengyuan Li and Huifang Yi and my husband Wei Sun for their love, encouragement and support.

Table of Contents

Table of Contents	iv
List of Tables	ix
List of Figures	xi
Abstract	xvi
Chapter 1 : Introduction	1
Chapter 2 : Scope of the Study	5
Chapter 3 : Literature Review	8
3.1 Overview of the Chemistry of Disinfectants	8
3.1.1 Aquatic Chemistry of Chlorine	8
3.1.2 Aquatic Chemistry of Chloramine	9
3.1.3 Aquatic Chemistry of Ozone	10
3.2 Mechanism of Disinfection and Bacterial Resistance to Disinfectants	12
3.2.1 The Composition and Structure of Bacterial Cells and Potential Targets for Disinfectants	12
3.2.1.1 Gram-positive Bacteria and Gram-negative Bacteria	12
3.2.1.2 Bacterial Spores	15
3.2.2 Mechanisms of Microbial Inactivation by Disinfectants	17
3.2.3 Resistance of Bacteria to Disinfectants	18
3.2.4 Quorum Sensing	22
3.2.4.1 Gram-negative Bacterial Communication	23
3.2.4.2 Gram-positive Bacteria Communication	24

3.2.4.3	Inter-species Communication	25
3.2.4.4	Genetic Control of Bacterial Resistance to Oxidative Stress	26
3.2.4.5	Cell Density-Dependent Resistance of Bacteria to Oxidative Stress	27
3.3	Review on Disinfection Kinetic Models	29
3.3.1	Chick Model	32
3.3.2	Chick-Watson Model.....	32
3.3.3	Hom Model.....	33
3.3.4	Rational Model (Power Law Model).....	34
3.3.5	Hom Power Law Model	35
3.3.6	Series-event Model.....	36
3.3.7	Multiple Target Model	37
3.3.8	Modified Multiple Target Model.....	38
3.4	Prior Research on Using CSTR (Continuously Stirred Tank Reactor) to Perform Disinfection.....	38
3.4.1	Continuous Flow System.....	40
3.4.2	Predicting Disinfection Performance in Continuously Stirred Tank Reactor from Batch Data.....	40
3.4.2.1	Segregated Flow Reactor	41
3.4.2.2	Completely Mixed Flow System.....	43
Chapter 4 :	Experimental Materials and Methods	46
4.1	Experimental Material	46
4.1.1	Laboratory Apparatus Preparation.....	46
4.1.2	Solution Preparation	51
4.1.3	Microbial Preparation.....	57
4.1.3.1	Growth media preparation	57
4.1.3.2	<i>Escherichia coli</i> preparation	59

4.1.3.3	<i>Bacillus subtilis</i> Preparation.....	63
4.2	Analytical Methods	67
4.3	CSTR Set Up and Characterization	69
4.3.1	CSTR Set Up.....	69
4.3.2	CSTR Characterization.....	74
4.3.2.1	Tracer Test Performance.....	74
4.3.2.2	F Curve	77
4.3.2.3	E Curve and Tanks-in-series Model.....	82
4.3.2.4	CSTR Characterization and Mixing Effect of the Reactor.....	88
4.3.2.5	Mean Residence Time Determination of the Reactor	91
4.4	Performance of Disinfection Experiments	97
4.5	Data Analysis.....	99
Chapter 5 :	Results and Discussion	102
5.1	Proposed and Achieved Experiments	102
5.2	Steady-state Condition Determination of the System.....	108
5.2.1	Monochloramine Disinfection System	108
5.2.2	Ozone Disinfection System	113
5.3	Prediction of CSTR Performance from Batch Kinetics and CSTR Data	115
5.3.1	Inactivation of <i>E. coli</i> in Stationary Phase Using Monochloramine.....	115
5.3.1.1	Batch Kinetics.....	115
5.3.1.2	CSTR Disinfection and Batch Predictions	115
5.3.1.3	Linear Regression between Observed and Predicted Data.....	130
5.3.1.4	Paired t-test between CSTR Observation and Batch Prediction	131
5.3.2	Inactivation of <i>E. coli</i> in Exponential Phase Using Monochloramine	131

5.3.2.1	Batch Kinetics.....	131
5.3.2.2	CSTR Disinfection and Batch Predictions	132
5.3.2.3	Linear Regression between Observed and Predicted Data.....	147
5.3.2.4	Paired t-test between CSTR Observation and Batch Prediction	147
5.3.3	Inactivation of <i>B. subtilis</i> Vegetative Cells in Exponential Phase Using Monochloramine.....	148
5.3.3.1	Batch Kinetics.....	148
5.3.3.2	CSTR Disinfection and Batch Predictions	149
5.3.3.3	Linear Regression between Observed and Predicted Data.....	163
5.3.3.4	Paired t-test between CSTR Observation and Batch Prediction	164
5.3.4	Inactivation of <i>B. subtilis</i> Spores Using Ozone	164
5.3.4.1	Batch Kinetics.....	164
5.3.4.2	CSTR Disinfection and Batch Predictions	165
5.3.4.3	Linear Regression between Observed and Predicted Data.....	179
5.3.4.4	Paired t-test between CSTR Observation and Batch Prediction	180
5.3.5	CSTR System Correction	180
5.3.5.1	Correction for Inactivation of <i>E. coli</i> in Stationary Phase Using Monochloramine	181
5.3.5.2	Correction for Inactivation of <i>E. coli</i> in Exponential Phase Using Monochloramine	186
5.3.5.3	Correction for Inactivation of <i>B. subtilis</i> Vegetative Cells in Exponential Phase Using Monochloramine	190
5.3.5.4	Correction for Inactivation of <i>B. subtilis</i> Spores Using Ozone	194
5.3.5.5	Summary of System Correction	198
5.4	The Effect of Initial Microbial Density on Disinfection in CSTR	200
5.4.1	Statistical Methods	201
5.4.2	Results from Four Series Disinfection Experiments.....	201
5.4.3	Comparison of the Effects of the Initial Microbial Density on Disinfection in CSTR System and Batch System.....	203

Chapter 6 :	Summary and Conclusion	205
Chapter 7 :	Engineering Significance and Future Work.....	207
List of References	210
Appendix A:	Derivation of Segregation Number Calculation	224
Appendix B:	Derivation of the Hom Power Law Model for CSTR Prediction	228
Appendix C:	Derivation of the Hom Model for CSTR Prediction.....	229
Appendix D:	Derivation of the Modified Multiple Target Model.....	230
Appendix E:	Matlab Program	232
Appendix F:	Experimental Data	237
Vita.....		250

List of Tables

4-1	Designed Mean Residence Times and Corresponding Flow Rates	76
4-2	Estimation of Parameters in Tanks-in-series Model	83
4-3	CSTR Characterization Parameters	89
4-4	Segregation Numbers for the Disinfection Experiments	90
4-5	Mean Residence Times Determined from Linear Regression Method	92
4-6	Mean Residence Times Determined from Non-linear Regression Method	97
4-7	Performed Disinfection Experiments	98
4-8	Disinfection Kinetic Models Applied in Batch Analyses	101
5-1	Disinfection Experiments Design in CSTR	102
5-2	Relative Standard Deviation of Disinfection Systems at Steady-state Condition	109
5-3	Batch Best-fit Model and Parameters for Stationary Phase <i>E. coli</i> Inactivation by Monochloramine	115
5-4	Linear Regression of Observation and Prediction (MES)	130
5-5	Paired t-test Comparison between Observed and Predicted Survival Ratio (ln units) for <i>E. coli</i> in Stationary Phase	131
5-6	Batch Best-fit Model and Parameters for Exponential Phase <i>E. coli</i> Inactivation by Monochloramine	132
5-7	Linear Regression of Observation and Prediction (MEE)	147
5-8	Paired t-test Comparison between Observed and Predicted Survival Ratio (ln units) for <i>E. coli</i> in Exponential Phase	148
5-9	Batch Best-fit Model and Parameters for Exponential Phase <i>B. subtilis</i> Vegetative Cells Inactivation by Monochloramine	149
5-10	Linear Regression of Observation and Prediction (MBE)	163
5-11	Paired t-test Comparison between Observed and Predicted Survival Ratio (ln units) for <i>B. subtilis</i> Vegetative Cells	164
5-12	Batch Best-fit Model and Parameters for <i>B. subtilis</i> Spores Inactivation by Ozone	165
5-13	Linear Regression of Observation and Prediction (OBS)	179

5-14	Paired t-test Comparison between Observed and Predicted Survival Ratio (ln units) for <i>B. subtilis</i> Spores	180
5-15	Linear Regression II of Observation and Prediction (MES).....	182
5-16	Linear Regression II of Observation and Prediction (MEE).....	187
5-17	Linear Regression II of Observation and Prediction (MBE)	191
5-18	Linear Regression II of Observation and Prediction (OBS)	195
5-19	Summary of Backwards Stepwise Regression and ANOVA for Disinfection Data.....	202
5-20	Effects of Initial Microbial Density on Disinfection in CSTR and Batch System.....	204

List of Figures

3-1	Structural Differences between Gram-positive Cell and Gram-negative Cell (Denyer and Stewart 1998).....	13
3-2	Schematic Layered Diagram of a Bacterial Spore (Russell 1995).....	16
3-3	The Molecular Structures of Two Typical HSL Signal Chemicals	24
3-4	The Molecular Structure of Autoinducer AI-2	25
3-5	Microbial Survival Curves under Disinfection.....	31
4-1	Standard Curves of Microbial Density of <i>E. coli</i> in Stationary Phase and Exponential Phase vs. Optical Density at 660 nm	61
4-2	Growth Curve of <i>E. coli</i>	62
4-3	Standard Curves of Microbial Density of <i>B. subtilis</i> cells in Exponential Phase and Spores vs. Optical Density at 660 nm.....	65
4-4	Growth Curve of <i>B. subtilis</i>	66
4-5	Schematic Sketch of CSTR	70
4-6	Monochloramine Disinfection System Configuration	71
4-7	Ozone Disinfection System Configuration.....	72
4-8	Conductivity Standard Curve of NaCl Solution	75
4-9	F Curve ($Q_1 = Q_2 = 125$ mL/min).....	78
4-10	F Curve ($Q_1 = Q_2 = 62.5$ mL/min).....	79
4-11	F Curve ($Q_1 = Q_2 = 41.7$ mL/min).....	80
4-12	F Curve ($Q_1 = Q_2 = 25$ mL/min).....	81
4-13	Tanks-in-series Model E(t) Fitting Curve.....	84
4-14	Tanks-in-series Model E(t) Fitting Curve.....	85
4-15	Tanks-in-series Model E(t) Fitting Curve.....	86
4-16	Tanks-in-series Model E(t) Fitting Curve.....	87
4-17	Linear Regression of Tracer Test ($Q_1 = Q_2 = 125$ mL/min)	93
4-18	Linear Regression of Tracer Test ($Q_1 = Q_2 = 62.5$ mL/min)	94

4-19	Linear Regression of Tracer Test ($Q_1 = Q_2 = 41.7$ mL/min)	95
4-20	Linear Regression of Tracer Test ($Q_1 = Q_2 = 25$ mL/min)	96
5-1	Proposed and Achieved Experiments (<i>E. coli</i> in Stationary Phase)	104
5-2	Proposed and Achieved Experiments (<i>E. coli</i> in Exponential Phase).....	105
5-3	Proposed and Achieved Experiments (<i>B. subtilis</i> Vegetative Cells in Exponential Phase)	106
5-4	Proposed and Achieved Experiments (<i>B. subtilis</i> Spores).....	107
5-5	Steady-state Condition Determination (<i>E. coli</i> in Stationary Phase, $\theta = 10.35$ minutes)	110
5-6	Steady-state Condition Determination (<i>E. coli</i> in Exponential Phase, $\theta = 6.20$ minutes)	111
5-7	Steady-state Condition Determination (<i>B. subtilis</i> Vegetative Cells in Exponential Phase, $\theta = 6.20$ minutes).....	112
5-8	Steady-state Condition Determination (<i>B. subtilis</i> Spores, $\theta = 4.11$ minutes).....	114
5-9	Inactivation of <i>E. coli</i> in Stationary Phase using Monochloramine ($N_0 = 10^3$ CFU/mL, $C = 0.75$ mg/L)	117
5-10	Inactivation of <i>E. coli</i> in Stationary Phase using Monochloramine ($N_0 = 10^4$ CFU/mL, $C = 0.75$ mg/L)	118
5-11	Inactivation of <i>E. coli</i> in Stationary Phase using Monochloramine ($N_0 = 10^5$ CFU/mL, $C = 0.75$ mg/L)	119
5-12	Inactivation of <i>E. coli</i> in Stationary Phase using Monochloramine ($N_0 = 10^5$ CFU/mL, $C = 0.75$ mg/L)	120
5-13	Inactivation of <i>E. coli</i> in Stationary Phase using Monochloramine ($N_0 = 10^3$ CFU/mL, $C = 1.0$ mg/L)	121
5-14	Inactivation of <i>E. coli</i> in Stationary Phase using Monochloramine ($N_0 = 10^4$ CFU/mL, $C = 1.0$ mg/L)	122
5-15	Inactivation of <i>E. coli</i> in Stationary Phase using Monochloramine ($N_0 = 10^4$ CFU/mL, $C = 1.0$ mg/L)	123
5-16	Inactivation of <i>E. coli</i> in Stationary Phase using Monochloramine ($N_0 = 10^5$ CFU/mL, $C = 1.0$ mg/L)	124
5-17	Inactivation of <i>E. coli</i> in Stationary Phase using Monochloramine ($N_0 = 10^3$ CFU/mL, $C = 1.5$ mg/L)	125

5-18	Inactivation of <i>E. coli</i> in Stationary Phase using Monochloramine ($N_0 = 10^3$ CFU/mL, $C = 1.5$ mg/L)	126
5-19	Inactivation of <i>E. coli</i> in Stationary Phase using Monochloramine ($N_0 = 10^4$ CFU/mL, $C = 1.5$ mg/L)	127
5-20	Inactivation of <i>E. coli</i> in Stationary Phase using Monochloramine ($N_0 = 10^5$ CFU/mL, $C = 1.5$ mg/L)	128
5-21	Overall Comparison of Observed vs. Predicted Survival Ratio (Inactivation of <i>E. coli</i> in Stationary Phase Using Monochloramine).....	129
5-22	Inactivation of <i>E. coli</i> in Exponential Phase Using Monochloramine ($N_0 = 10^3$ CFU/mL, $C = 0.75$ mg/L)	134
5-23	Inactivation of <i>E. coli</i> in Exponential Phase Using Monochloramine ($N_0 = 10^3$ CFU/mL, $C = 0.75$ mg/L)	135
5-24	Inactivation of <i>E. coli</i> in Exponential Phase Using Monochloramine ($N_0 = 10^4$ CFU/mL, $C = 0.75$ mg/L)	136
5-25	Inactivation of <i>E. coli</i> in Exponential Phase Using Monochloramine ($N_0 = 10^5$ CFU/mL, $C = 0.75$ mg/L)	137
5-26	Inactivation of <i>E. coli</i> in Exponential Phase Using Monochloramine ($N_0 = 10^3$ CFU/mL, $C = 1.0$ mg/L)	138
5-27	Inactivation of <i>E. coli</i> in Exponential Phase Using Monochloramine ($N_0 = 10^4$ CFU/mL, $C = 1.0$ mg/L)	139
5-28	Inactivation of <i>E. coli</i> in Exponential Phase Using Monochloramine ($N_0 = 10^5$ CFU/mL, $C = 1.0$ mg/L)	140
5-29	Inactivation of <i>E. coli</i> in Exponential Phase Using Monochloramine ($N_0 = 10^5$ CFU/mL, $C = 1.0$ mg/L)	141
5-30	Inactivation of <i>E. coli</i> in Exponential Phase Using Monochloramine ($N_0 = 10^3$ CFU/mL, $C = 1.5$ mg/L)	142
5-31	Inactivation of <i>E. coli</i> in Exponential Phase Using Monochloramine ($N_0 = 10^4$ CFU/mL, $C = 1.5$ mg/L)	143
5-32	Inactivation of <i>E. coli</i> in Exponential Phase Using Monochloramine ($N_0 = 10^4$ CFU/mL, $C = 1.5$ mg/L)	144
5-33	Inactivation of <i>E. coli</i> in Exponential Phase Using Monochloramine ($N_0 = 10^5$ CFU/mL, $C = 1.5$ mg/L)	145

5-34	Overall Comparison of Observed vs. Predicted Survival Ratio (Inactivation of <i>E. coli</i> in Exponential Phase Using Monochloramine).....	146
5-35	Inactivation of <i>B. Subtilis</i> Vegetative Cells in Exponential Phase Using Monochloramine ($N_0 = 10^3$ CFU/mL, $C = 1.0$ mg/L)	150
5-36	Inactivation of <i>B. Subtilis</i> Vegetative Cells in Exponential Phase Using Monochloramine ($N_0 = 10^3$ CFU/mL, $C = 1.0$ mg/L)	151
5-37	Inactivation of <i>B. Subtilis</i> Vegetative Cells in Exponential Phase Using Monochloramine ($N_0 = 10^3$ CFU/mL, $C = 1.0$ mg/L)	152
5-38	Inactivation of <i>B. Subtilis</i> Vegetative Cells in Exponential Phase Using Monochloramine ($N_0 = 10^4$ CFU/mL, $C = 1.0$ mg/L)	153
5-39	Inactivation of <i>B. Subtilis</i> Vegetative Cells in Exponential Phase Using Monochloramine ($N_0 = 10^3$ CFU/mL, $C = 1.5$ mg/L)	154
5-40	Inactivation of <i>B. Subtilis</i> Vegetative Cells in Exponential Phase Using Monochloramine ($N_0 = 10^3$ CFU/mL, $C = 1.5$ mg/L)	155
5-41	Inactivation of <i>B. Subtilis</i> Vegetative Cells in Exponential Phase Using Monochloramine ($N_0 = 10^4$ CFU/mL, $C = 1.5$ mg/L)	156
5-42	Inactivation of <i>B. Subtilis</i> Vegetative Cells in Exponential Phase Using Monochloramine ($N_0 = 10^5$ CFU/mL, $C = 1.5$ mg/L)	157
5-43	Inactivation of <i>B. Subtilis</i> Vegetative Cells in Exponential Phase Using Monochloramine ($N_0 = 10^3$ CFU/mL, $C = 2.0$ mg/L)	158
5-44	Inactivation of <i>B. Subtilis</i> Vegetative Cells in Exponential Phase Using Monochloramine ($N_0 = 10^3$ CFU/mL, $C = 2.0$ mg/L)	159
5-45	Inactivation of <i>B. Subtilis</i> Vegetative Cells in Exponential Phase Using Monochloramine ($N_0 = 10^4$ CFU/mL, $C = 2.0$ mg/L)	160
5-46	Inactivation of <i>B. Subtilis</i> Vegetative Cells in Exponential Phase Using Monochloramine ($N_0 = 10^4$ CFU/mL, $C = 2.0$ mg/L)	161
5-47	Overall Comparison of Observed vs. Predicted Survival Ratio (Inactivation of <i>B. subtilis</i> Vegetative Cells Using Monochloramine).....	162
5-48	Inactivation of <i>B. Subtilis</i> Spores Using Ozone.....	166
5-49	Inactivation of <i>B. Subtilis</i> Spores Using Ozone.....	167
5-50	Inactivation of <i>B. Subtilis</i> Spores Using Ozone.....	168
5-51	Inactivation of <i>B. Subtilis</i> Spores Using Ozone.....	169

5-52	Inactivation of <i>B. Subtilis</i> Spores Using Ozone.....	170
5-53	Inactivation of <i>B. Subtilis</i> Spores Using Ozone.....	171
5-54	Inactivation of <i>B. Subtilis</i> Spores Using Ozone.....	172
5-55	Inactivation of <i>B. Subtilis</i> Spores Using Ozone.....	173
5-56	Inactivation of <i>B. Subtilis</i> Spores Using Ozone.....	174
5-57	Inactivation of <i>B. Subtilis</i> Spores Using Ozone.....	175
5-58	Inactivation of <i>B. Subtilis</i> Spores Using Ozone.....	176
5-59	Inactivation of <i>B. Subtilis</i> Spores Using Ozone.....	177
5-60	Overall Comparison of Observed vs. Predicted Survival Ratio (Inactivation of <i>B. subtilis</i> Spores Using Ozone)	178
5-61	Blank Experiment of <i>E. coli</i> in Stationary Phase.....	184
5-62	Overall Comparison of Observed vs. Predicted Survival Ratio With and Without System Correction (Inactivation of <i>E. coli</i> in Stationary Phase Using Monochloramine).....	185
5-63	Blank Experiment of <i>E. coli</i> in Exponential Phase.....	188
5-64	Overall Comparison of Observed vs. Predicted Survival Ratio With and Without System Correction (Inactivation of <i>E. coli</i> in Exponential Phase Using Monochloramine).....	189
5-65	Blank Experiment of <i>B. subtilis</i> Vegetative Cells in Exponential Phase ($N_0 = 10^4$ CFU/mL).....	192
5-66	Overall Comparison of Observed vs. Predicted Survival Ratio With and Without System Correction (Inactivation of <i>B. subtilis</i> in Exponential Phase Using Monochloramine)	193
5-67	Blank Experiment of <i>B. subtilis</i> Spores ($N_0 = 10^3$ CFU/mL)	196
5-68	Overall Comparison of Observed vs. Predicted Survival Ratio With and Without System Correction (Inactivation of <i>B. subtilis</i> Spores Using Ozone).....	197

Abstract

Effects of Initial Microbial Density on Disinfection Efficiency
in a Continuous Flow System and Validation of
Disinfection Batch Kinetics in a Continuous Flow System

Lijie Li

Charles N. Haas Supervisor, Ph.D.

This work was designed with two primary objectives. One is to test the hypothesis that initial microbial density has a significant effect on disinfection in a continuous flow system. The other is to validate the disinfection kinetics obtained from the batch studies in a continuous flow system.

Four series of disinfection experiments were conducted at 15°C in phosphate buffer solution using a lab-scale continuously stirred tank reactor (CSTR). These experiments included the inactivation of *E. coli* in stationary phase using monochloramine (pH 7), the inactivation of *E. coli* in exponential phase using monochloramine (pH 7), the inactivation of *B. subtilis* vegetative cells in exponential phase using monochloramine (pH 7), and the inactivation of *B. subtilis* spores using ozone (pH 8). Prior to these experiments, the reactor was characterized as an ideal CSTR by performing step-input tracer tests.

Statistical analyses of the CSTR disinfection data indicated that the initial microbial density had a significant effect on the inactivation of *E. coli* in stationary phase using monochloramine in the CSTR system. This result was consistent with the conclusion drawn from batch disinfection data analysis in a previous study. Effects of initial microbial density on disinfection efficiency were not observed in the other three

series of experiments, suggesting that this effect might be specific to certain microorganisms in certain growth phases.

The disinfection efficiency in a CSTR was predicted from the mathematical expression obtained from batch inactivation kinetics and the CSTR hydraulic characteristics. The predicted survival ratio was compared with the observed CSTR survival ratio in natural log units. For *E. coli* in both stationary phase and exponential phase, no significant difference existed between the two sets of data after system correction of the change of *E. coli* density in the tubing system, indicating that this approach could be used to predict the behavior of *E. coli* using monochloramine in continuous flow system from batch kinetics. For *B. subtilis* cells and spores, systematic differences between continuous flow and batch systems precluded the use of batch data for CSTR inactivation estimation.

Chapter 1 : Introduction

The exposure to disease-causing organisms such as bacteria, viruses, and protozoa has caused great health concern and existed as a big challenge for drinking water suppliers. Disinfection, as a process designed to inactivate pathogenic microorganisms, has been widely used in water treatment utilities to reduce transmission of waterborne diseases.

In the United States, all public water systems (PWSs) using surface water sources or groundwater sources under the direct influence of surface water are regulated under the Surface Water Treatment Rule (SWTR) (USEPA 1989). Under this regulation, disinfection is required for both filtered and non-filtered systems. 99.9% removal/inactivation of *Giardia lamblia* cysts and 99.99% removal/inactivation of viruses are required through filtration and disinfection. Assuming conventional filtration can provide 2.5-log removal of *Giardia* and 2-log removal of viruses, disinfection is responsible for achieving the remainder of removal/inactivation (USEPA 1991).

The resistance of bacteria to disinfectants depends on the external environment (pH, temperature), the disinfectants (nature, concentration), and organisms inactivated (type, growth phase). It has been known that stationary-phase cells are more resistant to different kinds of environmental stresses than exponential-phase cells and cell density is believed to be an important factor which controls the growth phase of bacteria shifting from exponential to stationary (Kaiser and Losick 1993; Benjamin and Datta 1995; Sitnikov 1996; Datta and Benjamin 1999; Yamada 1999; Hengge-Aronis 2000; Lazazzera 2000). It has been suggested that bacteria can communicate with each other

and regulate their gene expression with respect to cell density by quorum sensing, so they can change their response to different environmental stresses, including oxidative agents (Storz 1990; Zambrano and Kolter 1996; Gray 1997; Eisenstark 1998; Surette and Bassler 1998; Bassler 1999; Kobayashi and Tagawa 1999; Storz and Imlay 1999; Thorne and Williams 1999; Gruenheid and Finlay 2000; Holden 2000; Whiteley 2000; Pomposiello and Demple 2001)

Since Chick (1908) first considered the analogy between the bacteria-disinfectant reaction and an elementary bimolecular chemical reaction and developed the Chick Model, a number of disinfection kinetic models have been developed to assess disinfection performance and the design of reactor systems. The disinfection rate was expressed as $\frac{dN}{dt}$ (organisms killed/volume-time) and the survival ratio in (natural) logarithmic scale was utilized to refer to the disinfection efficiency. Among the most frequently used disinfection models, the Chick model only considered the effect of contact time; the Chick-Watson model and the Hom model incorporated both the disinfectant concentration and the contact time; the Multiple Target model combined the number of targets contained in a particle (organism or clump of organisms) needed to be destroyed to kill the organism; and the Series-event model introduced a series levels of damaging reactions occurring in integral steps.

Earlier in the 1970s, the initial virus density was found to play a role in disinfection efficiency (Majumdar 1973). Studies since then also suggested that the initial microbial density could have significant effects in disinfection (Roy 1981; Crockford 1995; Walker 1995; Datta and Benjamin 1999). More sophisticated and statistically

accurate kinetic models such as the Power Law model and the Hom Power Law model were developed to take account of initial microbial density (Majumdar 1973; Roy 1981; Anotai 1996).

Appropriate disinfection criteria are very essential to ensure the protection of public health and to minimize the risk from chronic exposure to disinfection by-products (DBPs). The disinfection models are the basis to obtain the criteria. At present, the CT tables are used as the guidance for disinfection treatment in order to provide adequate control of those organisms under the SWTR. The CT value is defined as the product of the residual disinfectant concentration (C , in mg/L) with the contact time (T , in minute) between the point of disinfectant application and the point of residual measurement. For a particular continuous flow reactor, t_{10} value (time at which the first 10 percent of a tracer passes through a system) is used as a conservative measure of contact time in the CT calculation. Water utilities can calculate disinfection credit by either incorporating a safety factor into the CT values, or by performing pilot-scale studies to demonstrate the effectiveness of their disinfection systems.

Some issues exist with the current disinfection criteria. The CT approach was based on studies performed in buffered demand-free water in lab-scale batch system with high initial microbial density (Jarroll 1981; Rice 1982; Rubin 1989). The CT tables were derived from a simple Chick-Watson inactivation relationship without considering the effect of initial microbial density (Clark 1989). Also the t_{10} approach is based on a plug flow model with a crude correction for nonidealities in flow, which is usually not the case in real. Even though the SWTR allows utilities to demonstrate the effectiveness of their

disinfection through performance of pilot-scale studies, large expenses are involved and prohibitive for smaller water suppliers.

Chapter 2 : Scope of the Study

This research was conducted to study the effects of initial microbial density on disinfection in a laboratory continuously stirred tank reactor (CSTR) system.

One of the major objectives of this study is to examine the effect of initial microbial density on disinfection. Many types of microorganisms have been reported to be able to communicate with each other at high cell density and regulate their gene expression by producing and responding to secreted small signaling molecules (quorum sensing). These signaling molecules were reported to be different for Gram-negative bacteria and Gram-positive bacteria (Gray 1997; Lazazzera and Grossman 1998). However, very little work has been done to study the effect of initial microbial density on disinfection for different organisms. In this study, *Escherichia coli* and *Bacillus subtilis* in different growth phases were selected as the target bacteria to examine the effect of initial cell density on disinfection efficiency.

E. coli is a Gram-negative, non-spore-forming, rod-shaped, and facultative anaerobic bacterium. It is an abundant commensal found in the intestinal tract of humans and warm-blooded animals and has been employed widely in disinfection research as an indicator of fecal contamination in water for many decades (Boyd and Hoerl 1991; Haas 1999; Morin 2003). Prior research suggested that initial microbial density has significant effect on inactivation of Gram-negative bacteria *E. coli* in stationary phase with monochloramine in batch system (Kaymak 2003).

B. subtilis is a Gram-positive, endospore-producing, rod-shaped and aerobic bacterium (Davis 1990). Spores are formed under certain conditions such as starvation

and are highly resistant to disinfectants. Studies suggest that spores of *B. subtilis* which are easy to be cultured and non-pathogenic might be used as a surrogate to assess disinfection efficiency on *Giardia* cysts and *Cryptosporidium* oocysts in certain temperature ranges (Barbeau 1999; Facile 2000; Driedger 2001).

Bacteria display different resistance to environmental stresses including oxidative stress in exponential growth phase and stationary phase (Benjamin and Datta 1995; Datta and Benjamin 1999; Russell 1999; Hengge-Aronis 2000). Cell density is believed to be an important factor to regulate bacteria shifting from exponential phase to stationary phase (Kaiser and Losick 1993; Surette and Bassler 1998; Lazazzera 2000). In this study *E. coli* in different growth phases (exponential and stationary) were studied separately, as well as *B. subtilis* in dormant phase (spores) and exponential growth phase (vegetative cells).

Monochloramine was used to inactivate *E. coli* in stationary phase, *E. coli* in exponential phase, and *B. subtilis* vegetative cells in exponential phase. Ozone was used to disinfect *B. subtilis* spores.

Disinfection efficiency in continuous flow systems could also be predicted by a reactor engineering approach directly from kinetic data of a batch system and the hydraulic characteristics of a dynamic flow system (Trussell and Chao 1977; Selleck 1978; Haas 1988; Kouame 1990; Roustan 1991; Haas 1995; Haas 1997; Haas 1998; Chiu 1999; Greene 2003). This approach could be a way to get disinfection credits without the large expenses for performing pilot-scale studies.

Two continuously stirred tank reactor systems were set up in the laboratory, one for monochloramine disinfection and another for ozone disinfection. With a full CSTR

reactor characterization, a total of 52 disinfection experiments were performed at 15°C in demand-free buffered water. The initial microbial densities were 1×10^3 , 1×10^4 , and 1×10^5 colony forming units (CFU)/mL, with the purpose of investigating the effect of initial microbial density on disinfection efficiency.

The data were analyzed statistically to answer the following questions about the effects of initial microbial density on disinfection efficiency.

- Is this phenomenon valid for both Gram-negative bacteria (*E. coli*) and Gram-positive bacteria (*B. subtilis*)?
- Is this phenomenon valid for bacteria in dormant phase, stationary phase, and exponential phase?
- Is this phenomenon equally valid for continuous flow system and batch disinfection system?
- Can the batch disinfection kinetics be validated in continuous flow system?

Chapter 3 : Literature Review

3.1 Overview of the Chemistry of Disinfectants

3.1.1 Aquatic Chemistry of Chlorine

Chlorine has been widely used as the primary disinfectant for potable water treatment for over 100 years. Chlorine is highly soluble in water and is very easy to apply. It can be easily measured, easily controlled, and is relatively inexpensive comparing with other disinfectants. These properties make chlorine a very useful disinfectant (Qasim 2000). The concern about chlorine is the potentially carcinogenic disinfection by-products (DBPs) produced by chlorine with natural organic material (NOM) in water. And also chlorine is not an effective disinfectant against *Cryptosporidium* which presents a unique problem to water suppliers.

When dissolved in water, chlorine gas hydrolyzes rapidly to form hypochlorous acid (*HOCl*) and hydrogen chloride (*HCl*) according to



HOCl is a weak acid which is partially dissociated with the reaction



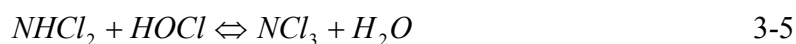
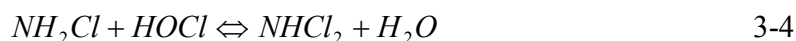
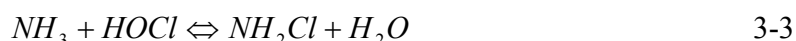
HOCl, *OCl⁻*, and *Cl₂* exist together in equilibrium as free available chlorine (FAC). Their relative proportions vary with pH, temperature, salinity, and the concentration of chlorine in solution. In natural water *HOCl* and *OCl⁻* are the predominant species. *HOCl*

is many times stronger a disinfectant than OCl^- , so the disinfecting power of chlorine decreases with increase in pH.

3.1.2 Aquatic Chemistry of Chloramine

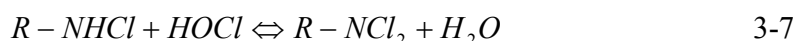
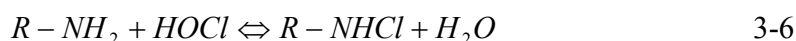
Chlorine can react with inorganic and organic nitrogen in water and accordingly produce inorganic chloramines and organic chloramines, which are called combined available chlorine (CAC). The source of inorganic nitrogen is ammonia, nitrate, and nitrite, while organic nitrogen is introduced by amino acids and proteins.

Free chlorine reacts with ammonia to form monochloramine (NH_2Cl), dichloramine ($NHCl_2$), and trichloramine (NCl_3) in a stepwise manner.

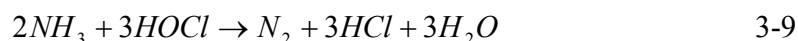


The relative distribution of the three inorganic chloramines depends on the proportion of chlorine and ammonia present, the reaction time, pH and temperature. Monochloramine is the most commonly used disinfectant in water treatment. If the chlorine to ammonia nitrogen ratio is less than 5:1 and the pH is 7.5 and higher, the combined residual will probably be 100 percent monochloramine (White 1999).

Reacting with nitrogen containing organic compounds, free chlorine can form organochloramines in accordance with the following equations:



With the increasing dosage of chlorine into water, the concentration of CAC will increase until a maximum combined residual is reached. Further addition of chlorine causes a decrease in CAC. This is observed as breakpoint chlorination. At this point, nitrogen gas will be released as an end product by the following equations.



A stable free residual can only be obtained after the breakpoint chlorination has been reached.

Chloramines are not very strong disinfectants, but they can result in a stable combined residual in the water distribution system and also can minimize organic byproduct formation, particularly the trihalomethanes (THMs) which are the subject of increasingly strict governmental regulation. In USA, approximately 20 percent of water utilities use ammonia addition in conjunction with chlorine or hypochlorite (Haas 1999). The concern about chloramination is that overdosing of ammonia can encourage the growth of nitrifying bacteria in the treatment processes and the distribution system, thereby affecting the quality of water supplied (Qasim 2000).

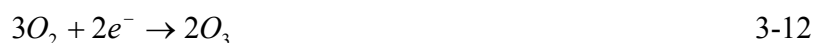
3.1.3 Aquatic Chemistry of Ozone

Ozone has been widely used for disinfection and for taste and odor control in water suppliers in Europe. Because of the growing concern about THM formation in chlorination in recent years, the interest on ozone as a disinfectant has been increased in the United States and Canada.

Ozone is a faintly blue, pungent-smelling, and unstable gas with high oxidation potential. It must be generated at the point-of-use by applying energy to oxygen or dried air. High-energy electrical field caused oxygen to dissociate. Each dissociated oxygen molecule reacts with another oxygen to form an ozone molecule (Qasim 2000).



The overall ozone formation is expressed by



When exposed to a neutral or alkaline environment (pH above 6), UV light, or hydrogen peroxide, ozone can decompose in water to produce more active hydroxyl free radicals. This reaction is accelerated at pH above 8.



The hydroxyl free radicals ($HO_2 \cdot$ and $HO \cdot$) are more effective oxidizing agents than the molecular ozone, but extremely short-lived. Ozone can only provide an adequate residual for a very short time in water.

Ozone has long been recognized as an excellent disinfectant and is also widely used in taste and odor control, color removal, as well as iron and manganese removal. Unlike chlorine, it produces little or no THM and does not produce dissolved and suspended solids.

Bromate control is a concern for water suppliers which use ozone as the disinfectant (Song 1997). Ozonation of water containing bromide (Br^-) and natural

organic matter (NOM) can produce bromate ion (BrO_3^-) which has demonstrated carcinogenicity in animal experiments. USEPA has set the maximum contaminant level (MCL) for bromate at 10 µg/L for Stage I of the Disinfectants/Disinfection Byproducts (D/DBP) Rule (USEPA 1998a).

3.2 Mechanism of Disinfection and Bacterial Resistance to Disinfectants

3.2.1 The Composition and Structure of Bacterial Cells and Potential Targets for Disinfectants

For vegetative bacterial cells, disinfectants can interact with three components: the cell wall, cytoplasmic membrane and cytoplasm (Denyer and Stewart 1998). Many factors determine the access of disinfectants to these regions including extracellular material, cell morphology and cellular chemical composition.

Bacterial spores are much more resistant to disinfectants than the vegetative cells due to the protective spore structure and the state of low hydration. The target sites of disinfectants are believed to be within the spore (Russell 1995).

3.2.1.1 Gram-positive Bacteria and Gram-negative Bacteria

The cell wall is the first potential target of a disinfectant. Based on a staining procedure called the Gram's stain, bacteria can be divided into two basic cell wall types: Gram-positive and Gram-negative. The cell walls of Gram-positive and Gram-negative bacteria are structurally different (Figure 3-1). The backbone material of both types is the

peptidoglycan layer which is composed of layers of polysaccharide chains linked by short peptides (Boyd and Hoerl 1991).

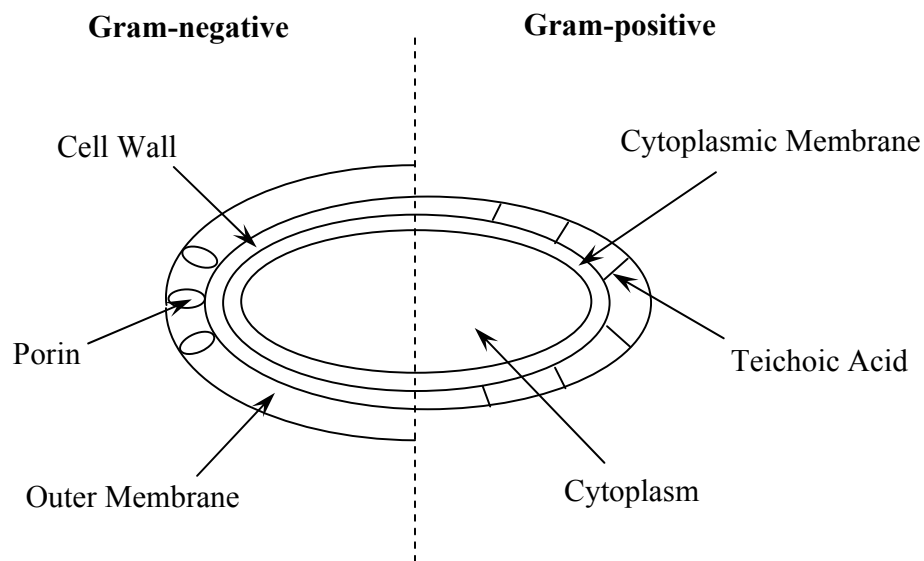


Figure 3-1 Structural Differences between Gram-positive Cell and Gram-negative Cell (Denyer and Stewart 1998)

The cell wall of Gram-positive bacteria is made of peptidoglycan (over 90% of cell wall) and teichoic acids. The peptidoglycan layer of Gram-positive bacteria is very thick compared to the Gram-negative peptidoglycan layer and provides a strong protective layer that protects the plasma membrane from lysis by osmotic shock. Teichoic acids are acidic polysaccharides not only permeate the peptidoglycan but also appear on

the surface of the cell wall. It makes the Gram-positive cell wall acidic and is very important in regulating autolytic activity (Atlas 1995).

Gram-negative cell walls are far more complex. The peptidoglycan layer of Gram-negative cells is very thin (only 5% to 10% of cell wall) and does not contain teichoic acids. Gram-negative cell walls also have other distinct structures called outer membranes which are semipermeable phospholipid bilayers made up of phospholipids (20-30%), lipopolysaccharide (30%) and protein (40-50%). The outer membrane is attached to the peptidoglycan layer by lipoproteins and has channels made of proteins called porins which can pass small polar molecules freely. Very large molecules are blocked by the outer membrane (Boyd and Hoerl 1991; Atlas 1995).

The cytoplasmic membrane is a phospholipid bilayer containing globular proteins. It provides a rich matrix of balanced interactions between phospholipid and enzymic/structural protein. The cytoplasmic membrane ensures a controlled impermeability and topological organization by which intracellular homeostasis and vectorial transport/metabolism are maintained.

The cytoplasm is the final region for disinfectant attack because of its inclusion within the cytoplasmic membrane. It offers a diverse range of target processes by the necessary replicative machinery, and many catabolic and anabolic processes (Denyer and Stewart 1998).

3.2.1.2 Bacterial Spores

Spores are the most resistant life forms known in bacteria (Bloomfield and Arthur 1994; Russell 1995; Russell 1999). Studies suggest that they might be used as surrogates or indicators for *Giardia* cysts and *Cryptosporidium* oocysts for assessing disinfection efficiency in certain temperature ranges (Barbeau 1999; Driedger 2001; Radziminski 2002; Larson and Marinas 2003). Spores are formed when conditions are unfavorable for the continued growth of bacteria. The two most important genera of bacteria producing spores are *Bacillus* and *Clostridium*. Many antibacterial compounds which can kill bacterial vegetative cells are not sporicidal but sporistatic, only retarding or inhibiting the germination or outgrowth of spores. A number of chemical compounds are sporicidal under the condition of much higher concentrations and longer contact times compared with bactericidal action.

Spores are the dormant, dehydrated forms of spore-forming vegetative cells. The structure of a “typical” bacteria spore includes core, plasma membrane, germ cell wall, cortex, inter and outer spore coat, and exosporium (present in some spores, but may surround just one spore coat), from inside to outside (Figure 3-2).

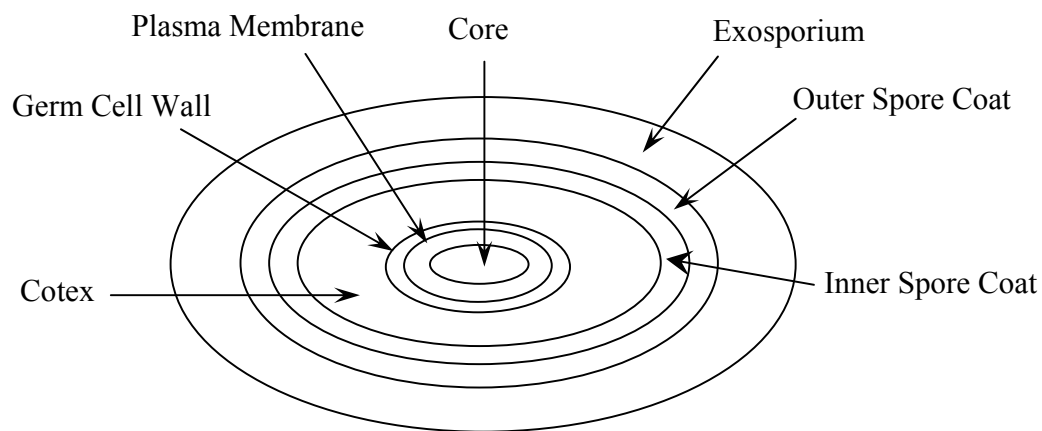


Figure 3-2 Schematical Layered Diagram of a Bacterial Spore (Russell 1995)

The spore coat is comprised predominantly of protein with smaller amounts of complex carbohydrates and lipid. The spore coat plays an important role in disinfectant resistance by limiting penetration to the underlying protoplast. Electron microscopy and chemical analysis indicates that the outer spore coat contains the alkali-resistant protein fraction and the inner spore coat contains the alkali-soluble fraction. The cortex consists largely of peptidoglycan which not only provides the mechanical protection to the spore, but also plays a role in maintaining dehydration of the spore protoplast. The cortical membrane (germ cell wall) is a dense inner layer of the cortex that develops into the cell wall of the emergent cell when the cortex is degraded during germination (Foster 1994). The protoplast is the location of RNA, DNA, dipicolinic acid (DPA) and most of the calcium, potassium, manganese and phosphorus in the spore (Bloomfield and Arthur 1994; Russell 1995; Saby 1999).

3.2.2 Mechanisms of Microbial Inactivation by Disinfectants

Effective disinfection requires disinfectant uptake by bacteria, subsequent transport of the sorbed disinfectants to the target sites of bacteria, and accumulation of disinfectants to damaging levels. The effect of disinfectants can also be magnified by bacterial self-destruction (autocidal) due to free radical accumulation through metabolic imbalance and impaired ionic homeostasis (Denyer and Stewart 1998). The targets of disinfectants include a range of cellular loci, such as the cytoplasmic membrane, respiratory function sites, enzymes and the genetic material (Cloete 2003). According to Denyer and Stewart (1998) , disinfection action can cause damages of different levels: “(1) disruption of the transmembrane proton motive force leading to an uncoupling of oxidative phosphorylation and inhibition of active transport across the membrane; (2) inhibition of respiration or catabolic/anabolic reactions; (3) disruption of replication; (4) loss of membrane integrity resulting in leakage of essential intracellular constituents such as potassium cation, inorganic phosphate, pentoses, nucleotides and nucleosides, and proteins; (5) lysis; (6) coagulation of intracellular material.” These lesions represent injury of increasing severity from bacteriostasis to rapid bactericidal action in order. Cell death can be caused from initial bacteriostatic damage if inactivation was maintained for sufficient duration or disinfectant dose was sufficiently high.

Disinfectants used in water treatment process are believed to produce various active oxygen species which seem to participate in the reaction with bacteria. Spin-trapping electron spin resonance (ESR) technique was used to measure unstable free radicals and it indicated the generation of hydroxyl radical in chlorination and ozonation

(Utsumi 1994; Hamada 1995). Glutathione, the predominant intracellular thiol compound in *E. coli* and many other bacteria, was found to be important in protecting bacteria against chlorination by acting as a scavenger (Chesney 1996; Saby 1999), and probably by being involved in the regulation of oxidative defense genes (Oktyabrsky 2001).

3.2.3 Resistance of Bacteria to Disinfectants

Venkobachar *et al.* (1975) demonstrated that chlorine affected the total dehydrogenase activity which closely correlated with the percent survivals of *E. coli* cells. The reaction with chlorine also inhibited the activity of succinic dehydrogenase which have sulfhydryl groups (-SH) essential for enzyme activity, indicating that the cytoplasmic membrane was affected. Chlorine treatment on *E. coli* caused the permeability changes of the membrane, cessation of phosphate uptake, and decrease in the oxygen uptake. Protein and RNA leakage were detected with chlorine doses of 1.5 mg/L, while DNA leakage was observed only at high chlorine doses (Venkobachar 1977). Haas and Engelbrecht (1980) conducted a series of experiments on *E. coli*, *Candida parapsilosis*, and *Mycobacterium fortuitum* to test their growth, UV release, TOC release, respiration, potassium uptake, thiomethyl- β -galactoside uptake, protein synthesis, DNA synthesis and Ames tests under chlorination. The results demonstrated that the lethal lesions caused by chlorine appeared to be a disruption of the cell membrane affecting cell permeability and a physical damage to the DNA of the cell.

Chloramine has relatively low reactivity as a disinfectant compared to free chlorine. Higher concentrations and longer contact times are usually needed to achieve

the same level of inactivation when applying chloramines as compared to free chlorine. Studies have suggested that chloramine might penetrate cell membranes easily and cause an internal destruction of bacterial cells, leading to a complete death rather than cell wall injury (Tosa 1995). Chloramine might lead to structural changes in the cell membrane by oxidation of thiol groups, which may allow other disinfectants to pass through and have synergistic inactivation effects (Kouame and Haas 1991; Straub 1995).

The mechanism of disinfection by ozone is different from that by chlorine. The mechanisms of ozone disinfection include: (1) direct oxidation/destruction of the cell wall with leakage of cellular constituents outside of the wall; (2) reactions with radical by-products of ozone decomposition; (3) damage to the constituents of the nucleic acids (purines and pyrimidines); and (4) breakage of carbon-nitrogen bonds leading to depolymerization (USEPA 1999). Ozone is a powerful disinfectant for virus and bacteria organisms (Roy 1981; Zhou and Smith 1994; Hunt and Marinas 1997; Hunt and Marinas 1999; Facile 2000) and can effectively inactivate *Giardia* cysts and *Cryptosporidium* oocysts which can not be killed easily by chlorine or chlorine dioxide (Roustan 1991; Gyurek 1999; Rennecker 1999; Driedger 2000; Rennecker 2000; Finch 2001; Li 2001; Corona-Vasquez 2002).

Bacterial resistance to disinfectants can be described as the temporary or permanent ability of an organism and its progeny to remain viable and/or multiply under the action of disinfectants. The mechanisms of bacterial resistance can be considered as being one of these two types: intrinsic resistance and acquired resistance. Intrinsic resistance is a natural chromosomally controlled property of a bacterial cell that enables the cell to avoid or overcome the action of a biocide. This kind of resistance is commonly

found in many Gram-negative bacteria, some Gram-positive bacteria like *Mycobacterium*, and bacterial spores. Biofilm is a kind of physiological adaptation which is considered as the modulation of the intrinsic resistance of bacteria. Acquired resistance results from genetic changes in a cell and develops either by mutation or by the acquisition of genetic material from another cell through transformation, transduction and conjugation (Russell 1995; Bower and Daeschel 1999). The activity of disinfectants depends on: (1) the external physical environment, *e.g.*, pH, temperature, presence of organic matter; (2) the nature, structure, composition and condition of the organism itself; and (3) the ability of the organism to degrade or inactivate the particular substance and convert it to an inactive form (Russell 1999).

Before reaching the target sites of bacteria, disinfectants encounter a number of structures and need to overcome physical and chemical diffusion barriers. Bacteria with effective penetration barriers usually display a higher inherent resistance, such as Gram-negative bacteria and spores. Bacteria also attempt to resist the action of disinfectants by exclusion of the active agents from the cellular loci of lethal destruction through efflux pumps and by enzyme mediated detoxification of the active agents (Russell 1995; Heinzl 1998; Cloete 2003). Bacteria populations can change their resistance by genetic adaptation in natural environment.

Growth conditions such as growth medium, temperature, pH, and other environmental factors may greatly influence the resistance of bacterial to disinfectants. Berg *et al.* (1982) studied the disinfection of *E. coli* by chlorine dioxide using cells grown in batch culture and in a chemostat with varied parameters. They demonstrated that the sensitivity of *E. coli* is markedly influenced by the qualitative nature of the growth

environment, degree of nutrient limitation, temperature, and density of the culture. The results showed that populations grown under conditions that more closely approximated natural aquatic environments were more resistant than those grown under commonly employed batch culture conditions in the lab. Also the bacteria grown at submaximal rates were more resistant than their counterparts grown at the maximal rates. Growth at 15°C led to greater resistance than did growth at 37°C. Low cell density during growth was conducive to enhanced resistance. They hypothesized that a population growing more rapidly had more easily damaged active substrate transport systems or genetic material. Matin and Harakeh (1990) reviewed the effect of starvation on bacterial resistance to disinfectants and concluded that non- or slowly-growing bacteria, such as those found in most natural environments, were more resistant to disinfectants than their lavishly-grown counterparts. Many studies demonstrated that the nature of growth-limiting nutrients and the specific growth rate of bacteria can significantly influence the structure and composition of their envelope (cell wall and outer membrane), thus influence their exclusion resistance mechanisms and the expression of outer-membrane proteins (Dean 1972; Gilbert and Brown 1978; Gilbert and Brown 1980; Sterkenburg 1984).

The growth phase is another important factor influencing bacteria resistance. Regulated by the signal of starvation, bacteria enter into stationary phase from exponential growth phase. The shift from exponential to stationary phase not only causes morphological and physiological changes of cells such as cell division leading to formation of short minicells as well as metabolic changes but also induces the expression of many distinct genes responding to various environmental stresses including oxidative

stress, thus increases bacteria resistance (Sitnikov 1996; Zambrano and Kolter 1996; Jorgensen 1999; Hengge-Aronis 2000; Lazazzera 2000; Whiteley 2000).

3.2.4 Quorum Sensing

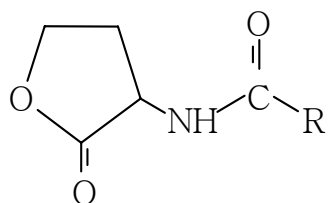
Quorum sensing is a cell density dependent gene regulation process that allows bacterial cells to express certain or specific genes only when they reach high cell density. The studies on quorum sensing started from the density-dependent expression of bioluminescence in the marine symbiotic bacterium *Vibrio fischeri* (Nealson 1970) and expanded to many processes regulation including growth, antibiotic production, virulence expression, conjugation, biofilm development, increased resistance in stationary phase, genetic competence, and sporulation in many species of bacteria (Lazazzera and Grossman 1998; Lazazzera 2000). The study by Surette and Bassler (1998) demonstrated that the quorum-sensing signal in *E. coli* and *Salmonella typhimurium* has the functions of allowing the cells to communicate their growth phase and the metabolic potential of the environment with each other.

Quorum sensing occurs at high cell density in many microorganisms (such as *E. coli* and *B. subtilis*) and modulates both intra- and inter-species cell-cell communications (Bassler 1999). It involves the production and detection of extracellular signaling molecules called autoinducers. The bacterial transition into stationary phase is regulated by quorum sensing and mediated by the produced signal stimulated by starvation (Lazazzera 2000). Such signal cannot be detected by bacteria that are present at low population densities. Only when the bacteria are at relatively high densities or are within

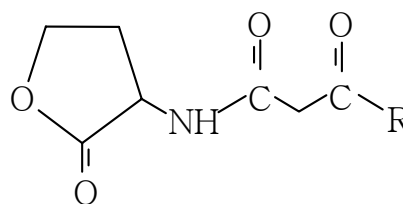
a confined environment can the signal accumulate to the concentration required for corresponding gene activation. Both Gram-negative and Gram-positive bacteria have their own cell-to-cell communication languages.

3.2.4.1 Gram-negative Bacterial Communication

In most Gram-negative bacteria, a particular subset of signaling molecules named acylated-homoserine lactones (HSL) are used by bacteria themselves to detect the relative number of bacteria within their own population. HSLs are soluble and diffusible molecules. The structures of two typical types of HSL signal molecules are shown in Figure 3-3, where 'R' stands for their acyl side-chain moiety with various length and degree of saturation (Zambrano and Kolter 1996; Gray 1997; Holden 2000; Michels 2000; Morin 2003). Specific HSL autoinducers diffuse passively across the bacterial membrane after being produced by autoinducer synthase protein I in response to the environmental stress. These signals cannot be detected by bacteria that are present at low population densities. Upon reaching the critical concentration, the autoinducer is bound by its cognate transcriptional activator protein R. Then the complex activates transcription of the target genes (Gray 1997; Bassler 1999). Various I/R systems have been reported in quorum sensing regulations of Gram-negative bacteria such as LuxI/LuxR in *Vibrio fischeri* and *Vibrio harveyi* (Fuqua 1994), SolI/SolR in *Ralstonia solanacearum* (Flavier 1997), LasI/LasR and RhII/RhlR in *Pseudomonas aeruginosa* (Glessner 1999).



N-Acylhomoserine Lactones



N-3-Oxoacylhomoserine Lactones

Figure 3-3 The Molecular Structures of Two Typical HSL Signal Chemicals**3.2.4.2 Gram-positive Bacteria Communication**

Different from Gram-negative bacteria, Gram-positive bacteria secrete processed peptide signaling molecules usually via a dedicated ABC (ATP-binding cassette) exporter protein. The peptide signals are recognized by cognate two-component sensor kinase proteins that interact with cytoplasmic response regulator proteins. In *B. subtilis*, two processed peptide signals, ComX and CSF (competence and sporulation factor), enable the bacteria to switch between competence for DNA uptake and sporulation. ComX pheromone can activate the ComP/ComA two-component system. CSF imported by an ABC transporter can promote competence development at low concentration and induce sporulation at high concentration (Lazazzera and Grossman 1998; Bassler 1999). In *B. subtilis*, Spo0A and RNA polymerase sigma factors (σ^A , σ^E , σ^F , σ^G , σ^H , σ^K) are the transcription factors responsible for the activation and expression of sporulation genes. σ^A and σ^H are the principal sigma factors which appear during all the stages of growth

and sporulation. Other alternative specific sigma factors appear sequentially during sporulation (Fujita and Sadaie 1998).

3.2.4.3 Inter-species Communication

In general, each bacterial species produces and responds to a unique autoinducer signal (AI-1) in intra-species communication. However, a type of autoinducer AI-2 has recently been discovered to function as a universal signal for inter-species communication related to cell-population density (Chen 2002; Xavier and Bassler 2003). Both Gram-negative and Gram-positive bacteria can produce, sense, and respond to AI-2 with the existence of the same gene *luxS*. AI-2 molecule is a novel furanosyl borate diester with no similarity to those autoinducers described previously (Figure 3-4) (Chen 2002). AI-2 controlled genes have been identified in many species of bacteria and in most cases related to virulence control (Anand and Griffiths 2003).

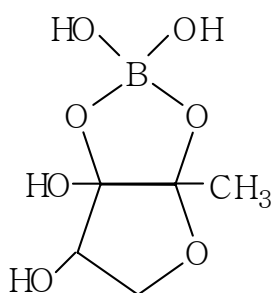


Figure 3-4 The Molecular Structure of Autoinducer AI-2

3.2.4.4 Genetic Control of Bacterial Resistance to Oxidative Stress

Bacteria have evolved sophisticated molecular mechanisms to monitor oxidant levels and to activate antioxidant defense genes. Antioxidant defense genes, such as *rpoS*, *oxyR* and *soxR*, can regulate the synthesis of molecules that protect cells from oxidative stresses (Storz 1990; Eisenstark 1998; Datta and Benjamin 1999; Kobayashi and Tagawa 1999; Storz and Imlay 1999; Pomposiello and Demple 2001).

In many Gram-negative bacteria like *E. coli* and *Pseudomonas aeruginosa*, σ^s , a sigma subunit of RNA polymerase encoded by *rpoS* gene, is believed to be a master regulator in the global gene expression responding to various environmental stresses mainly when cells are in stationary phase. σ^s is found to regulate more than 50 genes, many of which are involved in the oxidative stress response including *xthA* (encodes exonuclease involved in DNA repairs), *dps* (prevent formation of hydroxyl radicals), *katG* and *katE* (encodes catalases HPI and HPII), *gor* (encode glutathione reductase), *sodC* (encodes periplasmic superoxide dismutase) (Arnold and Kaspar 1995; Hengge-Aronis 2000; Whiteley 2000). It is also found to perform transcription of some genes related to cell morphology, membrane transport functions, and synthesis of additional cell components needed for survival during long and harsh periods of dormancy (Eisenstark 1998). Earlier studies indicated that *rpoS* expression was induced by HSL production (Huisman and Kolter 1994; Latifi 1996). Even though conflicting data were reported in recent studies showing that *rpoS* was not or probably only weakly controlled by quorum sensing, *rpoS*-transcribed genes might still be subjected to quorum sensing regulation (Sitnikov 1996; Baca-DeLancey 1999; Surette 1999; Hengge-Aronis 2002). In *P.*

aeruginosa, a relationship was indicated to exist between RpoS and quorum sensing and RpoS appeared to regulate the second quorum sensing system Rhl (Whiteley 2000).

3.2.4.5 Cell Density-Dependent Resistance of Bacteria to Oxidative Stress

Virus density has been reported to have an influence on inactivation. The batch and continuous flow studies conducted by Majumdar *et al.* (1973) demonstrated that poliovirus density played a part in ozonation. For batch experiments, they incorporated the poliovirus density into a general equation which was referred as the Power Law model today to express the inactivation rate in triple distilled water and primary and secondary wastewaters. The order of reaction with respect to virus density was 2.32. The data from the continuous flow studies was found to agree very well with the batch data. But not enough data was obtained to develop a defined relationship for continuous flow studies.

Roy *et al.* (1981) considered the effect of virus density on viral inactivation by ozone in demand-free buffered water using a continuous flow, completely-mixed reactor. They also used the Power Law model to describe ozone inactivation of Poliovirus. The average value of the order of reaction with respect to the density of virus was found to be 0.69 at constant temperature and pH conditions.

Bacterial density might also play a role in disinfection. It appears that bacteria have a way to communicate with each other and respond to the presence of other cells. Starvation will give bacteria a signal for entering into stationary phase from exponential

phase. Bacteria also show some cell density-dependent phenomena either in exponential phase or stationary phase.

Studies showed that initial microbial density had effects on microbial resistance to different kinds of environmental stresses. Glutathione plays a role as the intracellular thiol antioxidant in protection against oxidative stress (Chesney 1996; Saby 1999). When using glutathione-depleted Chinese hamster fibroblasts (HA1), increase of the cell density will result in the increase of the clonogenic cell survival after exposure to *NO*-containing medium. The results suggest that there is some non-glutathione-dependent mechanism(s) which can provide collective protection related to the total cell population (Walker 1995). The investigation by Crockford *et al.* (1995) found that the induction and subsequent repression of catalase activity of *Rhizobium leguminosarum* in exponential cultures is a cell-density-dependent phenomenon with maximum catalase activity at low initial cell density. It was proposed that catalase activity was repressed by the accumulation of an extracellular component in late-exponential phase. The cell density dependence of stationary-phase survival of *R. leguminosarum* under starvation was investigated and it turned out to be that high-density cultures survived with little or no loss of viability than low-density cultures and extracellular signal molecules has been involved (Thorne and Williams 1999). Datta and Benjamin (1999) studied the acid resistance of *E. coli* O157:H7 and found that stationary phase cells at low concentration were much more acid resistant than cells at high concentration. This phenomenon was not observed with exponential phase cells, *rpoS* mutant in stationary phase, and Gram-positive organisms. The experiments suggested that stationary phase cultures of *E. coli*

cells produced a substance which can enhance cell acid sensitivity at high concentration and depends on *rpoS*.

In the previous studies using batch systems conducted at Drexel University by Kaymak (2001; 2003), monochloramine and ozone were used separately to disinfect *E. coli* in exponential and stationary phase, *B. subtilis* vegetative cell in exponential phase, *B. subtilis* spores, and *Giardia muris* cysts. Initial concentration of microorganisms was demonstrated to be a statistically significant factor on inactivation of *E. coli* in stationary phase by monochloramine and inactivation of *G. muris* cysts by ozone. Both *E. coli* in stationary phase and *G. muris* cysts at high initial microbial concentration were found to be more sensitive to the disinfectants than which at low initial microbial concentration. This effect was not observed in the other cases. The results indicated that the effect of initial microbial density on disinfection might be microorganism-type dependent and also growth phase dependent.

3.3 Review on Disinfection Kinetic Models

Disinfection efficiency is usually expressed as log inactivation. Microorganisms undergoing disinfection have displayed different shapes in their survival curves (Figure 3-5). The studies on disinfection kinetics models started from Chick (1908) who first noticed the similarity between a chemical reaction and some disinfection reaction. She developed the model which was called the Chick model today to describe the most simple exponential kill curve. However, disinfection reactions are not simple bi-molecular, elementary reactions and can not be fully described by the simplest model in many cases.

More sophisticated models were developed to illustrate the deviations from exponential kill phenomena such as curves with a shoulder, curves with a tailing-off, and curves with both shoulder and tailing-off. Shoulders might be caused by inadequate mixing, clumps of microorganisms, and/or multiple targets necessary for inactivation (Hiatt 1964). Tailing off phenomena could be explained by the decay of disinfectant with contact time and the presence of several distinct subpopulations with varying resistance to a disinfectant (Cerf 1977).

Five most commonly used disinfection models are Chick, Chick-Watson, Hom, Power Law, and Hom Power Law model. These models can be derived from the following differential rate law:

$$\frac{dN}{dt} = -kmN^xC^n t^{m-1} \quad 3-15$$

where $\frac{dN}{dt}$ is the rate of inactivation; N is the number of survival bacteria at contact time t ; k is the reaction rate constant found experimentally; C is the concentration of the disinfectant; and m , n , and x are empirical constants.

Other different models have also been developed to fit the curves with a shoulder, curves with a tailing, and sigmoidal curves (Hiatt 1964; Severin 1984; Xiong 1999).

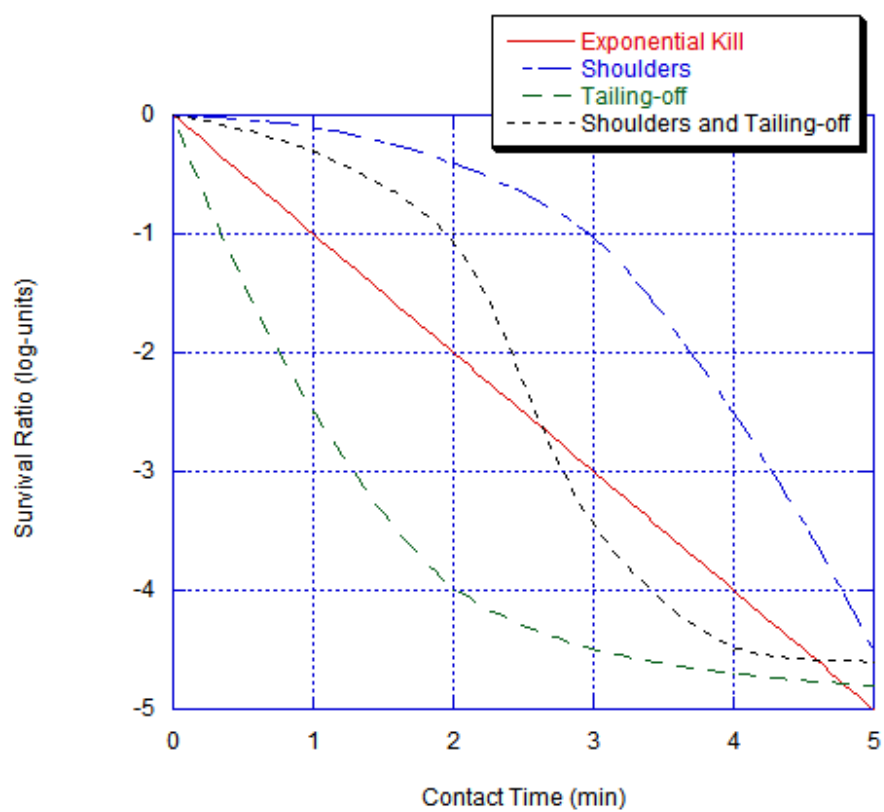


Figure 3-5 Microbial Survival Curves under Disinfection

3.3.1 Chick Model

Chick (1908) first noticed the analogy between a chemical reaction and disinfection. She suggested that disinfection could be expressed as a rate law similar to a chemical reaction in the following manner

$$r = \frac{dN}{dt} = -kN \quad 3-16$$

where r is the inactivation rate (organisms killed/volume-time); and k is the rate constant (time^{-1}). In a batch system, this kinetics results in an exponential decay in organisms.

3.3.2 Chick-Watson Model

Watson (1908) proposed that k is related to the disinfectant concentration C by

$$k = k' C^n \quad 3-17$$

where n is referred as the coefficient of dilution; k' is the pseudo first-order reaction rate constant (time^{-1}) and is assumed to be independent of disinfectant concentration and microorganism concentration.

In a batch system and assuming no disinfectant decay, the integration of Chick-Watson model yields

$$\ln \frac{N}{N_0} = -k' C^n t \quad 3-18$$

where N and N_0 are the concentrations of viable microorganisms at time t and time 0.

Watson also proposed an empirical logarithmic function to account for the effect of different disinfectant concentration

$$C^n T = \text{constant} \quad 3-19$$

where T is the time required to achieve a given level of inactivation. If $n < 1$, the contact time is more important; if $n > 1$, the disinfection dose is more important; if $n = 1$, the model is referred as the simple Chick-Watson model.

CT products derived from the simple Chick-Watson model has been widely used in disinfection system based on laboratory inactivation studies. The CT values for 99% inactivation were commonly used for the comparison of disinfectant efficiency for a specific microorganism.

The Chick-Watson model has been used to sufficiently describe the inactivation behavior of chlorine in homogeneous bacterial populations (Haas and Karra 1984) and ozone to *E. coli* (Zhou and Smith 1994).

3.3.3 Hom Model

Hom (1972) developed a flexible model to describe the curvilinear relationship between bacteria survival ratio and disinfectant contact time:

$$\frac{dN}{dt} = -k' m N C^n t^{m-1} \quad 3-20$$

Integration of this rate law with constant C gives

$$\ln \frac{N}{N_0} = -k' C^n t^m \quad 3-21$$

In the case of $m = 1$, the Hom model is simplified to the Chick-Watson model. The survival curve displays an initial shoulder when m is greater than unity and tailing-off when m is less than unity.

For continuous-flow system or a dynamically changing batch system, the batch kinetics can not be applied directly in the original form because of the change in concentration with time and varying hydraulics. Another form of Hom model was derived from the above expression (Haas 1995).

$$r = -mN(k' C^n)^{\frac{1}{m}} \left[-\ln \left(\frac{N}{N_0} \right) \right]^{\left(1 - \frac{1}{m}\right)} \quad 3-22$$

where r represents the number of organisms inactivated per unit volume per unit time.

Previous studies have demonstrated that the Hom model can give satisfactory fitting to data on inactivation of *Giardia* (Anmangandla 1993), *Cryptosporidium* (Driedger 2000), aerobic spore forming bacteria (Barbeau 1999), and HPC (heterotrophic plate count) bacteria (Pernitsky 1995).

3.3.4 Rational Model (Power Law Model)

A ‘rational’ model has been used to describe ozone inactivation of virus in a batch system (Majumdar 1973) and in a continuous flow system (Roy 1981). It can be written as

$$\frac{dN}{dt} = -k' C^n N^x \quad 3-23$$

which is the generalized rate law for $m = 1$ and can be simplified to Chick-Watson model with $x = 1$. Integration of this equation under demand free conditions (C, k' constant) results in the following relationship

$$\ln \frac{N}{N_0} = -\frac{1}{x-1} \ln \left[1 + (x-1)k' C^n t N_0^{x-1} \right] \quad 3-24$$

The rational model can describe shoulder ($x < 1$) and tailing-off ($x > 1$) phenomena. It can also describe the effect of initial microbial density on disinfection. If $x > 1$, the survival ratio will decrease with increasing of N_0 under the same disinfection conditions; and conversely if $x < 1$.

3.3.5 Hom Power Law Model

This generalized model was developed by combining the Hom model and the Rational model and incorporating the parameters of both models (k, m, n and x) (Anotai 1996).

$$\frac{dN}{dt} = -mk' C^n t^{m-1} N^x \quad 3-25$$

Upon integration, it can be expressed as

$$\ln \left(\frac{N}{N_0} \right) = -\frac{1}{x-1} \left[1 + N_0^{x-1} (x-1)k' C^n t^m \right] \quad 3-26$$

The Hom Power Law model can also be expressed as

$$r = -mk' C^n N^x \left\{ \frac{\left[\left(\frac{N}{N_0} \right)^{(1-x)} - 1 \right] N_0^{(1-x)}}{(x-1)k' C^n} \right\}^{\left(\frac{1}{1-x} \right)} \quad 3-27$$

This model may provide a somewhat better fit than the above models. However, since it has more parameters, it would be used as the best fit model only if it showed significant improvement over those models mentioned above.

3.3.6 Series-event Model

In the series-event model, the inactivation of a single organism can be idealized as occurring in a series of damaging reactions that occur in integer steps. The rate at which an organism passes from one event level to the next is assumed to be first order with respect to the disinfectant concentration and independent of the event level. There is a threshold n above which organisms are inactivated, and below which the organisms survive (Severin 1983).

For a batch reactor, the rate at which organisms pass through event level i is given by

$$r_{n_i} = kCN_{i-1} - kCN_i \quad 3-28$$

where N_i is the number of organisms which have reached event level i .

Solving from $i = 0$ to $i = n-1$ gives the expression of survival ratio in the series-event model

$$\ln \frac{N}{N_0} = -kCt + \ln \left(\sum_{i=0}^{n-1} \frac{(kCt)^i}{i!} \right) \quad 3-29$$

where i is the event level, and n is the number of events the organism must sustain prior to death.

3.3.7 Multiple Target Model

The basic assumption of multiple-hit theory is that each particle (organism or clump of organisms) contains n identical, critical targets. All of them must be hit once and destroyed to kill the organism (Hiatt 1964). Since the number of targets is finite, the probability of attaining the next hit is decreased as the reaction proceeds (Severin 1983). This model was first developed for irradiation studies on microorganisms and was then used to explain initial shoulders in survival curves of disinfection.

For a closed-batch reactor, the rate of attaining the i th hit in a particle r_{N_i} is

$$r_{N_i} = (n_c - i + 1)kCN_{i-1} - (n_c - i)kCN_i \quad 3-30$$

where k represents the inactivation rate constant with unit $[L/mg-s]$; n_c is the targets number contained in a particle; $(n_c - i + 1)$ and $(n_c - i)$ are probability factors accounting for the increased difficulty or specificity in hitting remaining targets as the reaction proceeds.

The probability of inactivating a specific target is $(1 - e^{-kCt})$ and the probability of survival of a particle with n_c critical targets is given by

$$\ln \frac{N}{N_0} = \ln \left[1 - (1 - e^{-kCt})^{n_c} \right] \quad 3-31$$

3.3.8 Modified Multiple Target Model

Based on the same assumptions as the Multiple Target model, the Modified Multiple Target Model was developed to describe non-first order kinetics of the destruction rate of particles and can be expressed as

$$\ln \frac{N}{N_0} = \ln \left[1 - \left(1 - e^{kC^n t} \right)^{n_c} \right] \quad 3-32$$

This model returns to the Multiple Target model at $n = 1$. It was first applied to describe the disinfection behavior of ozone on *B. subtilis* spores and had better fit than the other commonly used models (Kaymak 2003).

In continuous flow system, this model can be expressed as

$$r = -kn_c C^n N_0 \left[1 - \left(1 - \left(\frac{N}{N_0} \right)^{\frac{1}{n_c}} \right)^{n_c} \right] \left[\left(1 - \left(\frac{N}{N_0} \right)^{\frac{1}{n_c}} \right)^{\frac{n_c-1}{n_c}} \right] \quad 3-33$$

3.4 Prior Research on Using CSTR (Continuously Stirred Tank Reactor) to Perform Disinfection

The SWTR requires that all surface water treatment facilities provide adequate filtration and disinfection in order to achieve a 99.9% removal-inactivation of *G. lamblia* cysts and a 99.99% removal-inactivation of enteric viruses. Assuming 2.5-log removal of *Giardia* and 2-log removal of viruses through effective filtration by the SWTR, disinfection was required for the remainder of the removal-inactivation. 2-log removal of

Cryptosporidium is required by the IESWTR (Interim Enhanced Surface Water Treatment Rule) for systems that filter (USEPA 1998b).

The concept of the “CT” value was proposed by EPA to assure the attainment of primary disinfection at a minimum cost. It is defined as the product of the concentration of residual disinfectant C (mg/L) multiplied by the time T (minute), during which the disinfectant is present. The CT tables of the SWTR’s Guidance Manual (USEPA 1991) were mostly derived from laboratory studies conducted in buffered demand-free water which may be difficult to extrapolate to actual waters. And a simple Chick-Watson relationship for the inactivation was assumed even though the kinetics of microorganism disinfection was more complex. USEPA also used the t_{10} value (the time for 10 percent of the tracer mass to achieve breakthrough) as a conservative measure of contact time in implementing the CT guidance in continuous flow systems. This approach was based on a plug flow model which only crudely accounts for nonidealities in flow. Besides, SWTR also allows utilities to perform pilot-scale studies to demonstrate the effectiveness of their disinfection systems, which perhaps too expensive to conduct for smaller utilities.

Knowing the tracer information for a given reactor and the kinetic data for a batch system, it is possible to predict the disinfection behavior of continuous flow system (Trussell and Chao 1977; Selleck 1978; Nauman and Buffham 1983; Haas 1988; Haas 1998; Levenspiel 1999).

3.4.1 Continuous Flow System

There are two ideal continuous flow reactors with two limiting conditions of flow patterns: plug flow reactor (PFR) and continuously stirred tank reactor (CSTR). In a PFR, flow is assumed to be sufficiently turbulent such that the axial fluid velocity is uniform throughout any cross section, and elements of fluid are assumed to proceed through the reactor in an orderly and consistent manner. In a CSTR, the contents are completely mixed with an infinite amount of dispersion and the concentration is uniform throughout the volume. In reality, nonideal reactors with flow patterns between these two ideal conditions exist, and mass transport occurs by a combination of dispersion and advection (Levenspiel 1999).

It has been realized that a PFR is the most efficient reactor in disinfection facilities. And a CSTR is probably the poorest possible configuration for efficient disinfection. However a large number of CSTRs in series will approach the performance of a perfect plug flow reactor (Trussell and Chao 1977).

3.4.2 Predicting Disinfection Performance in Continuously Stirred Tank Reactor from Batch Data

Mixing of fluids during reaction is important for extremely fast reactions in homogeneous systems.

Two limiting circumstances can be assumed when calculating the degree of reaction in continuous flow reactor (Danckwerts 1958):

(1) “Completely segregated fluid or macrofluid: the incoming fluid is broken up into discrete fragments or streaks which are small compared to the tank and uniformly dispersed in it, but in which molecules entering together remain together indefinitely;”

(2) “Maximum micromixing fluid or microfluid: the inflowing material is dispersed on the molecular scale in a time much less than the reactor mean residence time; the environment of any particular molecule does not tend to contain an excess of molecules which entered at the same time as itself and the mixture is chemically uniform.”

3.4.2.1 Segregated Flow Reactor

The segregated flow model is used widely in chemical reactor and process engineering to deal with nonideal hydrodynamic behavior of real reactors. In the segregated flow or late mixing model, fluid elements of different age remain segregated and aggregates of molecules travel together until they exit a reactor. The fraction of bacteria remaining after disinfection will be the sum of the batch reactions of all small aggregates. So it is possible to predict performance of continuous flow system from batch disinfection kinetics and the hydraulic characteristics of the continuous flow system (Nauman and Buffham 1983; Levenspiel 1999).

With the same initial disinfectant dose, the inactivation in a continuous flow reactor can be computed by

$$S_{continuous} = \int_0^{\infty} E(t) S(t)_{batch} dt \quad 3-34$$

where $S_{continuous}$ is the predicted survival ratio in continuous flow reactor; $S(t)_{batch}$ is the batch survival ratio at time t ; and $E(t)$ is the normalized density function for residence time distribution (Haas 1995).

This approach was first applied to the design of chlorine contact facilities by Trussell and Chao (1977). Selleck *et al.* (1978) found that by using this approach, the disinfection results of the CSTR and batch experiments were consistent. Haas (1988) compared the disinfection effect between segregation flow prediction and maximum micromixing flow prediction and indicated that the effect of micromixing becomes particularly important at high degrees of inactivation. In other studies (Haas 1995; Haas 1998), experiments were conducted in both batch reactor and pilot plants with the same source water. Free chlorine, preformed monochloramine, and ozone were used to disinfect *E. coli*, *G. muris*, and bacteriophage MS2. The disinfection performance in dynamic systems was predicted by using batch kinetics and hydraulic characterization of pilot plants and compared with actual inactivation in pilot scale processes. The results demonstrated that it is possible to estimate the inactivation in continuous flow system by using the information obtained from laboratory batch systems. Roustan *et al.* (1991) compared two possible approaches for determination of *Giardia* cysts inactivation by ozone in continuous flow systems. One approach is based on the hydrodynamics data and the concept of CT value. The other is to predict the inactivation rate by integrating the inactivation kinetics and the hydraulic characteristics of the reactor into a mathematical model (segregated flow model, kinetics-and-hydraulics model). The difference in contact time values obtained by these two approaches was found to be very significant when high inactivation efficiency (3- to 4- logs) was required and the hydraulic behavior of the

reactor was close to that of a CSTR. In such a condition, the author suggested that the kinetics-and-hydraulics approach should be used since it gave more conservative prediction of the contact time needed. Chiu *et al.* (1999) employed the segregated flow model into UV disinfection system and modified it by incorporating UV dose.

3.4.2.2 Completely Mixed Flow System

The material balance equation in a completely mixed flow system is

$$QN_0 - QN + rV_R = V_R \frac{dN}{dt} \quad 3-35$$

where Q is the volumetric flow rate; V_R is the volume of the reactor; r is the inactivation rate; N_0 and N are the inlet bacterial concentration and the outlet bacterial concentration correspondingly.

Under steady-state conditions the accumulation is zero, and

$$\frac{N}{N_0} = 1 + \frac{r\tau}{N_0} \quad 3-36$$

where τ is the mean hydraulic residence time (HRT) and equals to the mean residence time θ in an ideal CSTR.

In well-mixed reactor which is a CSTR, a batch kinetic model can be applied in the above equation to compute the inactivation in CSTR. Farooq *et al.* (1977) used the Chick-Watson model to examine the influence of temperature and U.V. light on disinfection with ozone in two laboratory-scale, continuous flow systems. Roy *et al.* (1981) applied the Power Law model in a continuous flow, completely mixed reactor to access the kinetics of enteroviral inactivation by ozone. In another study, three kinetic

models (Chick-Watson model, Resistant Fraction model which considered both the induced resistance and the intrinsic resistance, and Series-event model) were tested to predict the inactivation process of *E. coli* by chlorine and monochloramine in a CSTR from batch data. The predictions were consistently lower in inactivation compared to the observed data and indicated more modeling efforts needed to obtain good prediction of a disinfection process in a CSTR from batch analysis (Kouame 1990). Five models were used to fit to the experimental data of *E. coli* inactivation by ozone obtained from a completely mixed reactor using statistical approaches by Zhou and Smith (1994). The study showed that the comprehensive models developed therein and the Chick-Watson model were adequate in predicting the bacterial survival.

Zwietering (1959) developed a performance expression for maximum mixed flow or early mixing microfluid. He introduced the concept of the life expectation λ which is defined as the time a molecule will spend in the system from a specified time until its leave. The expression can be written as

$$\frac{dN}{d\lambda} = r + \frac{E(\lambda)}{1 - F(\lambda)}(N - N_0) \quad 3-37$$

where r is the disinfection kinetics in batch reactor. The boundary condition of this expression is

$$\begin{cases} \lambda = \infty, \frac{dN}{d\lambda} = 0 & \text{at inlet} \\ \lambda = 0 & \text{at outlet} \end{cases} \quad 3-38$$

To solve the equation numerically, it is necessary to choose an estimated value of λ which is three or four times the mean residence time, and then integrate from zero to λ

(decreasing λ by small steps). For first order reaction, it was found that the expression of survival ratio was the same as obtained by using the segregated flow model and the inactivation was only dependent on the RTD. In an ideal CSTR, Equation 3-37 has the same expression with Equation 3-36. For a first-order reaction, Equation 3-37 can be converted to the same form as that has been found by segregation model (Equation 3-34).

Chapter 4 : Experimental Materials and Methods

4.1 Experimental Material

4.1.1 Laboratory Apparatus Preparation

Autoclave

AMSCO autoclave (American Sterilizer Co., Erie, PA) was used to sterilize all the solutions, media, and glassware for disinfection at 121°C for 15 minutes. Autoclave tape was used to check the success of sterilization.

Centrifuge

IEC clinical centrifuge (model Clinical Centrifuge, $r=7.5cm$, International Equipment Co., Needham Hts., MA) was used to wash and prepare microorganism suspension.

Colony Counter

Quebec Darkfield colony counter (Model 3325, Cambridge Instruments Inc., Buffalo, NY) was used to count the colonies on culture dishes after incubation.

Conductivity Meter

VWR digital conductivity meter (Model 2052, VWR Scientific Inc.) was used for conductivity measurement in tracer tests.

Filtration Units

The filter holding assembly (Gelman Sciences, Ann Arbor, MI) is a seamless funnel held in place by magnetic force. The design permits the membrane filter to be held securely on the porous plate of the receptacle without mechanical damage and allow all fluid to pass through the membrane during filtration. The assembly was autoclaved at 121°C for 15 minutes with top open portion covered tightly with aluminum foil and stored at 4°C before each experiment.

Flowmeter

Riteflow flowmeters (Bel-art Products, Inc., Pequannock, NJ) were used to control the flow rates of the liquids into the reactor. One flowmeter with Teflon body was used for ozone flow control.

Forceps

Smooth-tipped forceps without corrugation on the inner side of the tips were used to remove the filters from the filtration units after filtration and place the filter on culture dishes.

Glassware

All of the glassware was cleaned using Alconox detergent (Alconox, Inc., New York, NY) and rinsed in Milli-Q water.

All of the glassware used for disinfection experiments was sterilized at 121°C for 15 minutes.

Glass Tubes

Fisher glass tubes (150 mm x 16 mm) were capped and used as dilution tubes and slant tubes.

Incubator

Precision mechanical convection incubator (Model 4EM, Precision Scientific Inc., Chicago, IL) was used to incubate *E. coli* at 37±0.5°C and *B. subtilis* at 35±0.5°C with a high level of humidity.

VWR low temperature incubator (Model 2020, VWR Scientific Inc.) was used to store microorganisms, petri dishes, and solutions at 4°C.

Membrane Filter

Pre-sterilized, 47 mm GN-6 grid with 0.45 µm pore membrane filters (Gelman Sciences, Ann Arbor, MI) were used in the experiments.

Milli-Q Water System

A Milli-Q water system (Millipore Intertech., Bedford, MA) was used to generate all the water used in the laboratory. The process includes distillation, ion exchange, activated carbon adsorption, and membrane filtration.

Motor

Emerson motor (Model SA55NXGTE-4870, St. Louis, MO) was used to create partial vacuum for membrane filtration.

Multistirrer

Scinics Multistirrer (Model MC-303, Scinics Co., LTD., Tokyo, Japan) was used to provide the mixing in the reservoirs.

Ozone Generator

Polymetrics ozone generator (Model T408, Polymetrics Inc., Colorado Springs, Co.) was used to generate ozone gas for ozone disinfection on *B. subtilis* spores.

Petri Dishes

Gelman petri dishes (50 mm x 9 mm) and Millipore Petri dishes with pad (50 mm x 9 mm) were used to prepare the culture dishes for incubation of *E. coli* and *B. subtilis* using aseptic procedures.

pH Meter

Accumet pH meter (Model 25, Dever Instrument Co., LTD., Norfolk, UK) was used for pH measurement in the laboratory.

Pipettes

Sterile disposable pipettes were used for sampling and preparing dilution series.

Shaker

Orbit Environ-shaker (Model 3527, Lab-line Instruments Inc., Melrose Park, IL) was used to incubate microorganism in exponential phase with gentle shaking at 160 *rpm*.

Spectrophotometer

Turner digital spectrophotometer (Model 340, Barnstead/Thermolyne Co., Dubuque, IA) was used to measure concentration of chlorine and monochloramine at 515 *nm*, optical density of microbial suspension at 660 *nm*, and ozone concentration at 600 *nm*.

Stirrer

Labo stirrer (Model LR400C, Yamato Scientific Co., LTD., Tokyo, Japan) was used to provide the mixing in the CSTR reactor at 1000 *rpm*.

Water Bath

Precision water bath (Model 185, Precision Scientific Inc., Chicago, IL) was used to kill *B. subtilis* vegetative cells and activate spore germination at 75°C. The spore suspension and the samples were held in the water bath for 15 minutes for pasteurization.

Techne refrigerated bath (Model RB-12, Techne Inc., Princeton, NJ) was used to control the temperature of the CSTR system to be $15\pm 2^\circ\text{C}$.

4.1.2 Solution Preparation

Laboratory Water

The water used in the laboratory (conductivity of 18.2 MΩ) was produced by a Milli-Q water system.

Experimental Buffered Water

The experimental buffered water was prepared by adding 0.54 g/L of disodium hydrogen phosphate (Na_2HPO_4) and 0.884 g/L of potassium dihydrogen phosphate (KH_2PO_4) in Milli-Q water. Then it was adjusted to a pH of 7 or 8 with 1 N of NaOH .

The experimental buffered water was used as the matrix of disinfection reaction.

Dilution Water

Stock phosphate buffer solution was prepared by dissolving 34 g of potassium dihydrogen phosphate (KH_2PO_4) in 500 mL of Milli-Q water. It was adjusted to pH 7.2 ± 0.5 with 1 N of sodium hydroxide ($NaOH$) and diluted to 1 L with Milli-Q water.

Dilution water was prepared by adding 1.25 mL of stock phosphate buffer solution and 5 mL of magnesium chloride solution (81.1 g $MgCl_2 \cdot 6H_2O$ /L Milli-Q water) to 1 L of Milli-Q water. It was dispensed in amounts providing 9 ± 0.2 mL after autoclaving for 15 minutes.

The phosphate buffered dilution water was used for dilutions of organisms prior to plating in order to get better plate counts after incubation according to standard methods (APHA 1995). Bacteria were suspended in dilution water no more than 30 minutes at room temperature to avoid death or multiplication.

Demand Free Water

Chlorine Demand-free Water: Chlorine demand-free water was prepared from Milli-Q water by adding a sufficient quantity of stock chlorine solution to give 5 mg/L of free chlorine. After standing for two days, the solution should contain at least 2 mg/L of free chlorine. The remaining free chlorine was removed by irradiating the container with an ultraviolet lamp or placing it in direct sunlight.

Monochloramine Demand-free Water: The Milli-Q water has been tested for monochloramine demand and no significant demand of monochloramine was found.

Ozone Demand-free Water: Ozone demand-free water was prepared by bubbling ozone through Milli-Q water for 20 to 40 minutes to achieve at least 2 mg/L of ozone. The solution was allowed to stand for 60 minutes and then boiled.

Stock Chlorine Solution

A stock chlorine solution was prepared by bubbling chlorine gas into a weak alkaline solution to obtain a concentration of 150 ± 10 mg/L. The alkaline solution was prepared by the addition of 0.1 M sodium hydroxide (*NaOH*) to Milli-Q water to raise the final pH to at least 8.0. The chlorine solution was stored in a brown glass container under dark refrigerated conditions and discarded when the free chlorine concentration decreased below 140 mg/L.

Ammonium Chloride

A stock phosphate buffer solution was prepared by dissolving 34 g of potassium phosphate (KH_2PO_4) in 500 mL of Milli-Q water and the pH was adjusted to 8.0 with 1N of *NaOH*. Then it was diluted to 1 L with Milli-Q water.

A stock ammonium chloride solution of 150 mg/L was prepared by the addition of 150 mg of NH_4Cl to 1 L of stock phosphate buffer solution. The solution was stored in a brown glass container under dark refrigerated conditions.

Stock Monochloramine Solution

The preformed monochloramine solution was prepared daily as needed by mixing equal volumes of chlorine solution and ammonium chloride solution at a 3:1 ($Cl_2:N$) weight ratio and stirred for 30 minutes. The stock monochloramine solution was stored at room temperature and used within an hour after preparation.

Ozone Solution

The ozone solution was generated continuously at the point-of-use. Air containing ozone was generated by the ozone generator and bubbled through an ozone feed reservoir filled with 1 L of flowing Milli-Q water. Then the Milli-Q water containing dissolved ozone was used as the ozone solution for disinfection. The flow rate of fresh Milli-Q water flowing into ozone feed reservoir was the same as the flow rate of ozone solution leaving ozone feed reservoir (25 mg/L ~ 125 mg/L) so the volume of the solution in ozone feed reservoir remained constant. Effluent gas from ozone feed reservoir was neutralized by passing through the ozone neutralization solution to remove the excess ozone. For a certain liquid flow rate, ozone concentration in the Milli-Q water was controlled by adjusting either the air flow rate (0.7 ~ 1.0 L/minute) or ozone generator voltage (70V ~ 110V).

Potassium Permanganate Solution

The stock potassium permanganate solution was prepared by dissolving 891 mg of potassium permanganate ($KMnO_4$) in 1 L of Milli-Q water.

This solution was used to calibrate the colorimeter for chlorine measurement.

Stock N,N-diethyl-p-phenylenediamine Indicator Solution (for chlorine and monochloramine analysis)

The DPD solution was prepared by dissolving 1.1 g of anhydrous DPD sulfate in Milli-Q water containing 8 mL 1+3 H_2SO_4 and 200 mg disodium $EDTA$. Then the solution was made up to 1 L and stored in a dark bottle and kept in a dark cabinet. It was discarded when discolored.

Stock Phosphate Buffer Solution for DPD Method

The PBS solution was prepared by dissolving 24 g of anhydrous Na_2HPO_4 and 46 g of anhydrous KH_2PO_4 in Milli-Q water. It was then combined with 100 mL of Milli-Q water in which 800 mg of disodium ethylenediamine tetraacetate dihydrate ($EDTA$) was previously dissolved. The mixture was diluted to 1 L with Milli-Q water and with 20 mg of $HgCl_2$ added. The solution was covered and stored at room temperature.

Indigo Reagent (for ozone analysis)

The stock solution of indigo reagent was prepared by the addition of 1 mL of concentrated phosphoric acid to 500 mL of Milli-Q water in a 1 L volumetric flask. 770 mg of potassium indigo trisulfonate was added with stirring. Then Milli-Q water was added to the final volume of 1 L. The stock solution was stored in a dark bottle and kept in a dark cabinet for up to 4 months.

Indigo reagent #2 was prepared by adding 100 mL of indigo stock solution, 10 g of sodium dihydrogen phosphate, and 7 mL of concentrated phosphoric acid to a 1 L volumetric flask. Final volume was brought up to 1 L by the addition of Milli-Q water. The solution was stored in a dark bottle and kept in a dark cabinet for use within one week.

Sodium Chloride Solution

A 0.1 N sodium chloride solution was prepared by dissolving 5.844 g of sodium chloride ($NaCl$) in 1 L of Milli-Q water. It was then covered and stored at room temperature.

Sodium Hydroxide Solution

A 1 N sodium hydroxide solution was prepared by dissolving 40 g of $NaOH$ in 1 L of Milli-Q water. The solution was covered and stored at room temperature.

Sodium Thiosulfate Solution

A 100 mg/L sodium thiosulfate solution was prepared by adding 50 mg of sodium thiosulfate ($Na_2S_2O_3$) to 500 mL of water. This solution was autoclaved at 121°C for 15 minutes before use and stored at room temperature.

The sodium thiosulfate solution was used to stop the disinfection reaction upon sample collection.

Ozone Neutralization Solution

The ozone neutralization solution was prepared by Milli-Q water with 132 g/L of sodium thiosulfate ($Na_2S_2O_3$) and 3 g/L of potassium iodide (KI) added.

This solution was used to eliminate ozone from the exhaust gas stream by passing the gas through the solution during ozone generation.

4.1.3 Microbial Preparation

4.1.3.1 Growth media preparation

(a) *Escherichia coli* (ATCC 13706)

Bacto Nutrient Broth: This medium was prepared by dissolving 8 g of nutrient broth powder (Difco No. 0003-17-8) in 1 L of milli-Q water. The solution was sterilized at 121°C for 15 minutes. The final pH was 6.8 ± 0.2 at 25°C.

The Bacto nutrient broth was used for the first incubation of *E. coli* received from ATCC and for the preparation of *E. coli* in exponential phase.

Nutrient Agar: This medium was prepared by mixing 23 g of nutrient agar powder (Difco No. 0001-17) in 1 L of Milli-Q water and boiling for 1 minute to dissolve completely. It was then sterilized at 121°C for 15 minutes. The final pH was 6.8 ± 0.2 at 25°C.

The nutrient agar was used for the maintenance of the working stock culture and growth of the experimental cultures.

(b) *Bacillus subtilis* (ATCC 6633)

Bacto Nutrient Broth: The same medium for *E. coli* was used for the first incubation of *B. subtilis* from ATCC and for the preparation of *B. subtilis* vegetative cells in exponential phase.

R2A Agar: This medium was prepared by suspending 18.2 g of agar powder (Difco No. 1826-17) in 1 L of Milli-Q water. It was mixed well, boiled for 1 minute to dissolve the powder completely, then autoclaved at 121°C for 15 minutes. The final pH was 7.2 ± 0.2 .

The R2A agar was used for maintenance of the working stock culture, growth of the experimental cultures, and preparation of *B. subtilis* spores.

Trypticase Soy Broth: This medium was prepared by suspending 30 g of trypticase soy broth powder (BBL No. 4311768) in 1 L of Milli-Q water. It was mixed thoroughly, warmed gently to dissolve the powder completely, then autoclaved at 121°C for 15 minutes. The final pH was 7.3 ± 0.2 .

The trypticase soy broth was used for the incubation of *B. subtilis* after disinfection.

4.1.3.2 *Escherichia coli* preparation

Permanent Stock Culture Preparation: The *E. coli* strain (ATCC 13706) was obtained from American Type Culture Collection (Manassas, VA) as freeze-dried cultures. It was revived and propagated according to the ATCC instructions. A permanent stock culture was prepared and stored at 4°C.

Working Stock Culture Preparation: The working stock culture was prepared from the permanent stock culture following the procedures described by Kouame (1990). Aseptically an aliquot of permanent stock culture was transferred to capped assay tubes containing sterile nutrient agar slants. These tubes were placed in an incubator at 37°C for 24 hours. The capped tubes were then sealed with parafilm and stored at 4°C. A new set of working stock cultures was prepared every three weeks from the assay tubes.

E. coli in Stationary Phase Preparation: To prepare *E. coli* in stationary phase, capped assay tubes containing sterile nutrient agar were inoculated with *E. coli* from the working stock culture. These assay tubes were incubated at 37°C for 16-19 hours. Then the microorganisms were harvested by washing with buffered demand-free water and centrifuging at 6000 *rpm* for 10 minutes. The concentrate was washed twice with dilution water. Appropriate amounts of the final suspension were dosed in the buffered experimental water to achieve the desired initial microbial density.

E. coli in Exponential Phase Preparation: To prepare *E. coli* in exponential phase, a loopful of the overnight culture suspension at stationary phase was inoculated in nutrient broth and incubated in a shaker at 37°C with gently shaking at 160 *rpm*. Based

on the relationship between optical density and cell density (Figure 4-1) and the growth curves of *E. coli* (Figure 4-2) obtained from previous experiments conducted by Kaymak (2003), the incubation time has been determined to be around 3 hours with the optical density of the suspension in the range of 0.4~0.6 at 660 *nm*. The microorganisms in exponential phase were harvested by centrifuging at 6000 *rpm* for 10 minutes and washed twice with buffered demand-free water. The final suspension was dosed in buffered experimental water.

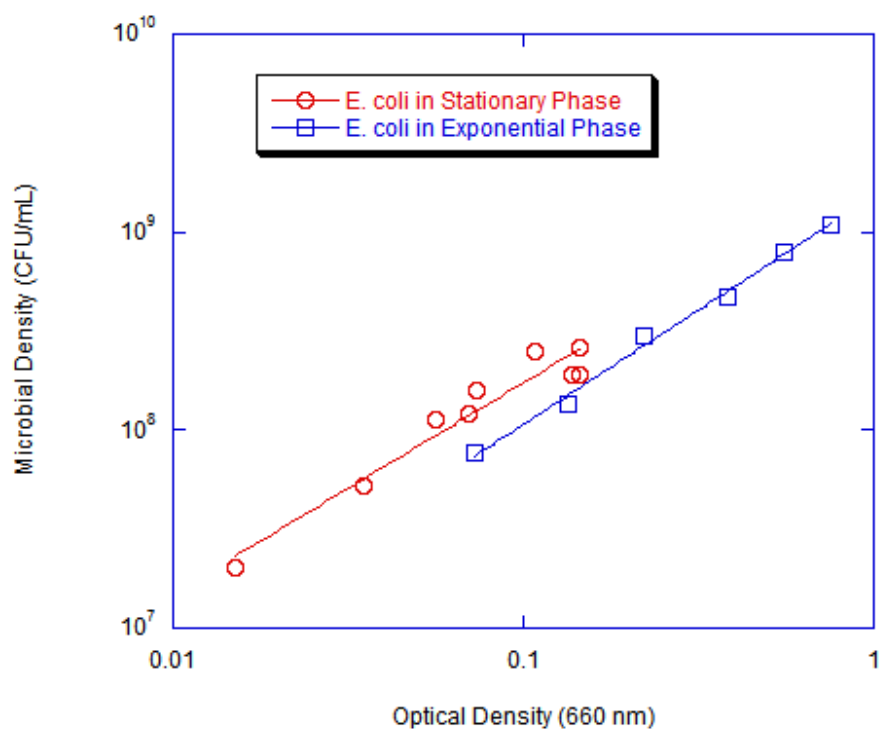


Figure 4-1 Standard Curves of Microbial Density of *E. coli* in Stationary Phase and Exponential Phase vs. Optical Density at 660 nm

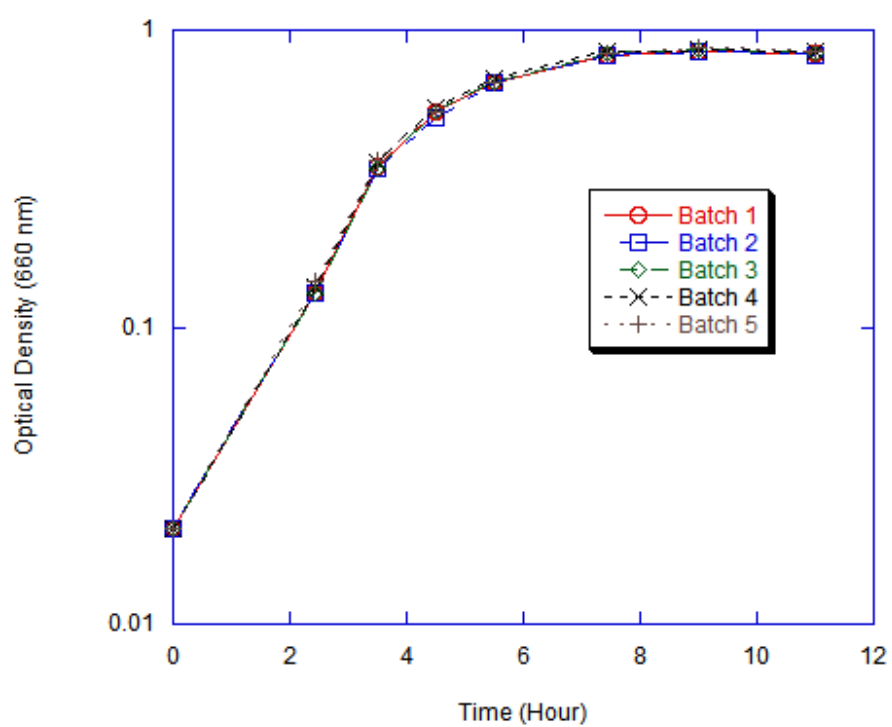


Figure 4-2 Growth Curve of *E. coli*

4.1.3.3 *Bacillus subtilis* Preparation

Permanent Stock Culture Preparation: The *B. subtilis* strain (ATCC 6633) was obtained from American Type Culture Collection (Manassas, VA) as freeze-dried cultures. It was revived and propagated according to the ATCC instruction. A permanent stock culture was prepared and stored at 4°C.

Working Stock Culture Preparation: An aliquot of the permanent stock culture of *B. subtilis* was transferred to capped assay tubes containing sterile R2A agar slant. These tubes were placed in the incubator at 35°C for 24 hours. The capped tubes were then sealed with parafilm and stored at 4°C. A new set of working stock cultures was prepared every three weeks from the assay tubes.

B. subtilis Spores Preparation: To prepare *B. subtilis* spores, a loop of *B. subtilis* was inoculated onto R2A slants from the working stock culture and incubated at 35°C for 10 days to sporulate. The spores were collected by rinsing the slants with sterile phosphate buffer and centrifuging at 4000 *rpm* for 4 minutes. Then the supernatant was withdrawn and washed twice with buffered demand-free water and centrifuged at 6000 *rpm* for 10 minutes. The final sporulated suspension was pasteurized in a 75°C water bath for 15 minutes with the purpose of killing all vegetative cells (Barbeau 1997; Barbeau 1999). The spore suspension was stored at 4°C for no more than one week and dosed in the buffered experimental water for disinfection experiments.

B. subtilis Vegetative Cells in Exponential Phase Preparation: To prepare *B. subtilis* in exponential phase, the microorganisms were incubated on R2A slants overnight. *B. subtilis* cells were collected from the media by rinsing the slants with sterile

buffered water and the suspension was centrifuged at 4000 *rpm* for 4 minutes. Then the supernatant was inoculated in tripticase soy broth and incubated at 35°C with gently shaking at 160 *rpm*. Based on the relationship between optical density and cell density (Figure 4-3) and the growth curves of *B. subtilis* (Figure 4-4) obtained by Kaymak (2003), the incubation time was determined to be 11~12 hours with the optical density of the suspension in the range of 0.3~0.4 at 660 *nm*. The microorganisms in exponential phase were harvested by centrifuging at 6000 *rpm* for 10 minutes and washed twice with buffered demand-free water. The final suspension was dosed in buffered experimental water for disinfection experiments.

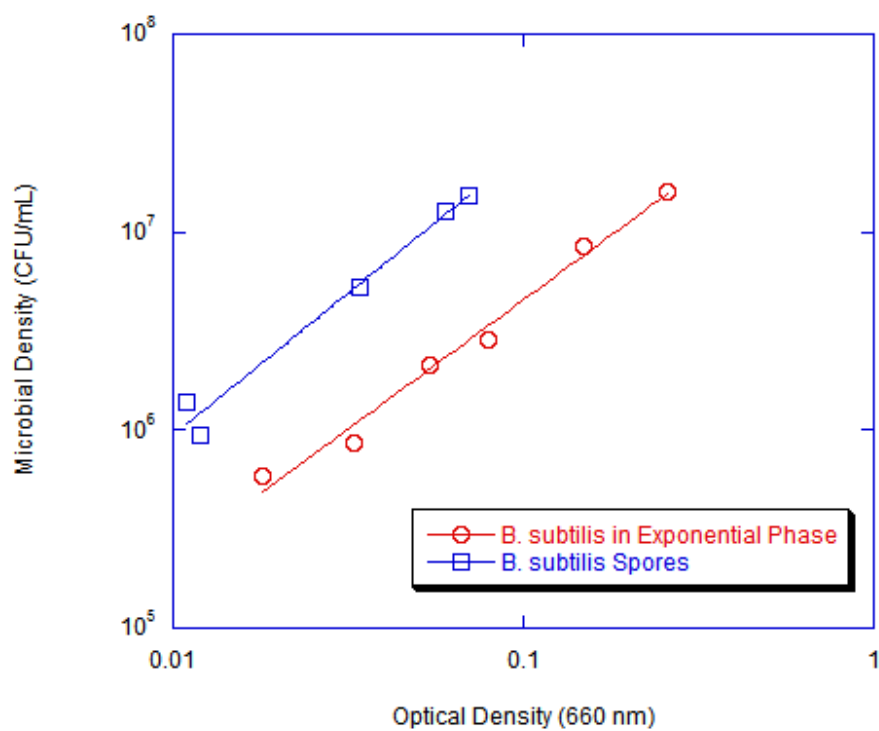


Figure 4-3 Standard Curves of Microbial Density of *B. subtilis* cells in Exponential Phase and Spores vs. Optical Density at 660 nm

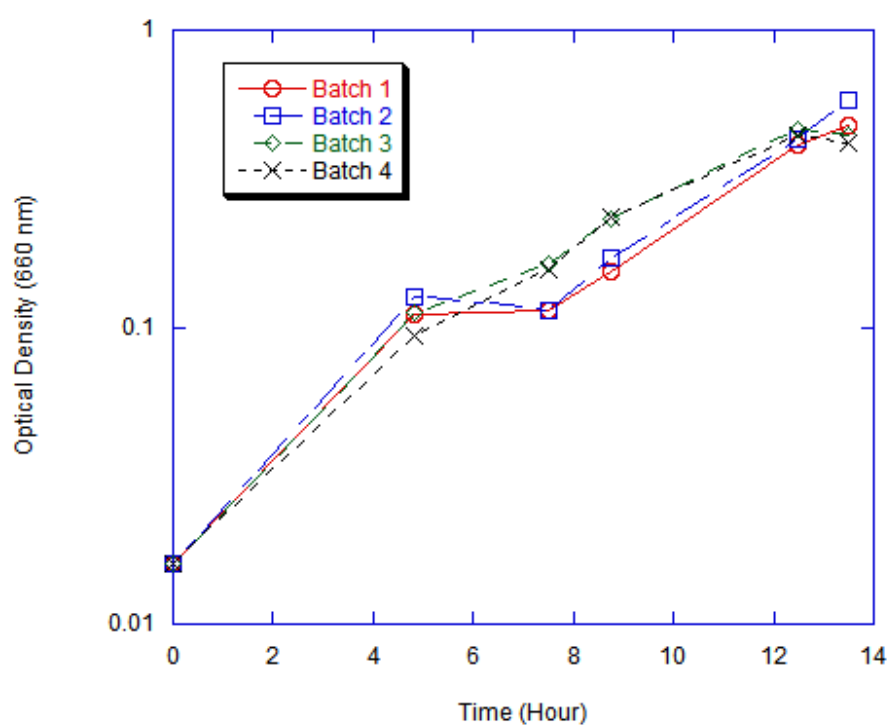


Figure 4-4 Growth Curve of *B. subtilis*

4.2 Analytical Methods

Analysis of Chlorine Residual

The free chlorine level in the solution was determined at 515 nm using a spectrophotometer by the DPD colorimetric method 4500-Cl G (APHA 1995).

Analysis of Monochloramine Residual

The free chlorine and total chlorine levels were both determined at 515 nm by the DPD colorimetric method 4500-Cl G (APHA 1995). The monochloramine purity was computed and was equal or approximate 100%.

Analysis of Ozone Residual

The ozone residual was determined at 600 nm by the indigo colorimetric method 4500-O₃ B (APHA 1995).

Microbial Enumeration

To terminate the disinfection reaction, 0.9 mL of sample was taken, added to 0.1 mL of sodium thiosulfate solution, and mixed well. Samples were kept at 4°C after taking and before analysis.

The membrane filter method 9215 D described below was used to enumerate *E. coli* and *B. subtilis* vegetative cells in the samples (APHA 1995). Nutrient agar was used

for incubation of *E. coli* and trypticase soy broth was used for incubation of *B. subtilis* vegetative cells.

Dilution: Decimal dilutions of samples were prepared by adding 1 mL of sample to pre-sterilized dilution tubes containing 9 mL of dilution water. Further decimal dilutions were prepared in the same way with the dilution tubes vortexed thoroughly at each step. The dilution tubes were stored at 4°C before filtration step and were stored at room temperature no more than 30 minutes.

Filtration: For each dilution sample three replicates were filtered. 1 mL of each dilution sample was added to a membrane filter holder using aseptic technique. An aliquot of 20 to 30 mL of Milli-Q water was added to the membrane filter holder to ensure a uniform distribution over the membrane filter. The filters were removed from the filter holding assembly by sterilized forceps and placed on the culture petri dishes. Then the dishes were put into the incubator. The membrane filter holders were rinsed with sterilized Milli-Q water every time after removing membrane filters from the filter holding assembly. The petri dishes labeled with date and sample ID were prepared in advance with pouring nutrient agar into dishes for *E. coli* culture and filling trypticase soy broth into dishes with pad for *B. subtilis* culture.

Incubation and Enumeration: the culture dishes were incubated for 24~25 hours at 37°C for *E. coli* and 22~24 hours at 35°C for *B. subtilis*. After the incubation, the number of colonies in the plates was counted by using a Quebec Colony Counter.

Determination of Bacteria Concentration: The microbial concentration was computed and expressed as colony forming units (CFU) per mL.

$$CFU / mL = \frac{\sum N_i}{\sum V_i} \quad 4-1$$

where the summation is taken over all plates of the particular sample. N_i is the colonies counted in a plate. V_i is the actual volume (mL) of the sample in a plate.

The viability of *B. subtilis* spores was determined by modified membrane filtration method (Barbeau 1997). Prior to filtration, the samples were pasteurized in a 75°C water bath for 15 minutes to kill all the vegetative cells and to activate spore germination. Then the heat-treated samples were diluted, filtered as above mentioned filtration procedures. The membrane filters were placed on pads saturated with trypticase soy broth in culture dishes using aseptic technique. The colonies were counted after incubation at 35°C for 22~24 hours.

4.3 CSTR Set Up and Characterization

4.3.1 CSTR Set Up

A Continuously Stirred Tank Reactor (CSTR) was used for disinfection experiments in this study. It was a glass tank with four baffles distributed symmetrically along the wall and an outlet at the bottom of the wall. The solution volume in the reactor was designed to be 500 mL. The schematic sketch of the CSTR was shown in Figure 4-5.

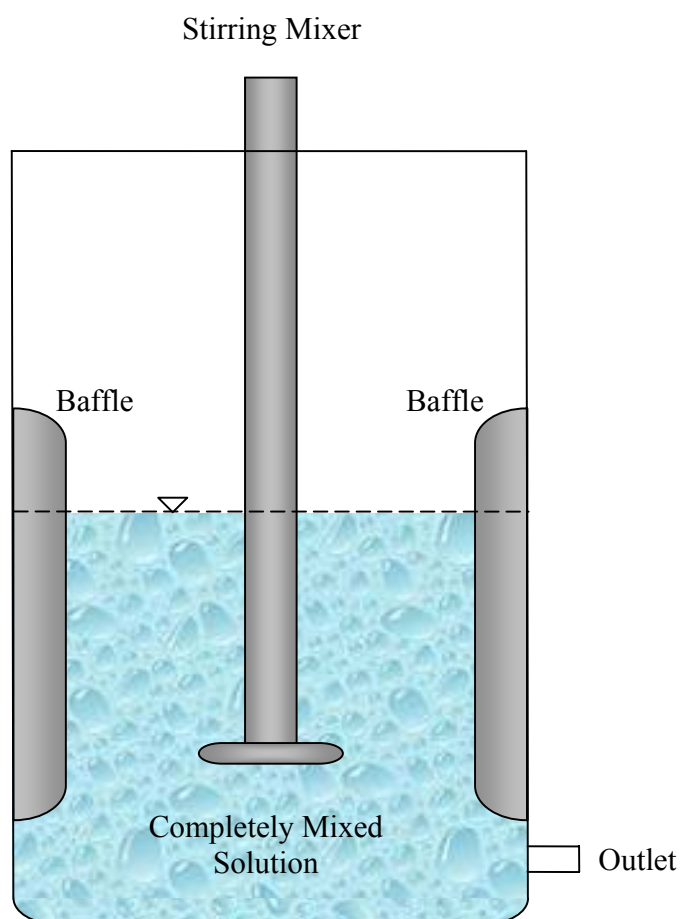


Figure 4-5 Schematic Sketch of CSTR

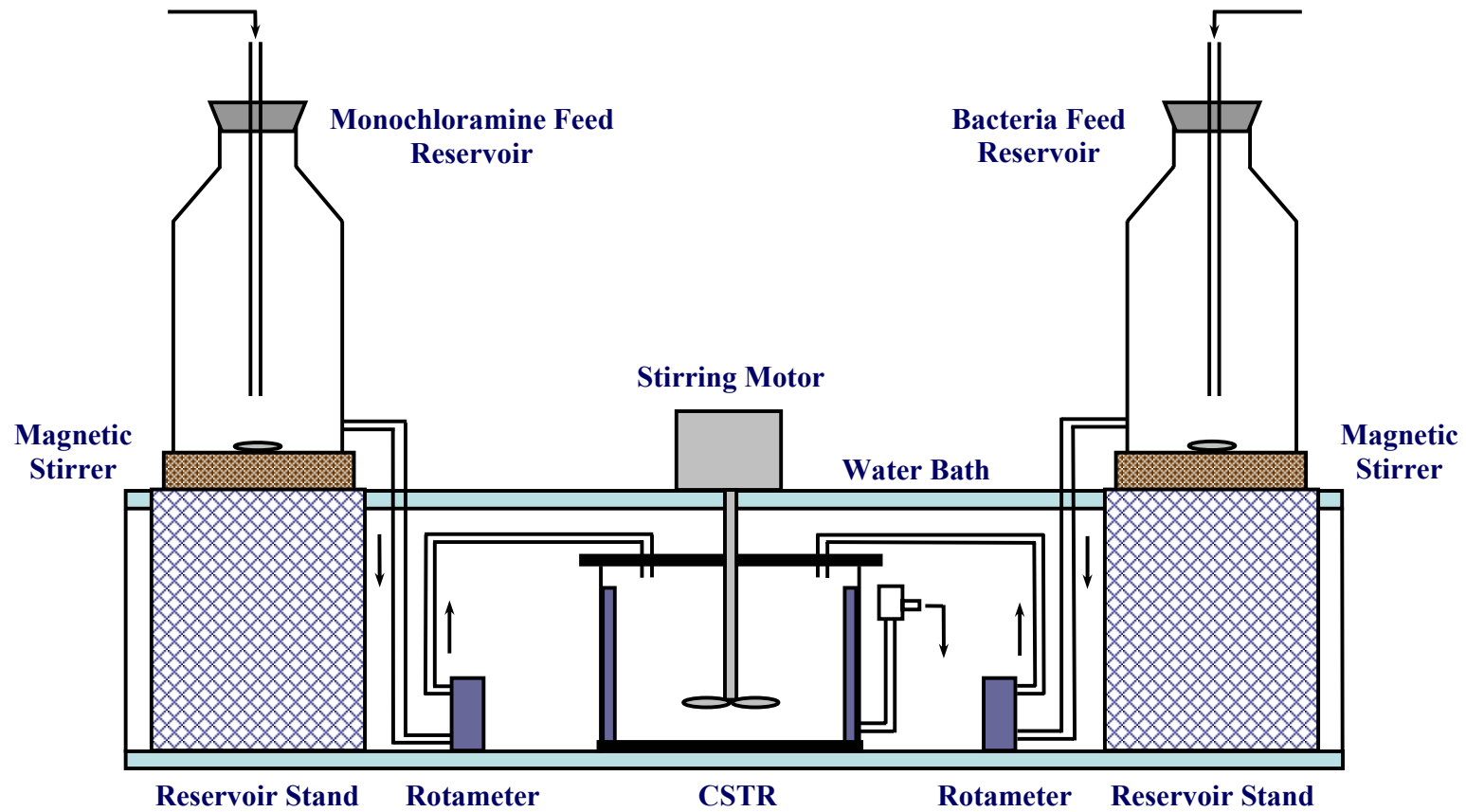


Figure 4-6 Monochloramine Disinfection System Configuration

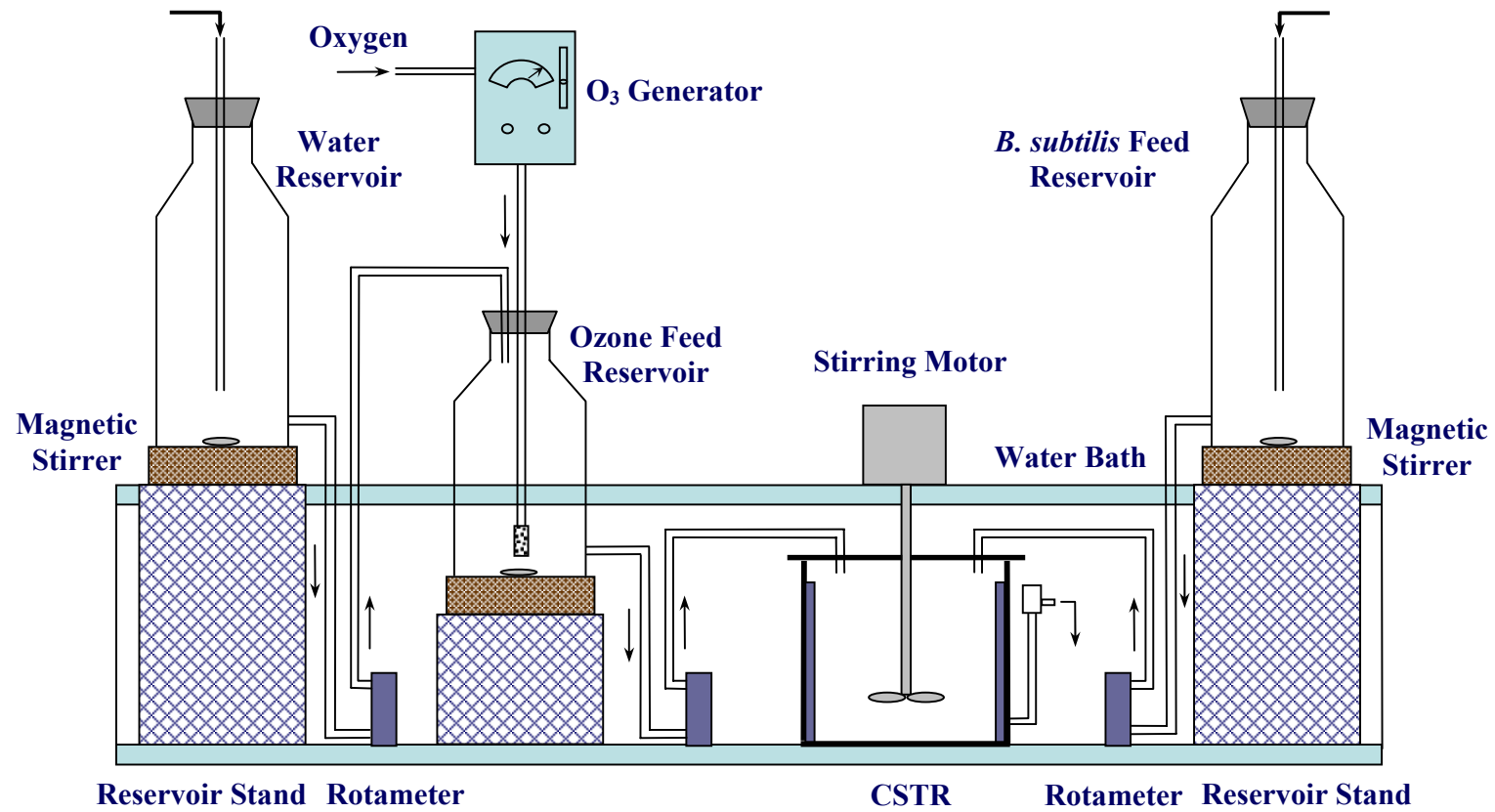


Figure 4-7 Ozone Disinfection System Configuration

Two CSTR systems were built up to perform disinfection experiments. One system was used for monochloramine disinfection and the other system was used for ozone disinfection. The system configurations were displayed in Figure 4-6 and Figure 4-7.

The principal components of the monochloramine disinfection system were two reservoirs, two rotameters, one stirring motor, and one reactor. The two reservoirs were filled with preformed monochloramine solution and bacterial suspension (*E. coli* in stationary phase, *E. coli* in exponential phase, and *B. subtilis* vegetative cells in exponential phase) under aseptic condition. Flows from both reservoirs were introduced into the reactor simultaneously with flow rates controlled by the two rotameters. The reactor has a volume of 1000 mL and was designed to hold about 500 mL of solution during experiments. A two-bladed stirring propeller ($d = 0.028m$) driven by a motor (1000 rpm) provided rapid mixing in the reactor. The temperature in the reactor was controlled by a water bath.

Since ozone is very reactive and easy to decay, it was generated continuously during ozone disinfection experiments. The ozone-oxygen gas mixture generated from an ozone generator was introduced into the bottom of ozone feed reservoir through a gas sparger. Milli-Q water was fed into ozone reservoir at the same time from water reservoir. Then ozone solution and bacteria suspension (*B. subtilis* spores) was introduced into the reactor simultaneously.

4.3.2 CSTR Characterization

4.3.2.1 Tracer Test Performance

Tracer tests provide a profile of tracer in the effluent of a reactor as a function of time, which is known as the RTD (residence time distribution). A step input tracer test was conducted to obtain the tracer concentration curve over time in the reactor for this study, which was achieved by introducing the tracer into the reactor at time zero and subsequently maintaining the constant concentration of tracer in the reactor influent. Sodium chloride (*NaCl*) was used as the non-reactive tracer in this study since sodium chloride has the same diffusivity in water as that of chlorine ($1.5 \times 10^{-5} \text{ cm}^2 / \text{sec}$) (Kouame 1990). The influent samples were collected from the reservoirs and the effluent samples were collected from the outlet of the reactor. A conductivity meter was used to measure the conductivity of the samples. The linear relationship was confirmed between the conductivity and the concentration of sodium chloride solution (Figure 4-8).

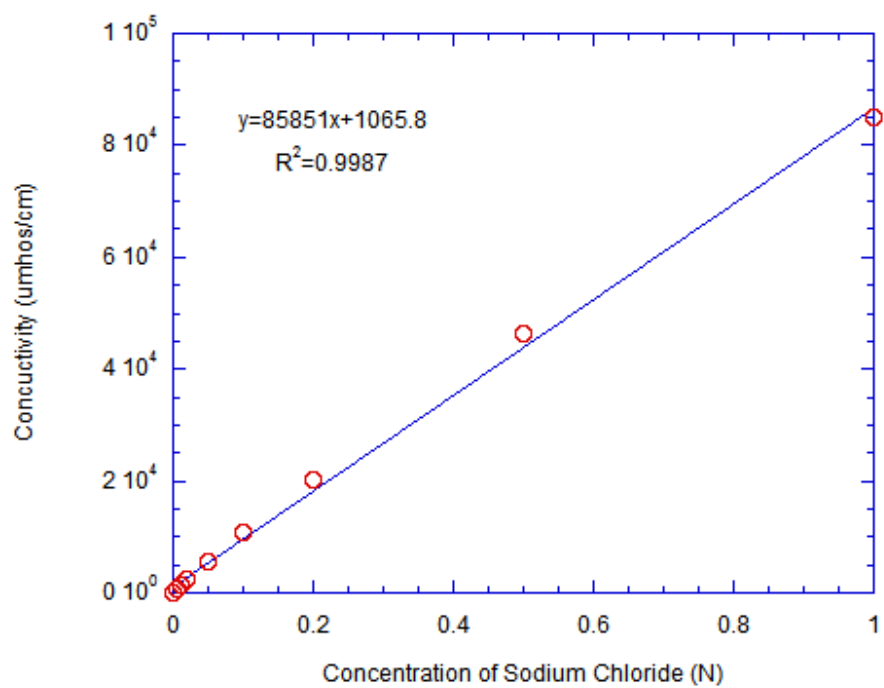


Figure 4-8 Conductivity Standard Curve of NaCl Solution

Four tracer tests were conducted in the monochloramine disinfection system with four designed mean residence times θ (min) and the corresponding flow rates Q (mL/min) from each reservoir (Table 4-1). The relationship was computed by the following equation.

$$Q = Q_1 + Q_2 = \frac{V}{\theta} \quad 4-2$$

where Q_1 is the flow rate of disinfectant solution; Q_2 is the flow rate of bacteria suspension; V is the solution volume in the reactor which was designed as 500 mL; and θ is the mean residence time for each experiment. The flow rates are the same for flows from each reservoir in this study.

At time zero, 0.1 N of sodium chloride solution was introduced into the reactor from one reservoir with predetermined flow rates and the flow rates were kept the same during the test. The phosphate buffered solution was introduced into the reactor from another reservoir with the same flow rates at the same time. Samples were taken from the outlet for a duration equal to six residence times. The effluent concentration was measured as a function of time. The background specific conductivity of the phosphate buffer solution was measured and subtracted from experimental data.

Table 4-1 Designed Mean Residence Times and Corresponding Flow Rates

Designed Mean Residence Time θ (min)	2	4	6	10
Flow Rate from Both Reservoirs $Q_1 = Q_2$ (mL/min)	125	62.5	41.7	25

4.3.2.2 F Curve

F curve is the cumulative residence time distribution function. $F(t)$ is the fraction of tracer molecules that exit the reactor before time t . For a step input test, it is the ratio of effluent concentration of tracer over step input concentration of tracer and will finally approach one after a steady-state condition is reached (Levenspiel 1999).

$$F(t) = \frac{C_{out}}{C_{in}} \quad 4-3$$

$F(t)$ curves obtained from tracer tests are plotted in Figure 4-9, Figure 4-10, Figure 4-11, and Figure 4-12, corresponding to different mean residence times and flow rates.

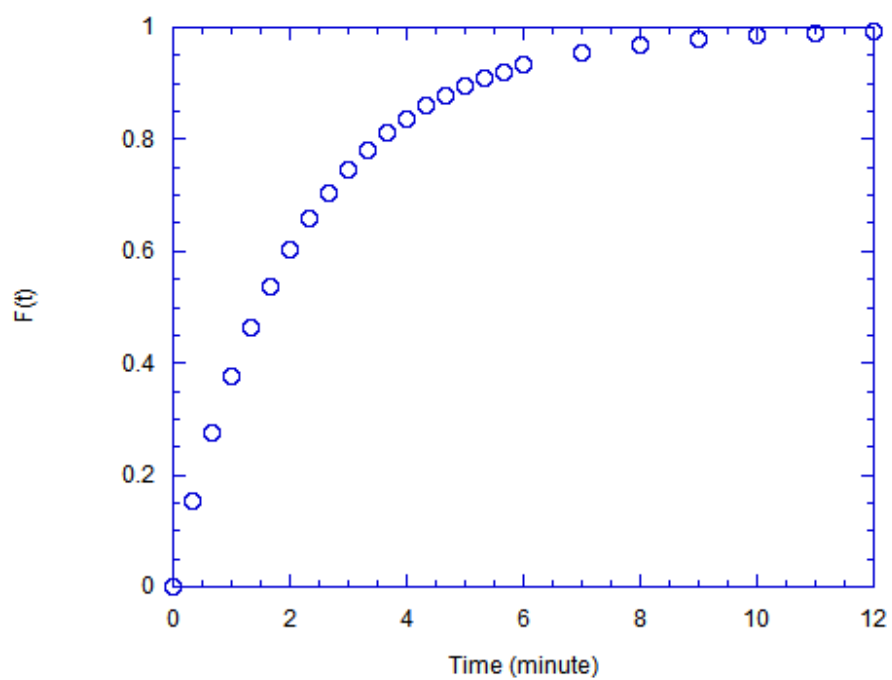


Figure 4-9 F Curve ($Q_1 = Q_2 = 125$ mL/min)

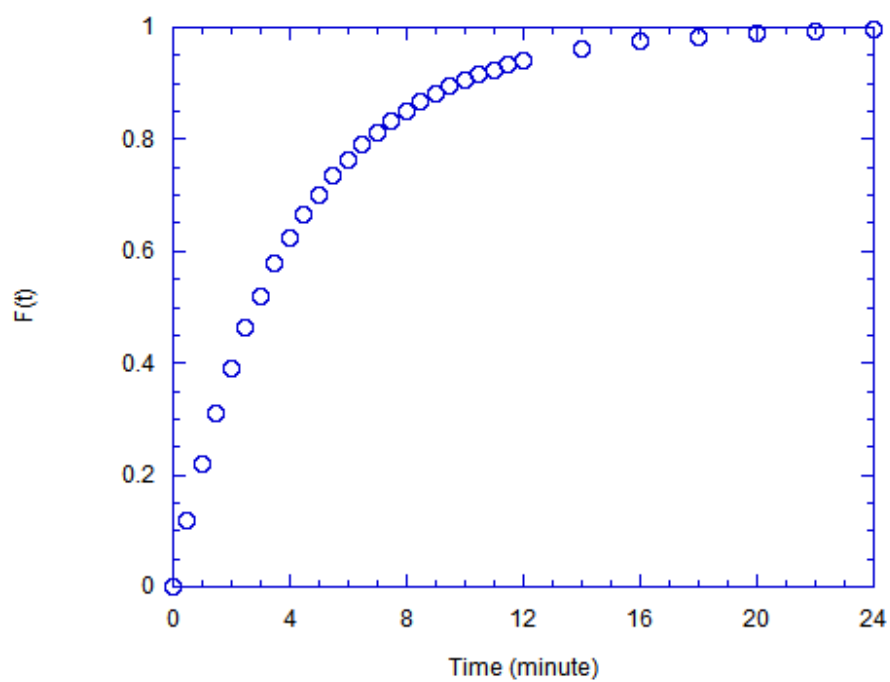


Figure 4-10 F Curve ($Q_1 = Q_2 = 62.5$ mL/min)

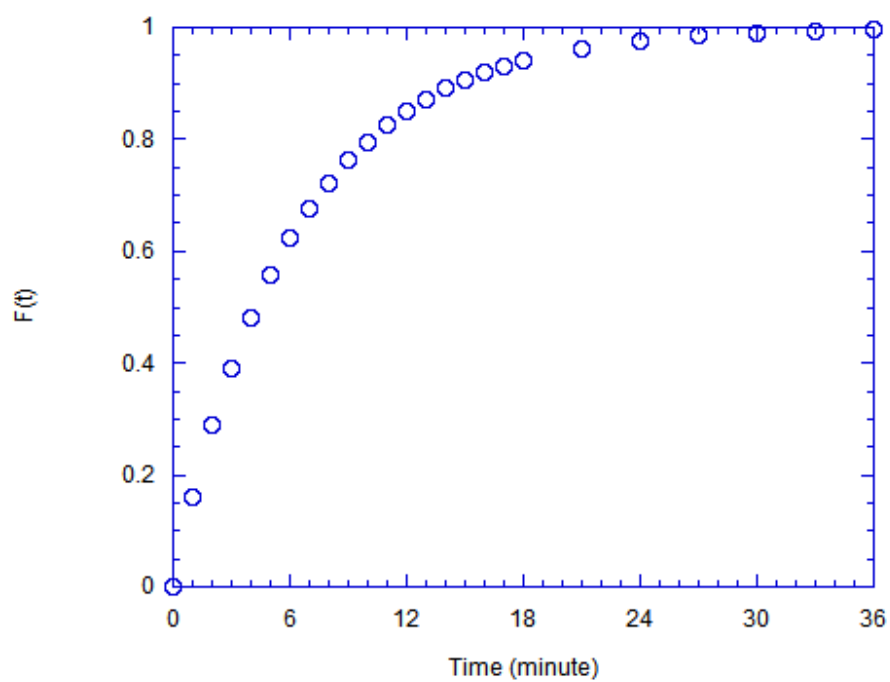


Figure 4-11 F Curve ($Q_1 = Q_2 = 41.7$ mL/min)

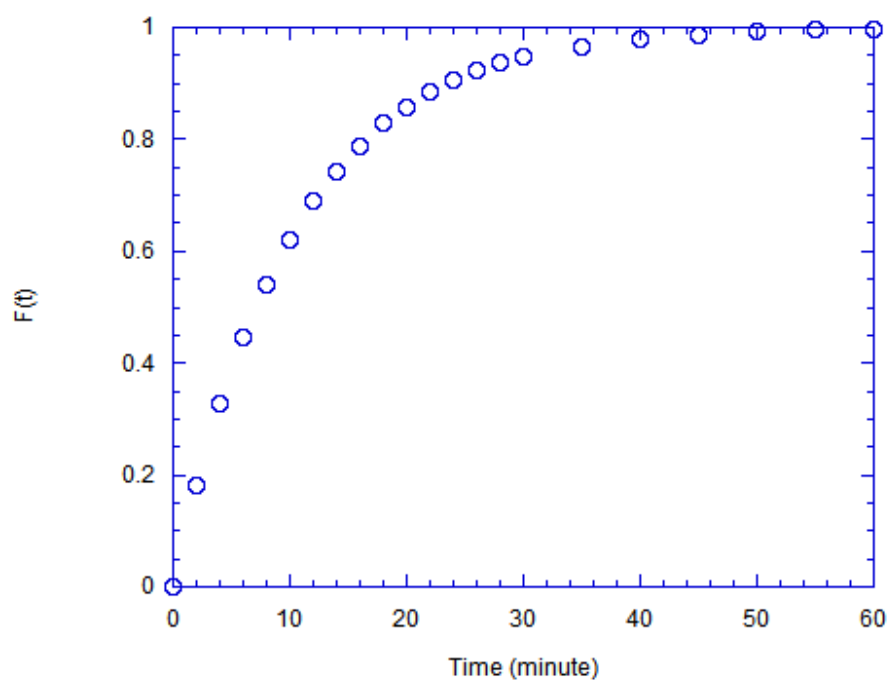


Figure 4-12 F Curve ($Q_1 = Q_2 = 25$ mL/min)

4.3.2.3 E Curve and Tanks-in-series Model

The E curve, the exit age or residence time distribution curve, can be derived from step tracer test data. $E(t)dt$ is the fraction of material exiting at a residence time between t and $t+dt$. The relation between E curve and F curve can be expressed as below

$$E(t) = \frac{dF(t)}{dt} \quad 4-4$$

$$F(t) = \int_0^t E(t)dt \quad 4-5$$

In many actual cases the RTD of a reactor shows an intermediate behavior between two types of ideal reactor – CSTR and PFR. Some RTD models have been developed to deal with nonideal in environmental engineering. The tanks-in-series model is one of the frequently used RTD models (Westerterp 1984; Haas 1997; Levenspiel 1999).

The tanks-in-series model comes from a system of N identical CSTRs in series. This model is expressed as (Nauman and Buffham 1983)

$$E(t) = \frac{1}{t\Gamma(N)} \left(\frac{Nt}{\theta} \right)^N \exp\left(-\frac{Nt}{\theta} \right) \quad 4-6$$

in the case for all $N > 0$ (including fractional) and dimensionless variance ν in the range $0 < \nu < \infty$, where θ is the mean residence time and Γ is the mathematical gamma function defined as

$$\Gamma(N) = \int_0^\infty e^{-x} x^{N-1} dx \quad 4-7$$

After $E(t)$ data being derived from F curve, nonlinear regression method was applied to estimate the value of unknown parameters (θ and N) in tanks-in-series model

with t as the independent variable. The best estimates for the unknown parameters in tanks-in-series model are obtained by minimizing ESS (error sum of squares).

$$ESS = \sum_{i=1}^n \left[E(t)_{\text{experimental}} - E(t)_{\text{predicted}} \right]^2 \quad 4-8$$

The analysis was done by using Microsoft Excel solver function (Microsoft Corporation). The experimental $E(t)$ data and fitted tanks-in-series model $E(t)$ curve were shown in Figure 4-13, Figure 4-14, Figure 4-15, and Figure 4-16. The values of parameters were listed in Table 4-2.

Table 4-2 Estimation of Parameters in Tanks-in-series Model

Flow Rate from Both Reservoirs $Q_1 = Q_2 \text{ (mL/min)}$	125	62.5	41.7	25
Mean Residence Time $\theta \text{ (min)}$	2.195	4.117	6.160	10.341
The Number of Ideal CSTR Reactor N	0.956	0.975	0.945	0.995

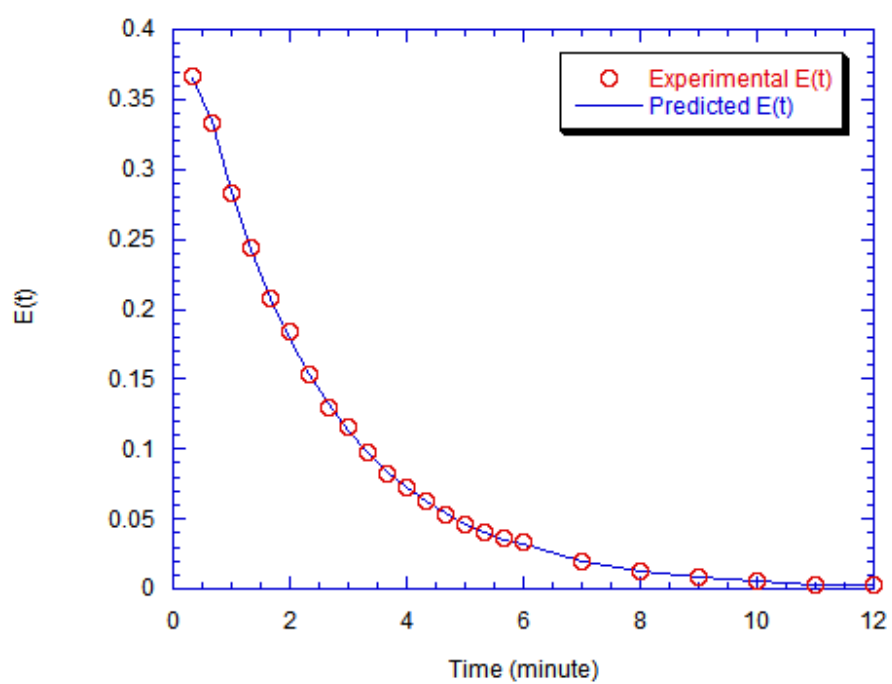


Figure 4-13 Tanks-in-series Model $E(t)$ Fitting Curve

$$(Q_1 = Q_2 = 125 \text{ mL/min})$$

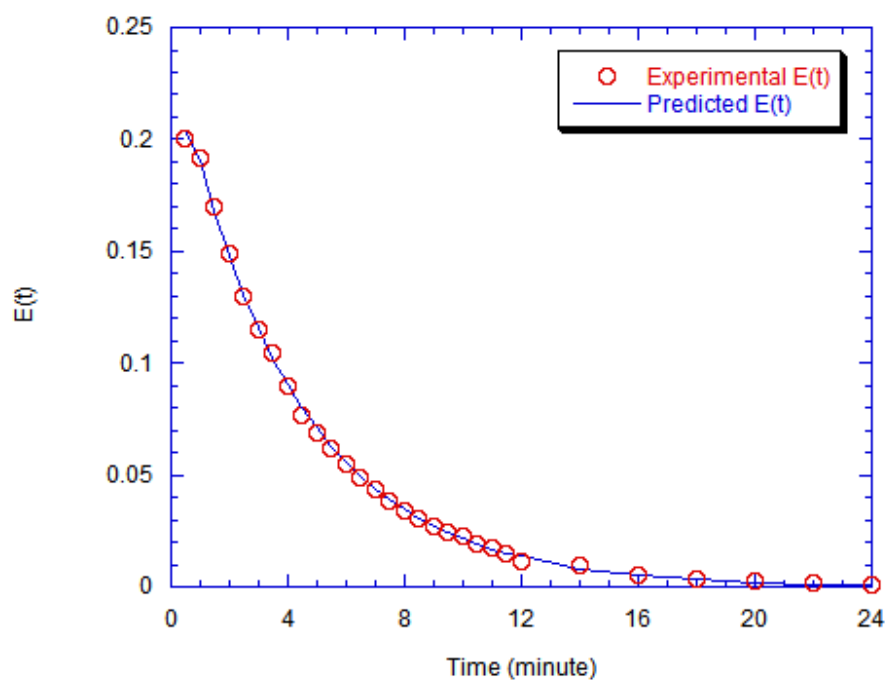


Figure 4-14 Tanks-in-series Model $E(t)$ Fitting Curve

$$(Q_1 = Q_2 = 62.5 \text{ mL/min})$$

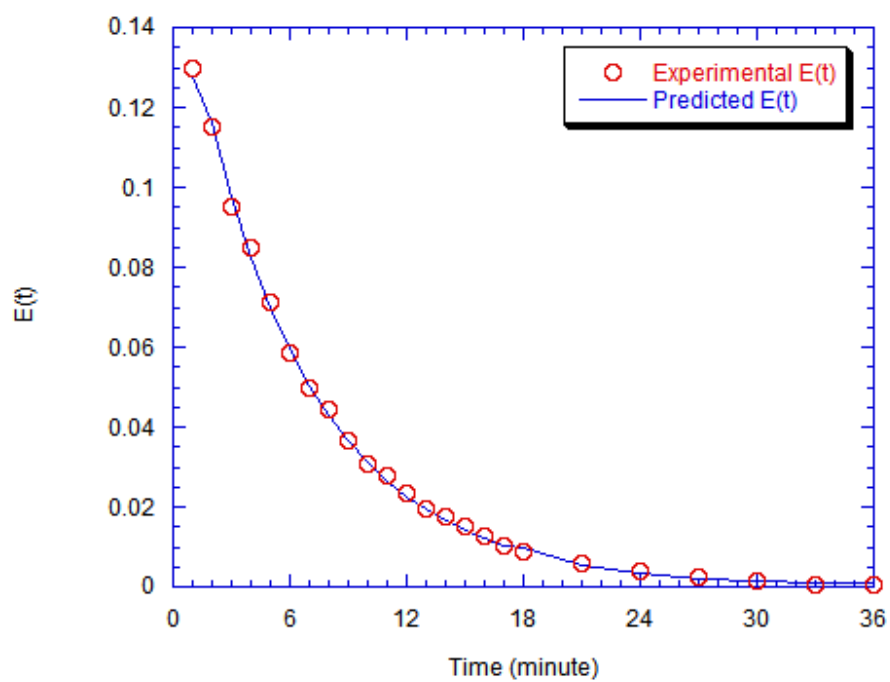


Figure 4-15 Tanks-in-series Model E(t) Fitting Curve

$$(Q_1 = Q_2 = 41.7 \text{ mL/min})$$

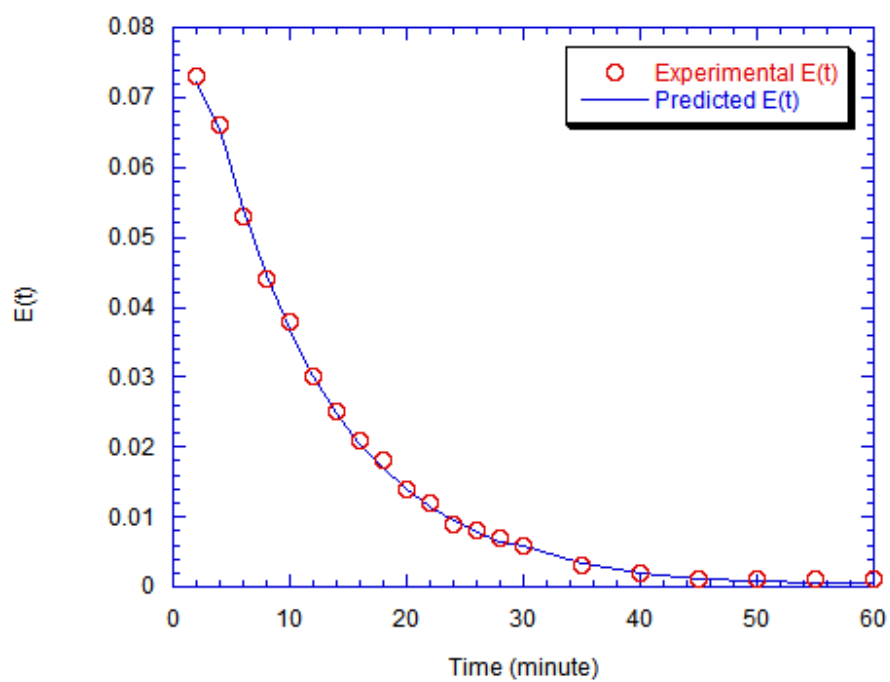


Figure 4-16 Tanks-in-series Model $E(t)$ Fitting Curve

$(Q_1 = Q_2 = 25 \text{ mL/min})$

4.3.2.4 CSTR Characterization and Mixing Effect of the Reactor

Two parameters were used to characterize the reactor: Pe (Peclet number) and N (the number of identical CSTRs in tanks-in-series model).

The Peclet number (Pe) is the reciprocal of dispersion number which is a dimensionless group defined as the ratio of axial dispersion coefficient to the product of velocity and length $\left(\frac{D}{uL}\right)$ (Levenspiel 1999). For a system with closed boundary condition, the Peclet number can be computed by

$$\nu = \frac{2}{Pe} - \frac{2}{Pe^2}(1 - e^{-Pe}) \quad 4-9$$

in which ν is the normalized variance and can be derived from

$$\nu = \frac{1}{N} \quad 4-10$$

In CSTR, the contents are completely mixed with an infinite amount of dispersion, and the concentration is uniform throughout the volume. For an ideal CSTR the dispersion number is infinity and the Peclet number is zero (Haas 1999). The number of N in tanks-in-series model should also be one for an ideal CSTR.

Table 4-3 listed the value of N and Pe derived from tanks-in-series model for four tracer tests. By performing t-test, the both hypotheses of $N=1$ ($p=0.0586$) and $Pe=0$ ($p=0.1641$) could not be rejected with significance level of 5%. So the hypothesis that the reactor can be considered as an ideal CSTR could not be rejected.

Table 4-3 CSTR Characterization Parameters

Flow Rate $Q_1 = Q_2 \text{ (mL/min)}$	125	62.5	41.7	25
<i>The Number of CSTR Reactors</i> N	0.956	0.975	0.945	0.995
Normalized Variance ν	1.046	1.026	1.058	1.005
Peclet Number Pe	2.53×10^{-6}	9.98×10^{-6}	2.21×10^{-6}	6.16×10^{-7}

While each flow pattern of fluid has its RTD, the same RTD can describe a number of different flow patterns. For example, earlier mixing and later mixing of fluids might give the same RTD. For a first-order reaction, the segregation has no influence on the performance of reactor. For a non-first-order reaction, a rise in segregation improves reactor performance for orders greater than unity but lowers performance for reaction orders smaller than unity (Levenspiel 1999).

A dimensionless segregation number was used to estimate the degree of mixing in the reactor:

$$S_g = \frac{\mu^{1.5}}{4\pi^2 \rho^{1.5} \varepsilon^{0.5} D \theta} \quad 4-11$$

where S_g is the segregation number; μ is the dynamic viscosity of liquid; ρ is the density of liquid; ε is the power dissipated per unit mass of liquid; D is the molecular diffusivity of liquid; and θ is the mean residence time (Nauman and Buffham 1983). Segregation is

considered to be unimportant and the reactor is well mixed for $S_g < 0.1$, while some segregation effects exist for $S_g > 1.0$.

ε is defined as

$$\varepsilon = \frac{P}{V\rho} \quad 4-12$$

where V is the volume of the reactor; P is the power imparted to the water by a mixer and can be calculated by

$$P = 2\pi nT \quad 4-13$$

where n is the impeller speed (*rps*); and T is the impeller shaft torque (Qasim 2000).

Under the experimental condition ($\rho_{15^\circ C} = 999.1 \text{ kg/m}^3$, $\mu_{15^\circ C} = 1.14 \times 10^{-3} \text{ N-s/m}^2$, $D = 1 \times 10^{-9} \text{ m}^2/\text{s}$, $n = 1000 \text{ rpm}$, $V = 500 \text{ mL}$), the following equation can be derived (Appendix A).

$$S_g = \frac{0.035}{\theta(\text{sec})} \quad 4-14$$

The computed segregation numbers for the disinfection experiments are shown in Table 4-4. All of them were much less than 0.1, which indicated that the reactor was micromixed and the segregation effects was not significant in the reactor.

Table 4-4 Segregation Numbers for the Disinfection Experiments

Mean Residence Time $\theta(\text{min})$	2	4	6	10
Segregation Number S_g	2.92×10^{-4}	1.46×10^{-4}	9.72×10^{-5}	5.83×10^{-5}

4.3.2.5 Mean Residence Time Determination of the Reactor

From the CSTR characterization analysis, the reactor for disinfection experiments in the continuous flow system can be considered as an ideal CSTR with no significant segregation effect. The actual mean residence time hereby can be estimated by two methods: unsteady-state mass balance equation estimation and Tanks-in-series model ($N=1$) estimation.

(a) Mass Balance Method (Linear Regression)

For nonreactive tracer step test, an unsteady-state mass balance equation for CSTR can be written as

$$\frac{dC(t)}{dt} = \frac{Q}{V}(C_0 - C(t)) \quad 4-15$$

where C_0 is the input tracer concentration; $C(t)$ is the outflow tracer concentration at any time t ; Q is the volumetric flow rate; and V is the volume of solution in the reactor.

Upon integration of the unsteady-state mass balance relationship for the nonreactive tracer in a CSTR with $C(t) = 0$ at $t = 0$, the following expression can be derived:

$$\ln\left(1 - \frac{C(t)}{C_0}\right) = -\frac{t}{\theta} \quad 4-16$$

For an ideal CSTR, the plot of $\ln\left(1 - \frac{C(t)}{C_0}\right)$ vs. t should give a straight line with

slope equal to $\frac{1}{\theta}$ and intercept equal to zero. By linear regression (Figure 4-17, Figure

4-18, Figure 4-19, Figure 4-20), the mean residence times were computed from the slope of the regression lines (Table 4-5).

Table 4-5 Mean Residence Times Determined from Linear Regression Method

Designed Mean Residence Time (<i>min</i>)	2	4	6	10
Actual Mean Residence Time (<i>min</i>)	2.29	4.29	6.39	10.30

When conducting the tracer test study, the liquid volume in the reactor was observed to fluctuate depending on the flow rates. An increase in liquid volume was observed with the increase of flow rate. So the actual liquid volume in the reactor was larger than 500 mL during the experiments, which caused the increase of the mean residence time.

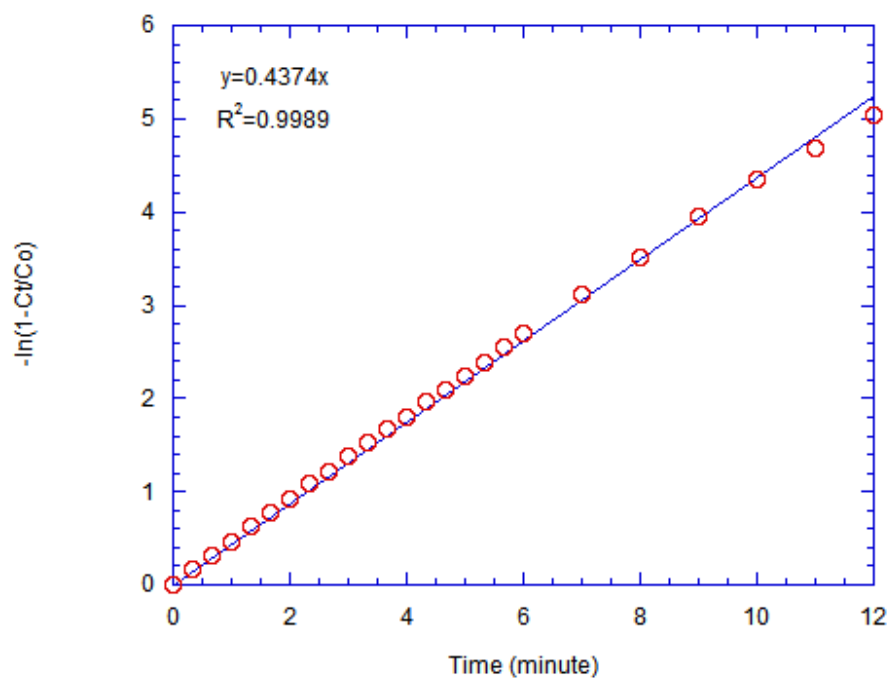


Figure 4-17 Linear Regression of Tracer Test ($Q_1 = Q_2 = 125$ mL/min)

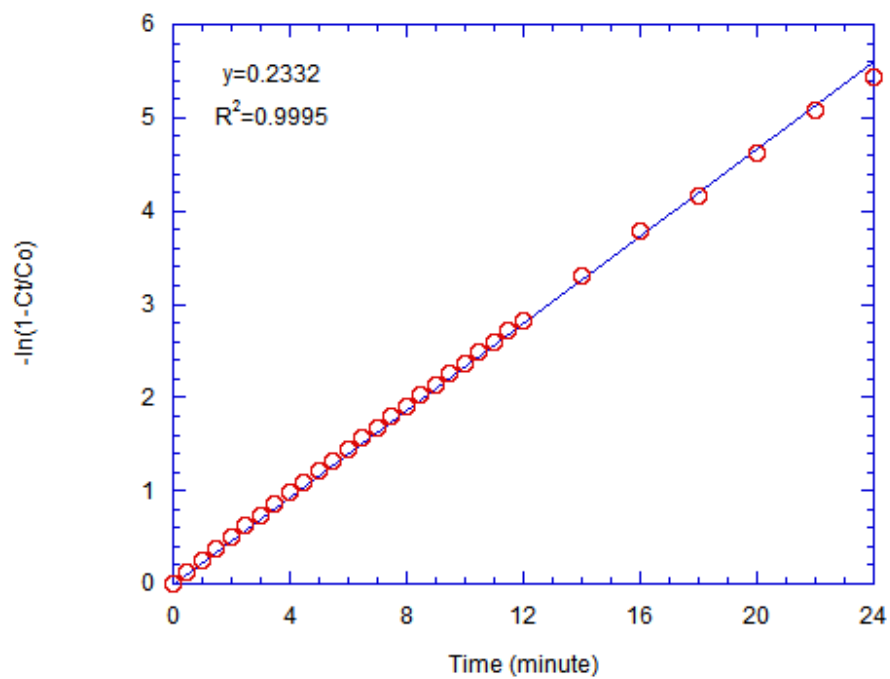


Figure 4-18 Linear Regression of Tracer Test ($Q_1 = Q_2 = 62.5$ mL/min)

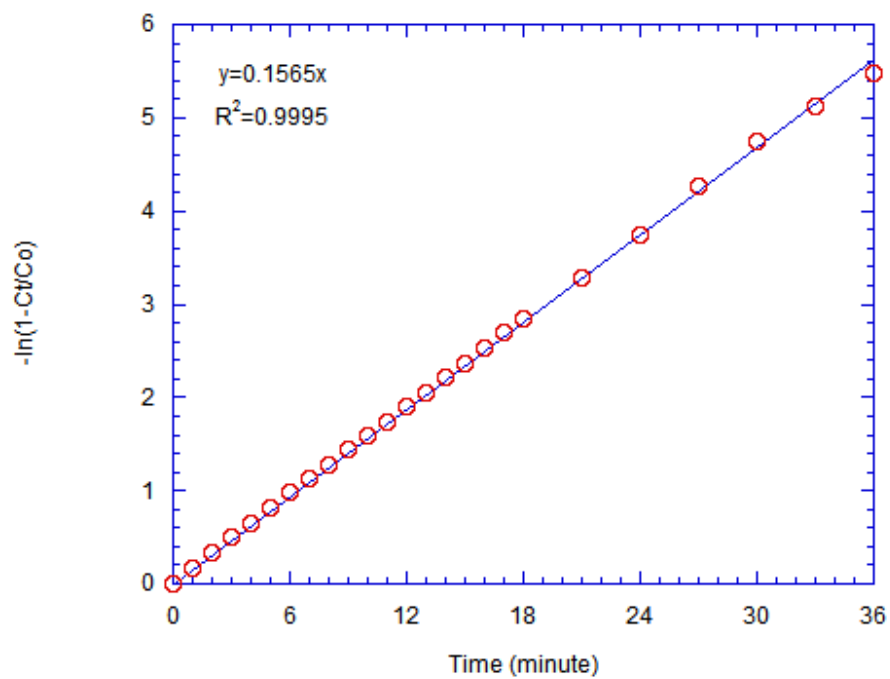


Figure 4-19 Linear Regression of Tracer Test ($Q_1 = Q_2 = 41.7$ mL/min)

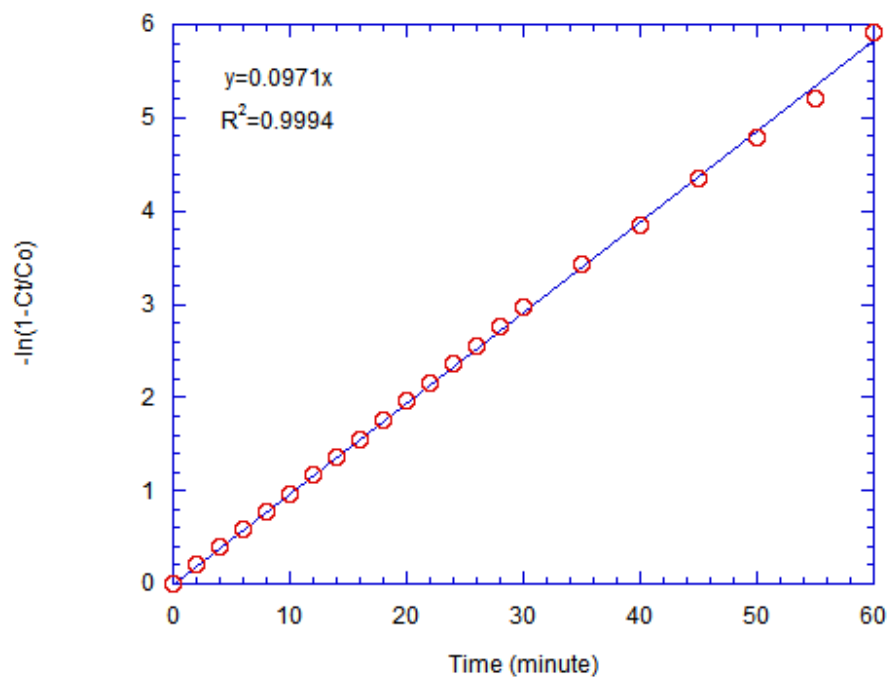


Figure 4-20 Linear Regression of Tracer Test ($Q_1 = Q_2 = 25$ mL/min)

(b) Tanks-in-series Model Method (Non-linear Regression)

The Tanks-in-series model was also applied to determine the mean residence time for the CSTR by setting the N value to be one and using nonlinear regression method.

Table 4-6 Mean Residence Times Determined from Non-linear Regression

Method				
Designed Mean Residence Time (<i>min</i>)	2	4	6	10
Actual Mean Residence Time (<i>min</i>)	2.20	4.11	6.20	10.35

Nonlinear regression is a superior method to linear regression of transformed data and produces more accurate results (Motulsky and Ransnas 1987). Even though linear regression is intuitively straightforward, it is not optimal because the transformation can distort the experimental errors. In this study, linear regression on the log-transformed data could enhance the errors associated with the points with large t values and overemphasize the importance of the points with large t values. Based on this, the mean residence time derived by nonlinear regression method will be used for the analysis of experimental data.

4.4 Performance of Disinfection Experiments

Four series of disinfection experiments were performed in the CSTR (Table 4-7) based on the batch disinfection experiments conducted under the similar experimental

conditions (temperature, disinfection dose range, initial microbial density) (Kaymak 2003). They are:

- (1) Inactivation of *E. coli* in stationary phase using monochloramine (MES);
- (2) Inactivation of *E. coli* in exponential phase using monochloramine (MEE);
- (3) Inactivation of *B. subtilis* vegetative cells in exponential phase using monochloramine (MBE);
- (4) Inactivation of *B. subtilis* spores using ozone (OBS).

Table 4-7 Performed Disinfection Experiments

Experiments	Initial Microbial Density (CFU/mL)	Mean Residence Time (min)	Temperature (°C)	pH
MES	10^3 , 10^4 , 10^5	2.20, 6.20, 10.35	15	7
MEE	10^3 , 10^4 , 10^5	2.20, 6.20, 10.35	15	7
MBE	10^3 , 10^4 , 10^5	2.20, 6.20, 10.35	15	7
OBS	10^3 , 10^4 , 10^5	2.20, 6.20, 10.35	15	8

The monochloramine disinfection experiments were performed at 15°C and pH 7 in the monochloramine disinfection system (Figure 4-6). Initial microbial density was determined at three levels of 10^3 , 10^4 , and 10^5 CFU/mL. The mean residence times in the CSTR were 2.20, 6.20 and 10.35 minutes.

The ozone disinfection experiments were conducted at 15°C and pH 8 in the ozone disinfection system (Figure 4-7). Initial microbial density was also set at three levels of 10^3 , 10^4 , and 10^5 CFU/mL. The mean residence times in the CSTR were 2.20, 4.11 and 6.20 minutes.

Bacterial suspension flow and disinfectant solution flow were simultaneously fed into the CSTR from the two reservoirs at predetermined flow rates. After steady-state conditions being achieved (3 to 4 residence times, which were determined by experiments and detailed in section 5.1), two test samples were taken from the reactor outlet for bacteria survival determination and disinfectant residual analysis; and two control samples were taken from the bottom of the reservoirs to determine the initial microbial density and the stock disinfectant concentration by correction for dilution in the reactor.

4.5 Data Analysis

The purposes of the disinfection experiments and data analysis were: (1) to determine the effects of initial microbial density on disinfection efficiency; (2) to test the predictability of the inactivation of *E. coli* and *B. subtilis* in the dynamic flow system from batch inactivation data.

StataTM 7 (Stata Corporation, College Station, TX) was applied to run the statistic analysis for the data. Three factors were controlled for each disinfection experiment: initial microbial density, disinfection dose, and mean residence time. Statistical methods

were used to test if these three factors had significant effects on inactivation efficiency in CSTR and what were the extents of such effects, especially initial microbial density.

Seven models have been used in batch disinfection kinetic analysis, which are summarized in Table 4-8. By using non-linear regression method, the best-fit model for each series of disinfection experiments and corresponding best-fit parameters were obtained in batch data analysis.

The predicted survival ratio in CSTR under steady-state condition was computed by combining the best-fit kinetics derived from batch data by:

$$\left(\frac{N}{N_0} \right)_{\text{predicted in CSTR}} = 1 + \frac{r_{\text{batch}} \theta}{N_0} \quad 3-36$$

where N_0 is the initial bacteria concentration; N is the predicted bacterial concentration in CSTR under steady-state condition; r is the microbial inactivation kinetics in batch system, and θ is the mean residence time.

A Matlab program was written (Appendix E) to predict the bacteria survival ratio in CSTR by using Matlab 5.2 (The MathWorks, Inc., Natick, MA). The results were also double-checked by using Excel solver function (Microsoft Corporation, Redmond, WA).

Table 4-8 Disinfection Kinetic Models Applied in Batch Analyses

Disinfection Models	Disinfection Rate Expression	Batch Survival Ratio Expression (demand-free)
Chick Model	$r = -kN$	$\ln \frac{N}{N_0} = -kt$
Chick-Watson Model	$r = -k' C^n N$	$\ln \frac{N}{N_0} = -k' C^n t$
Hom Model	$r = -k' m C^n t^{m-1} N$	$\ln \frac{N}{N_0} = -k' C^n t^m$
Power Law Model	$r = -k' C^n N^x$	$\ln \frac{N}{N_0} = -\frac{1}{x-1} \ln [1 + (x-1)k' C^n t N_0^{x-1}]$
Hom Power Law Model	$r = -k' m C^n t^{m-1} N^x$	$\ln \frac{N}{N_0} = -\frac{1}{x-1} [1 + (x-1)k' C^n t^m N_0^{x-1}]$
Series-event Model	$r_{n_i} = kCN_{i-1} - kCN_i$	$\ln \frac{N}{N_0} = -kCt + \ln \left(\sum_{i=0}^{n-1} \frac{(kCt)^i}{i!} \right)$
Multiple Target Model	$r_{N_i} = (n_C - i + 1)kCN_{i-1} - (n_C - i)kCN_i$	$\ln \frac{N}{N_0} = \ln [1 - (1 - e^{KCT})^{n_c}]$
Modified Multiple Target Model	$r_{N_i} = (n_C - i + 1)kC^n N_{i-1} - (n_C - i)kC^n N_i$	$\ln \frac{N}{N_0} = \ln [1 - (1 - e^{KC^n T})^{n_c}]$

Chapter 5 : Results and Discussion

5.1 Proposed and Achieved Experiments

A total of 48 (12 x 4) disinfection experiments were performed in the CSTR at a temperature of 15°C with three initial microbial density levels, three disinfectant dose levels, and three mean residence time levels. The pH was set at 7 for monochloramine disinfection and 8 for ozone disinfection. The experimental design matrix is displayed in Table 5-1. Three more duplicate experiments were performed for each series of disinfection experiments.

Table 5-1 Disinfection Experiments Design in CSTR

Experiments	MES	MEE	MBE	OBS
Initial Microbial Density (CFU/mL)	$10^3, 10^4, 10^5$	$10^3, 10^4, 10^5$	$10^3, 10^4, 10^5$	$10^3, 10^4, 10^5$
Disinfection Dose (mg/L)	0.75, 1.0, 1.5	0.75, 1.0, 1.5	1.0, 1.5, 2.0	1.5, 2.0, 2.5
Mean Residence Time (Minutes)	2.20, 6.20, 10.35	2.20, 6.20, 10.35	2.20, 6.20, 10.35	2.20, 6.20, 10.35
Temperature (°C)	15	15	15	15
pH	7	7	7	8

The proposed and achieved experiments are shown through Figure 5-1 to Figure 5-4. Most of the proposed experiments were achieved, except for the inactivation of *B. subtilis* vegetative cells using monochloramine at the initial microbial density level of 10^5 CFU/mL. 144 observations were obtained.

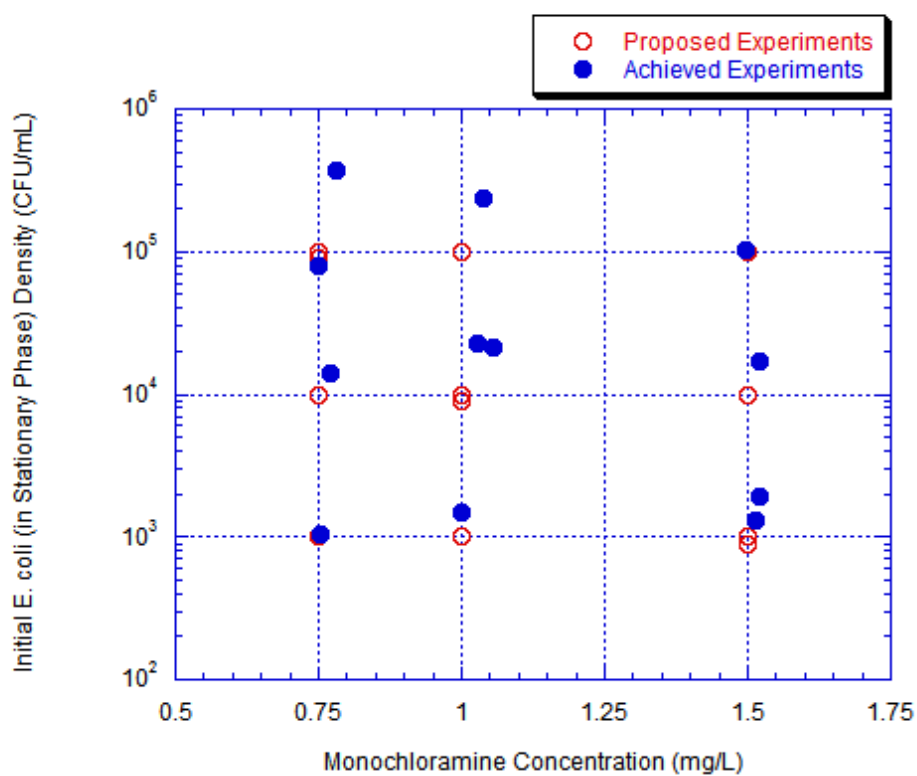


Figure 5-1 Proposed and Achieved Experiments

(*E. coli* in Stationary Phase)

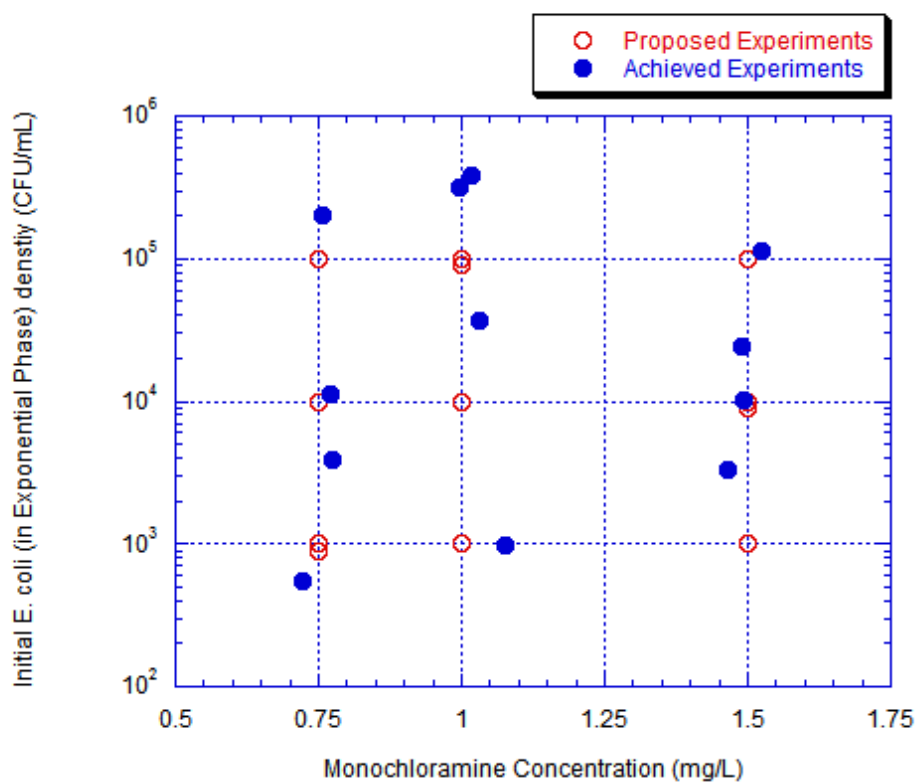


Figure 5-2 Proposed and Achieved Experiments

(*E. coli* in Exponential Phase)

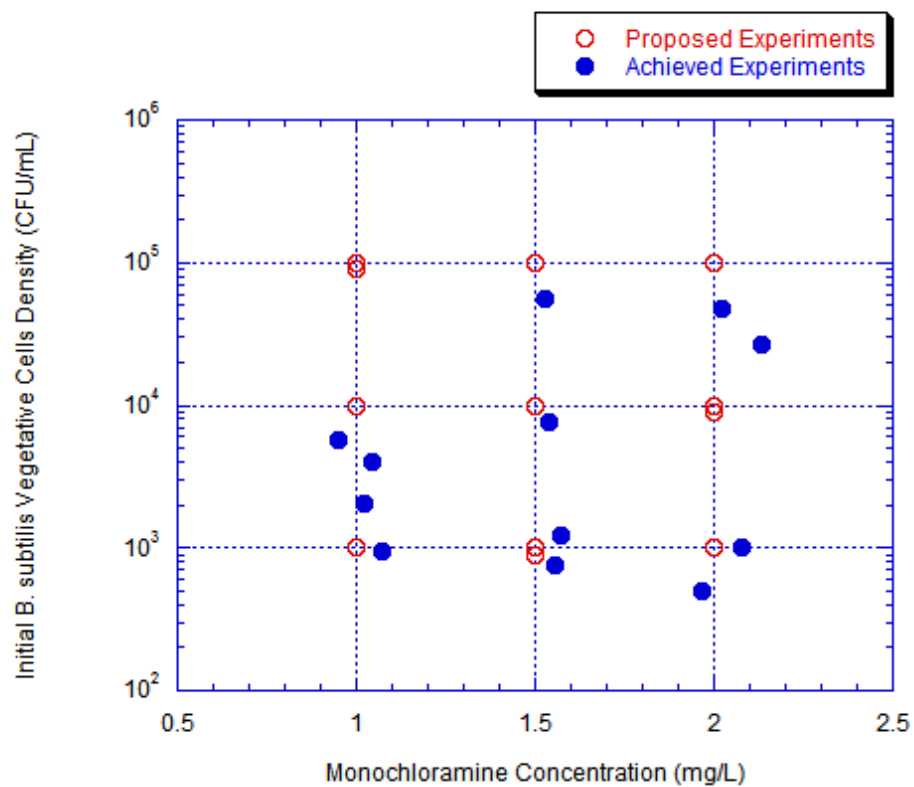


Figure 5-3 Proposed and Achieved Experiments

(*B. subtilis* Vegetative Cells in Exponential Phase)

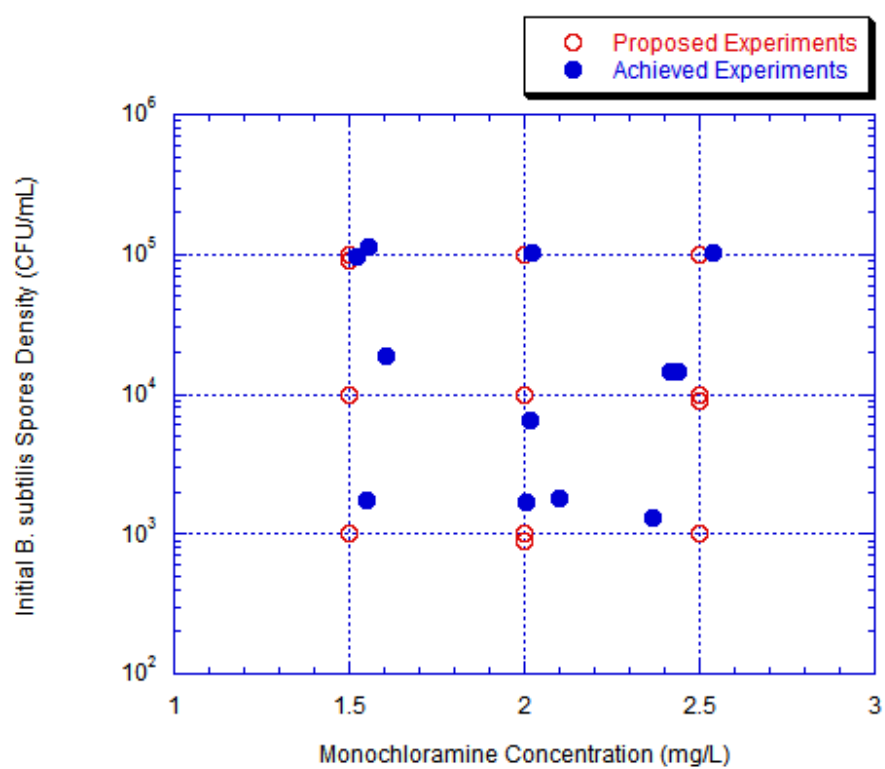


Figure 5-4 Proposed and Achieved Experiments (*B. subtilis* Spores)

5.2 Steady-state Condition Determination of the System

Before each series of disinfection experiments, one experiment was conducted in the CSTR system under the same experimental condition to determine the minimum time needed for the system to achieve steady-state condition. To start the experiment, the microbial suspension and the disinfectant solution were fed into the CSTR simultaneously at the pre-determined flow rate at time zero. Samples were taken at times equal to one through six mean residence times.

5.2.1 Monochloramine Disinfection System

Three series of disinfection experiments were conducted in the monochloramine disinfection system. After two mean residence times, the concentrations of both monochloramine and bacteria (*E. coli* in stationary phase, *E. coli* in exponential phase, and *B. subtilis* vegetative cells in exponential phase) remained steady (Figure 5-5, Figure 5-6, and Figure 5-7). The sampling time for the subsequent disinfection experiments was then determined to be at three mean residence times from the start of the experiment. The standard deviation of monochloramine concentration and bacteria survival ratio after two residence times are shown in Table 5-2. No monochloramine decay was observed in both reservoir and reactor.

Table 5-2 Relative Standard Deviation of Disinfection Systems at Steady-state

Condition				
Experiments	MES	MEE	MBE	OBS
RSD of Disinfectant Concentration	0.029	0.017	0.011	0.038
RSD of Bacteria Survival Ratio (ln units)	0.057	0.084	0.283	0.034
# of Data Points	5	5	5	4

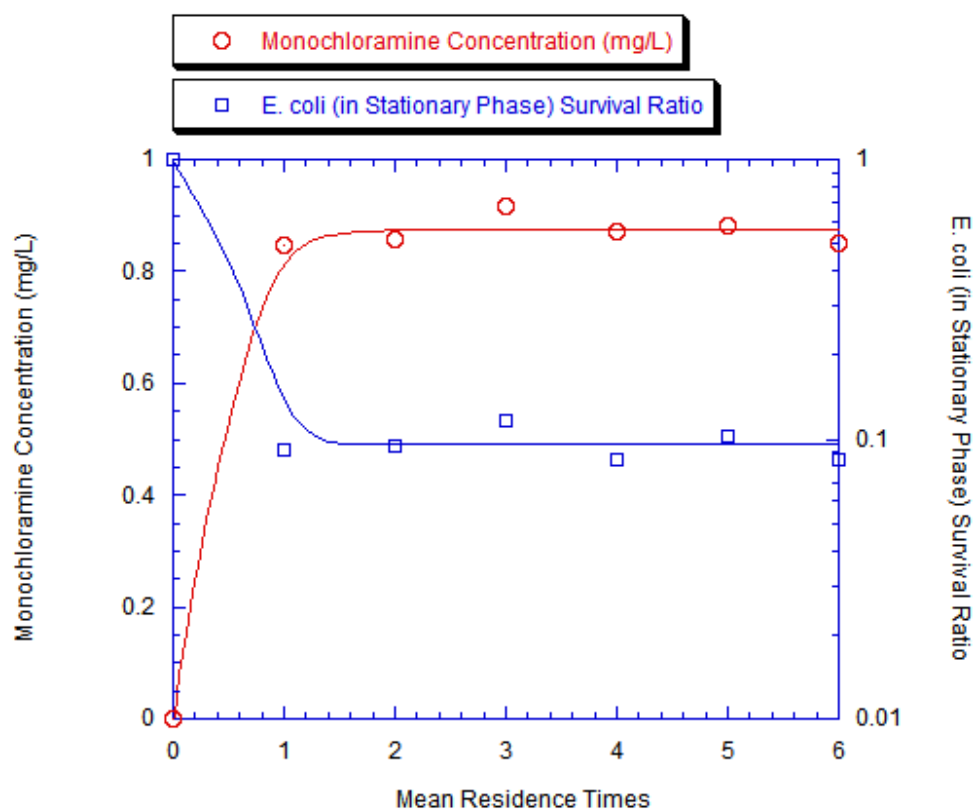


Figure 5-5 Steady-state Condition Determination

(*E. coli* in Stationary Phase, $\theta = 10.35$ minutes)

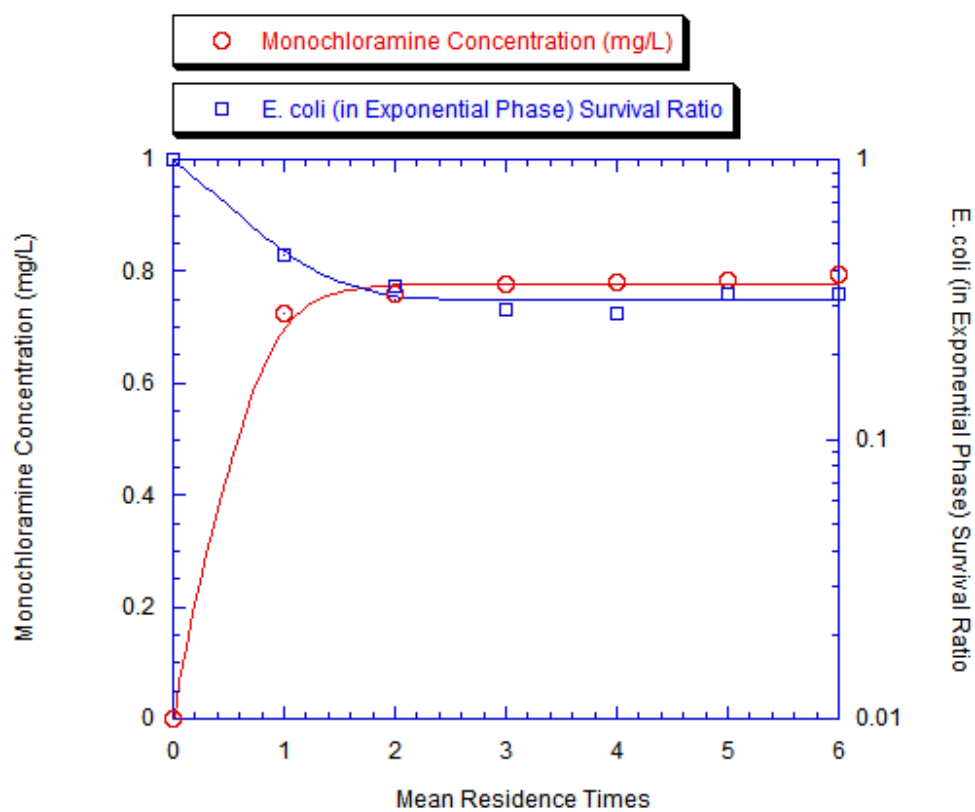


Figure 5-6 Steady-state Condition Determination

(*E. coli* in Exponential Phase, $\theta = 6.20$ minutes)

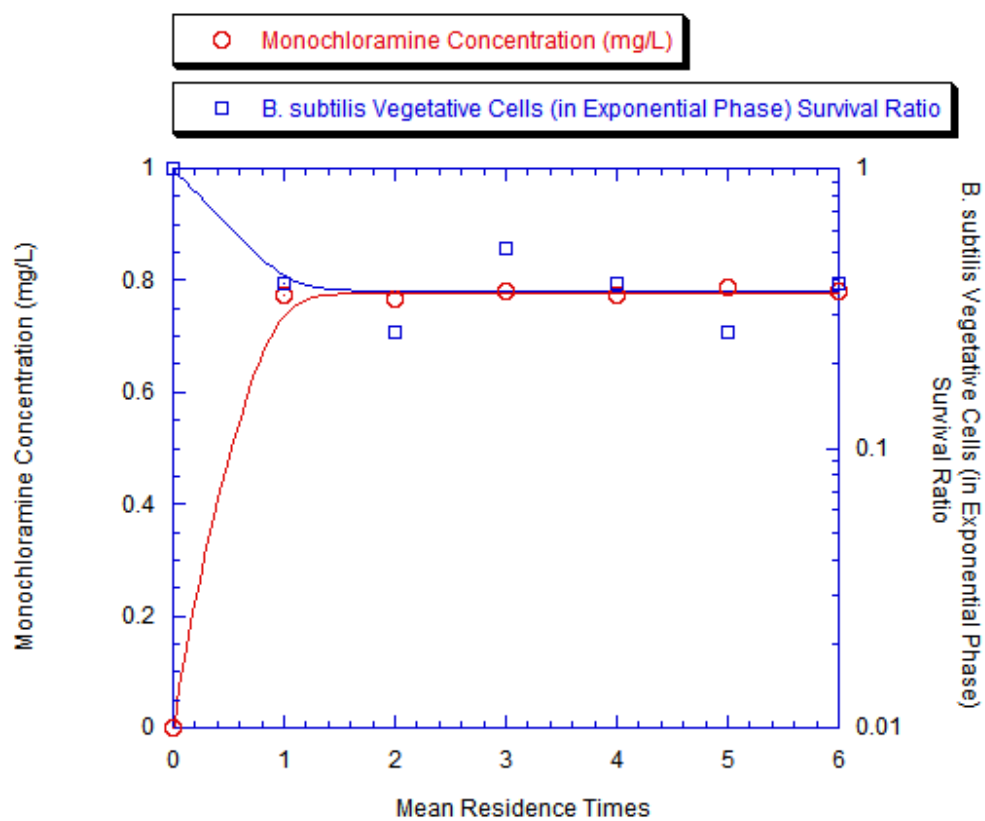


Figure 5-7 Steady-state Condition Determination

(*B. subtilis* Vegetative Cells in Exponential Phase, $\theta = 6.20$ minutes)

5.2.2 Ozone Disinfection System

Ozone disinfection on *B. subtilis* spores experiments were conducted in the ozone disinfection system. After three mean residence times, the concentrations of both ozone and *B. subtilis* spores remained steady (Figure 5-8 and Table 5-2). So the sampling time for the following ozone disinfection experiments was determined to be at four mean residence times.

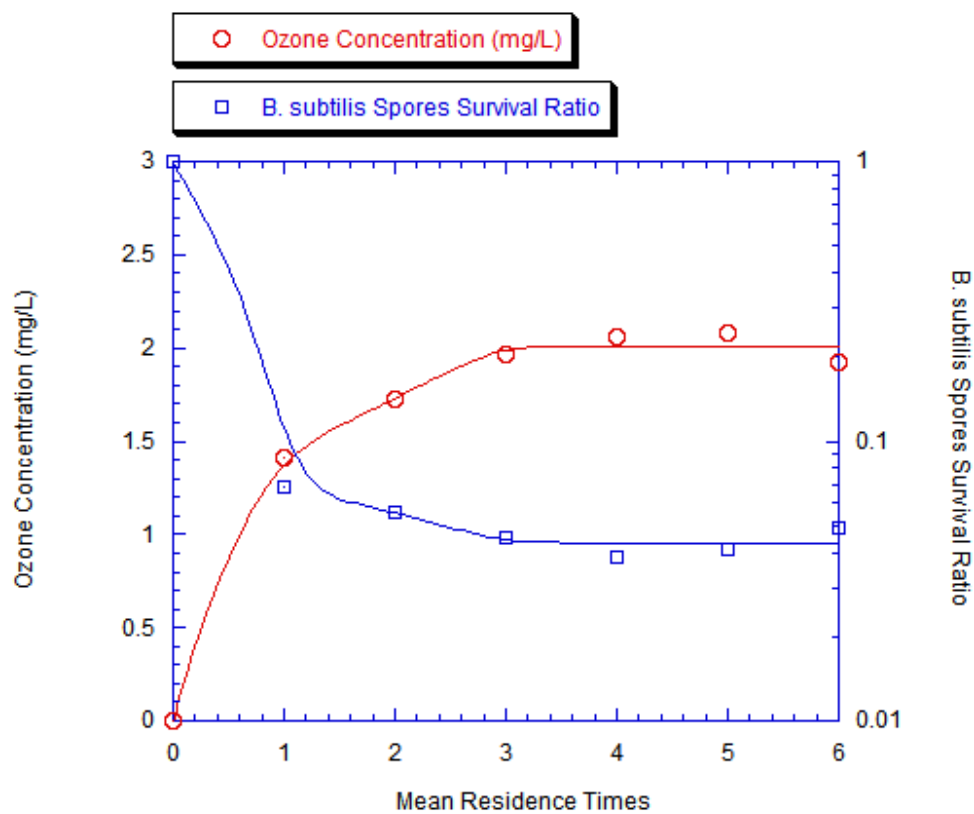


Figure 5-8 Steady-state Condition Determination

(*B. subtilis* Spores, $\theta = 4.11$ minutes)

5.3 Prediction of CSTR Performance from Batch Kinetics and CSTR Data

5.3.1 Inactivation of *E. coli* in Stationary Phase Using Monochloramine

5.3.1.1 Batch Kinetics

Disinfection kinetics were reported from experiments conducted in a batch system by Kaymak (2003) for the inactivation of *E. coli* in stationary phase using monochloramine. The Hom Power Law model was found to be the best-fit model with the values of best-fit parameters given below in Table 5-3.

**Table 5-3 Batch Best-fit Model and Parameters for Stationary Phase *E. coli*
Inactivation by Monochloramine**

Best-fit Model	Best-fit Parameters			
	$k' \text{ (min}^{-1}\text{)}$	n	m	x
Hom Power Law	0.004832	2.4737	2.9479	1.2180

5.3.1.2 CSTR Disinfection and Batch Predictions

Based on the steady-state mass balance relationship in CSTR and the Hom Power Law inactivation kinetics expression in batch reactor, the following equation was derived to predict the *E. coli* (in stationary phase) survival ratio in CSTR (Appendix B).

$$\left(\frac{N}{N_0}\right)_{predicted} = 1 - mk'C^n \theta \left(\frac{N}{N_0}\right)_{predicted}^x N_0^{x-1} \left\{ \frac{\left[\left(\frac{N}{N_0}\right)_{predicted}^{1-x} - 1\right] N_0^{1-x}}{(x-1)k'C^n} \right\}^{\left(\frac{1}{1-m}\right)} \quad 5-1$$

The observed results and the predicted results for each disinfection experiment on *E. coli* in stationary phase are shown from Figure 5-9 to Figure 5-20. The overall comparison was displayed in Figure 5-21.

Generally, the comparison data points distributed evenly around the diagonal on which observed survival ratio is equal to predicted survival ratio. The power regression line (linear regression line if the survival ratio being expressed in logarithm units) of comparison data is parallel to but under the diagonal, which means the over-prediction of survival ratio in CSTR from batch system. The differences between observed survival ratio (in ln units) and predicted survival ratio (in ln units) have a mean of -0.3427 and a standard deviation of 0.8510.

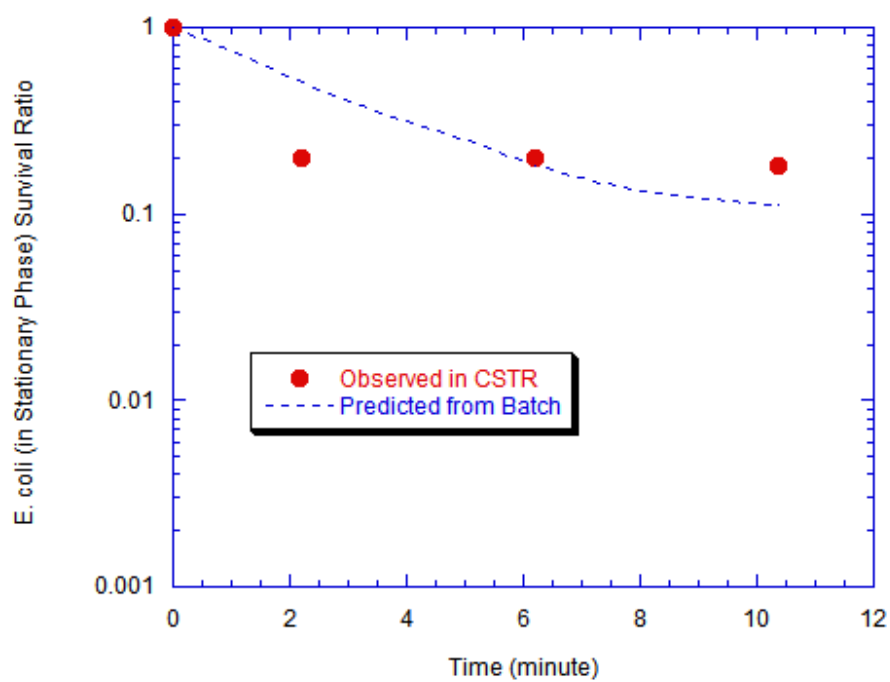


Figure 5-9 Inactivation of *E. coli* in Stationary Phase using Monochloramine
 $(N_0 = 10^3 \text{ CFU/mL}, C = 0.75 \text{ mg/L})$

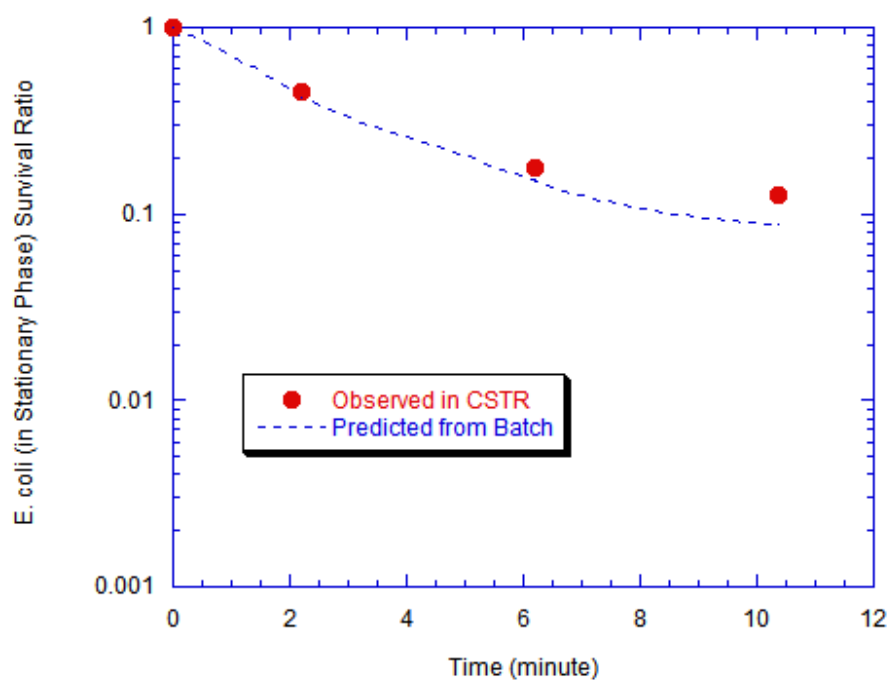


Figure 5-10 Inactivation of *E. coli* in Stationary Phase using Monochloramine

($N_0 = 10^4$ CFU/mL, $C = 0.75$ mg/L)

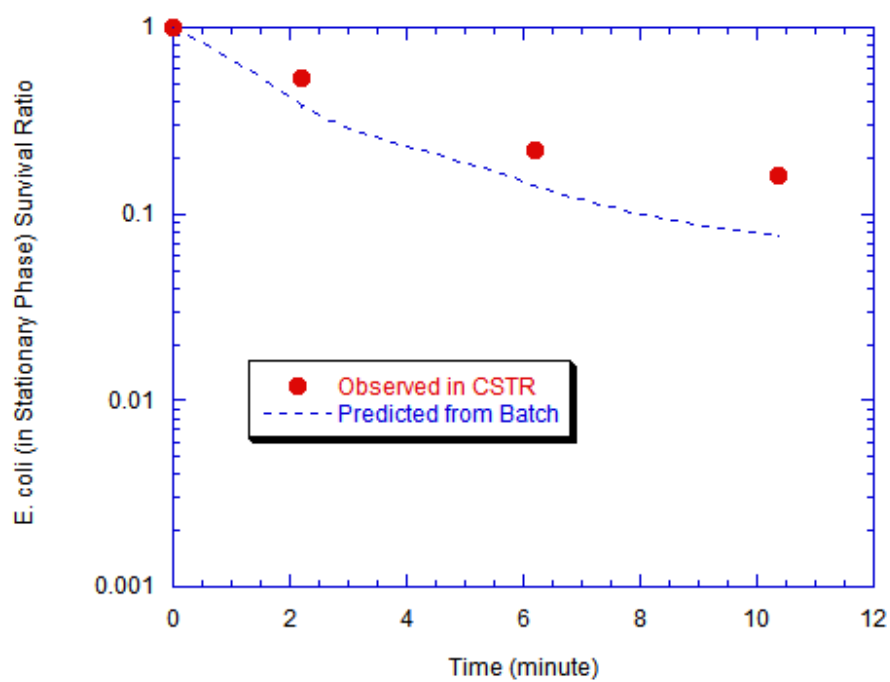


Figure 5-11 Inactivation of *E. coli* in Stationary Phase using Monochloramine

$(N_0 = 10^5 \text{ CFU/mL}, C = 0.75 \text{ mg/L})$

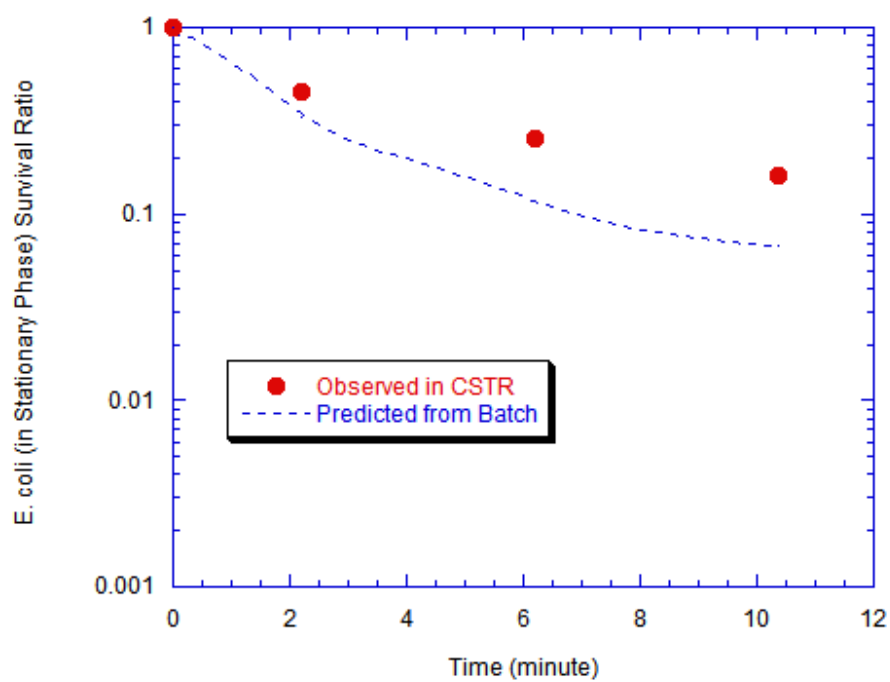


Figure 5-12 Inactivation of *E. coli* in Stationary Phase using Monochloramine

$(N_0 = 10^5 \text{ CFU/mL}, C = 0.75 \text{ mg/L})$

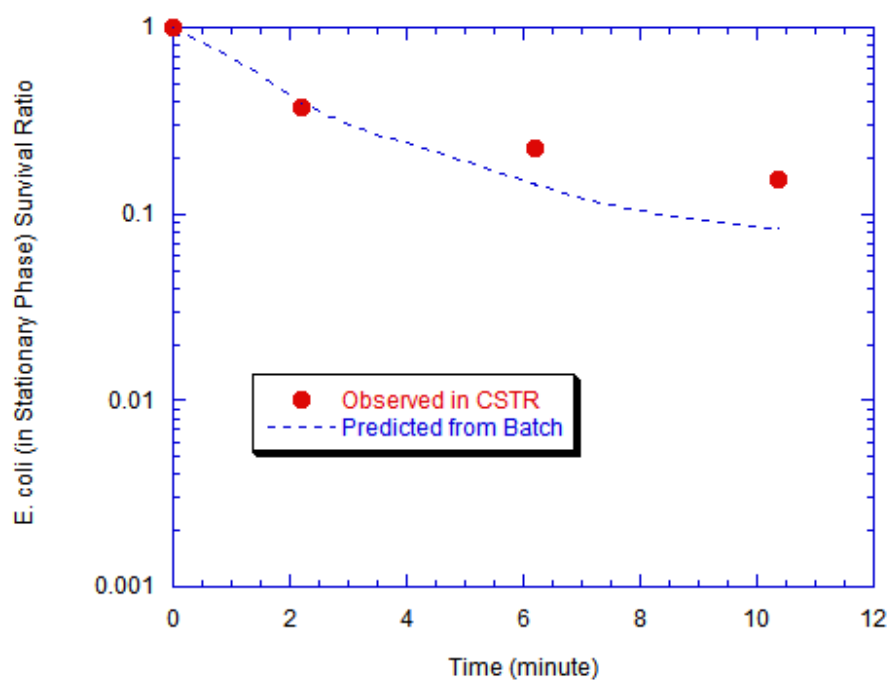


Figure 5-13 Inactivation of *E. coli* in Stationary Phase using Monochloramine

$(N_0 = 10^3 \text{ CFU/mL}, C = 1.0 \text{ mg/L})$

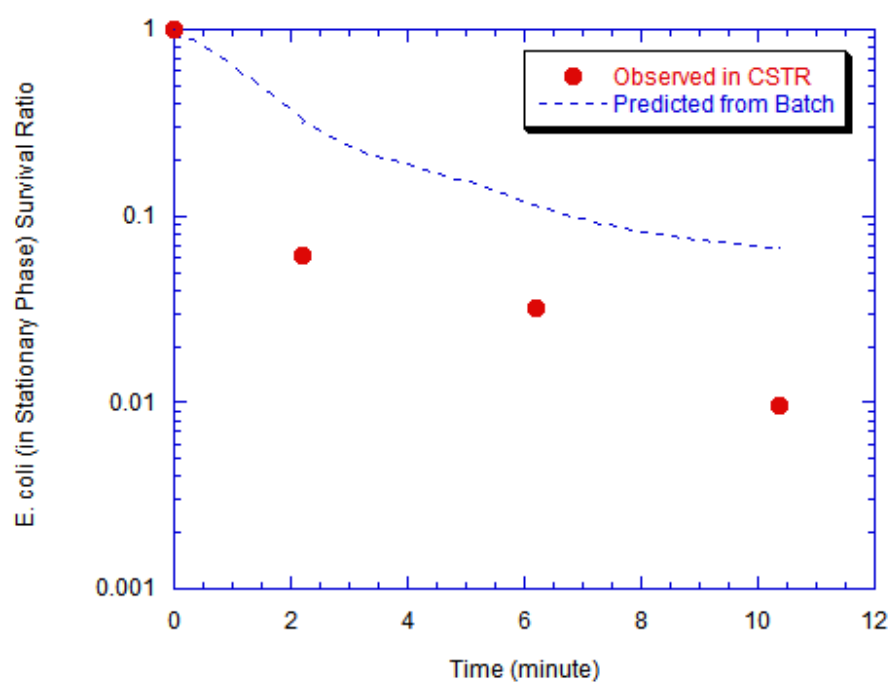


Figure 5-14 Inactivation of *E. coli* in Stationary Phase using Monochloramine

$(N_0 = 10^4 \text{ CFU/mL}, C = 1.0 \text{ mg/L})$

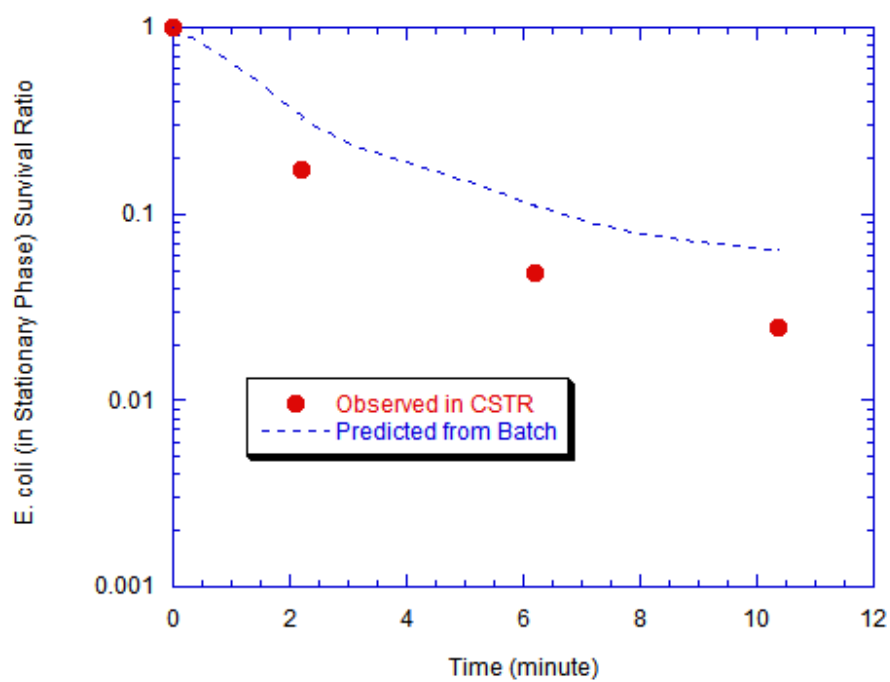


Figure 5-15 Inactivation of *E. coli* in Stationary Phase using Monochloramine

($N_0 = 10^4$ CFU/mL, $C = 1.0$ mg/L)

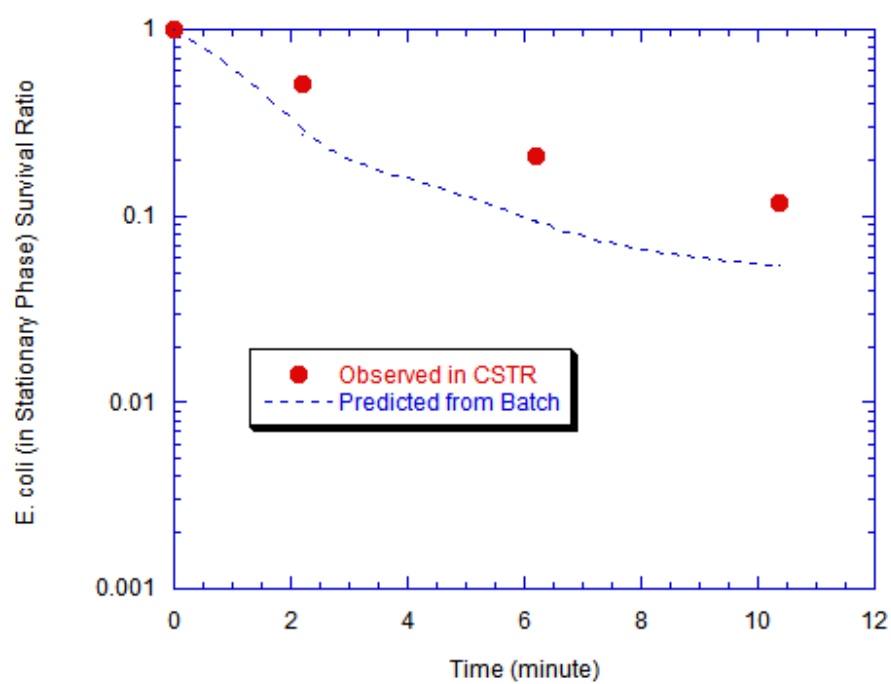


Figure 5-16 Inactivation of *E. coli* in Stationary Phase using Monochloramine

$(N_0 = 10^5 \text{ CFU/mL}, C = 1.0 \text{ mg/L})$

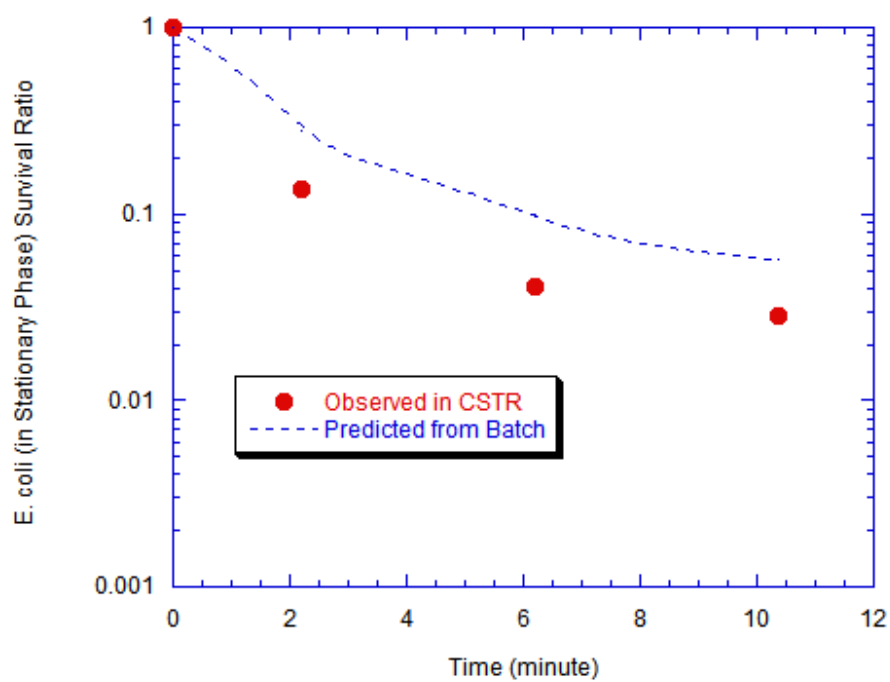


Figure 5-17 Inactivation of *E. coli* in Stationary Phase using Monochloramine
($N_0 = 10^3$ CFU/mL, $C = 1.5$ mg/L)

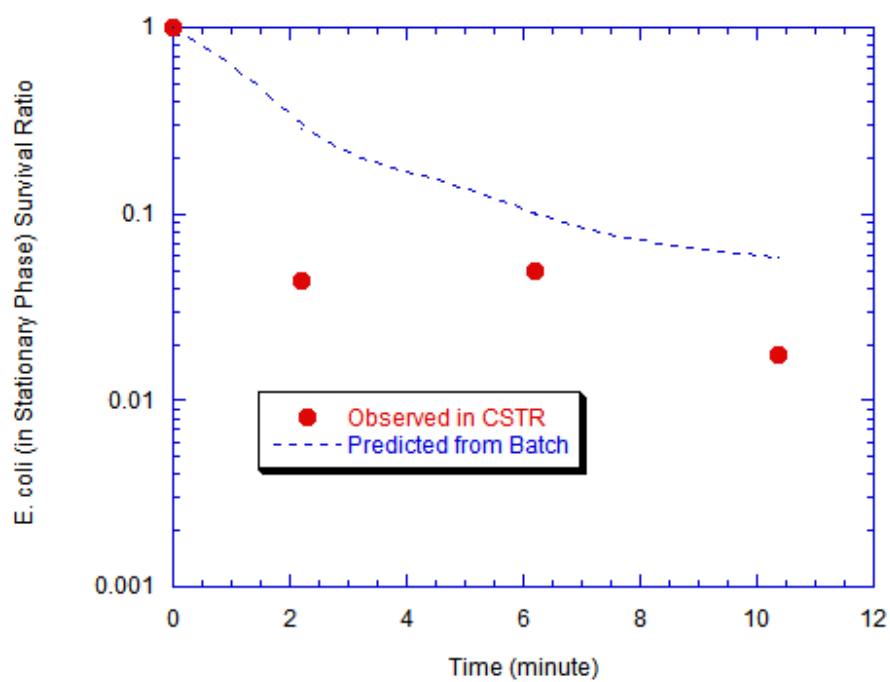


Figure 5-18 Inactivation of *E. coli* in Stationary Phase using Monochloramine

($N_0 = 10^3$ CFU/mL, $C = 1.5$ mg/L)

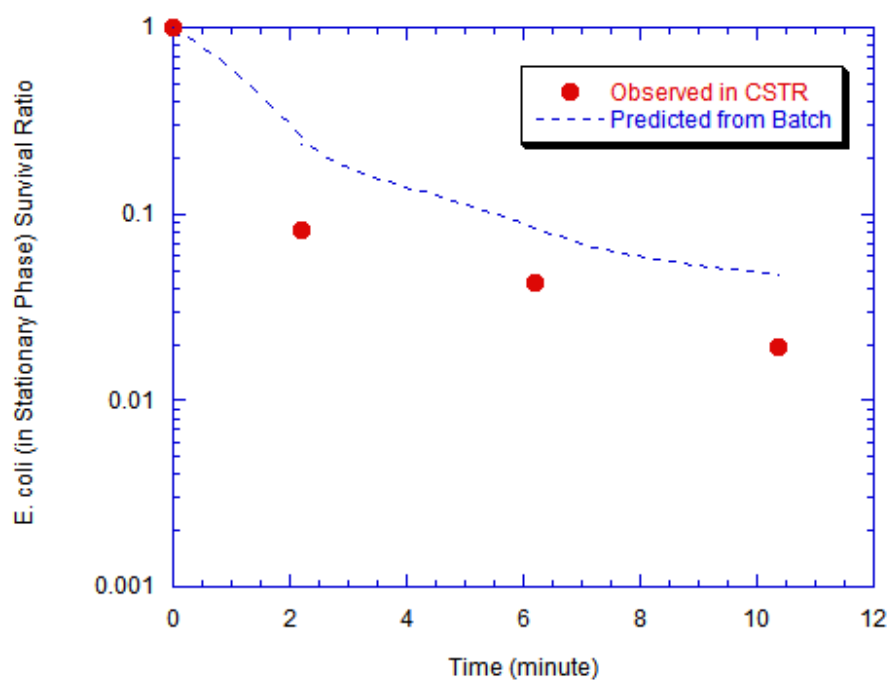


Figure 5-19 Inactivation of *E. coli* in Stationary Phase using Monochloramine

$(N_0 = 10^4 \text{ CFU/mL}, C = 1.5 \text{ mg/L})$

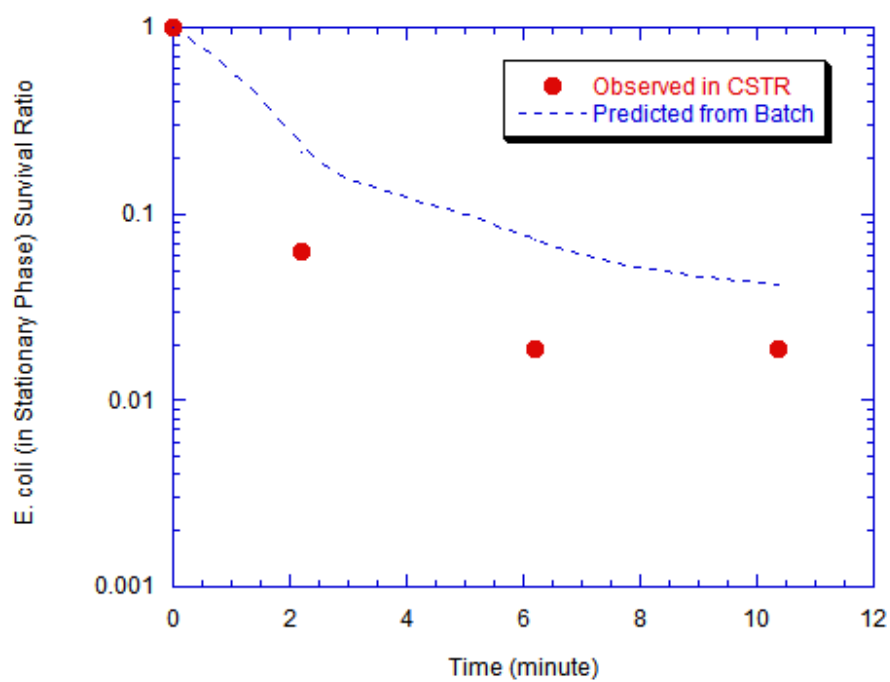


Figure 5-20 Inactivation of *E. coli* in Stationary Phase using Monochloramine

$(N_0 = 10^5 \text{ CFU/mL}, C = 1.5 \text{ mg/L})$

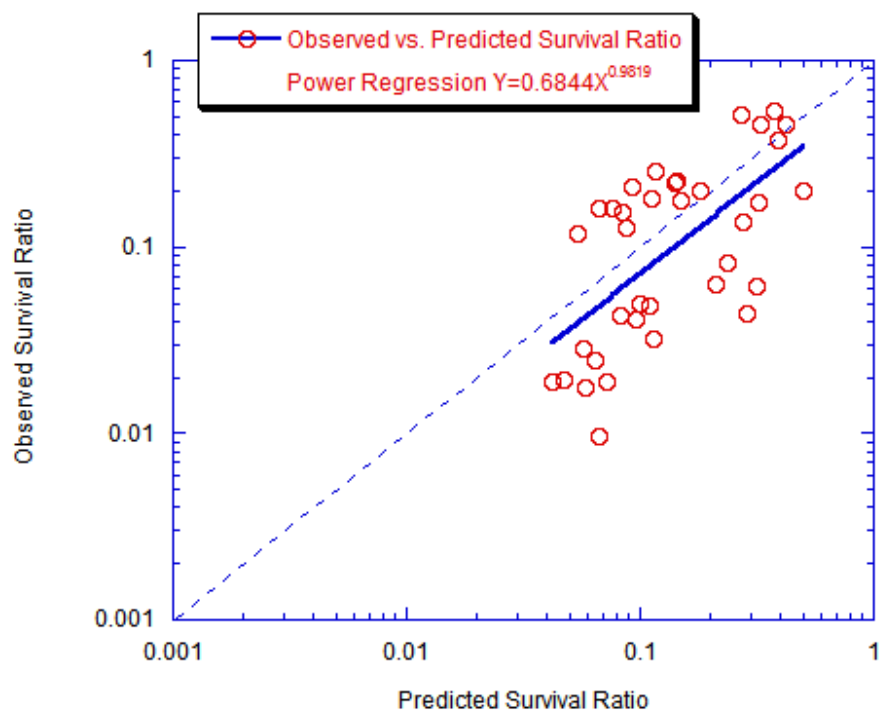


Figure 5-21 Overall Comparison of Observed vs. Predicted Survival Ratio
(Inactivation of *E. coli* in Stationary Phase Using Monochloramine)

5.3.1.3 Linear Regression between Observed and Predicted Data

The linear regression was made between observed survival ratios (-ln units) and predicted survival ratios (-ln units) from Chick, Chick-Watson, Hom, Power Law, and Hom Power Law model. The regression equations and R-square values were listed in Table 5-4, where $SR_{observed}$ is *E. coli* survival ratio computed from experimental data in –ln units and $SR_{predicted}$ is *E. coli* survival ratio predicted from batch kinetics in –ln units.

Table 5-4 Linear Regression of Observation and Prediction (MES)

Model	Linear Regression Equation	R ²
Chick	$SR_{observed} = 1.3928 \times SR_{predicted} - 0.0275$	0.4979
Chick-Watson	$SR_{observed} = 1.3822 \times SR_{predicted} - 0.0006$	0.4742
Hom	$SR_{observed} = 1.0785 \times SR_{predicted} + 0.4276$	0.4687
Power Law	$SR_{observed} = 1.3817 \times SR_{predicted} - 0.0092$	0.4541
Hom Power Law	$SR_{observed} = 0.9819 \times SR_{predicted} + 0.3792$	0.4041

Note: SR is $-\ln(\text{Survival Ratio})$.

A t-test was used to test two hypotheses from the linear regressions: (1) the slope is equal to one; (2) the intercept is equal to zero. With a significance level of 5%, neither the hypothesis one ($P = 0.0512$) nor the hypothesis two ($P = 0.2067$) can be rejected.

5.3.1.4 Paired t-test between CSTR Observation and Batch Prediction

Paired t-test was applied to compare the observed survival ratio (ln units) of *E. coli* in stationary phase in CSTR and the predicted survival ratio (ln units) from batch kinetics for five models. The hypothesis of observed survival ratios (ln units) were statistically equal to predicted survival ratios (ln units) was examined at a significance level of 5%. None of the models' prediction passed paired t-test (Table 5-5).

Table 5-5 Paired t-test Comparison between Observed and Predicted Survival Ratio (ln units) for *E. coli* in Stationary Phase

Model	Probability ($\alpha = 5\%$)
Chick	3.223×10^{-5}
Chick-Watson	3.650×10^{-5}
Hom	0.00016
Power Law	0.00005
Hom Power Law	0.02106

5.3.2 Inactivation of *E. coli* in Exponential Phase Using Monochloramine

5.3.2.1 Batch Kinetics

From the kinetic analysis on batch disinfection data, the Hom model was considered to be the best-fit model to describe the disinfection behavior of

monochloramine on *E. coli* in exponential phase in batch system (Kaymak 2003). The values of best-fit parameters are given below in Table 5-6.

Table 5-6 Batch Best-fit Model and Parameters for Exponential Phase *E. coli* Inactivation by Monochloramine

Best-fit Model	Best-fit Parameters		
	$k' \text{ (min}^{-1}\text{)}$	n	m
Hom	0.0780	2.3796	2.5989

5.3.2.2 CSTR Disinfection and Batch Predictions

The equation used for predicting *E. coli* (in exponential phase) survival ratio in CSTR was derived from CSTR mass balance relationship and batch Hom model kinetics (Appendix C).

$$\left(\frac{N}{N_0}\right)_{\text{predicted}} = 1 - m(k'C^n)^{\frac{1}{m}} \theta \left(\frac{N}{N_0}\right)_{\text{predicted}} \left[-\ln\left(\frac{N}{N_0}\right)_{\text{predicted}} \right]^{\left(1-\frac{1}{m}\right)} \quad 5-2$$

The observed results and the predicted results for each disinfection experiment on *E. coli* in exponential phase are demonstrated from Figure 5-22 to Figure 5-33. The overall comparison was displayed in Figure 5-34.

To summarize the comparison, most predictions from the Hom model seemed to underestimate the corresponding observed survival ratios. The power regression line (linear regression line with the survival ratio being expressed in logarithm units) of comparison data is almost parallel to the diagonal. The regression line locates above the

diagonal and means the under-prediction of survival ratio in CSTR from batch system. The differences between observed survival ratio (in ln units) and predicted survival ratio (in ln units) have a mean of 0.2701 and a standard deviation of 0.4900.

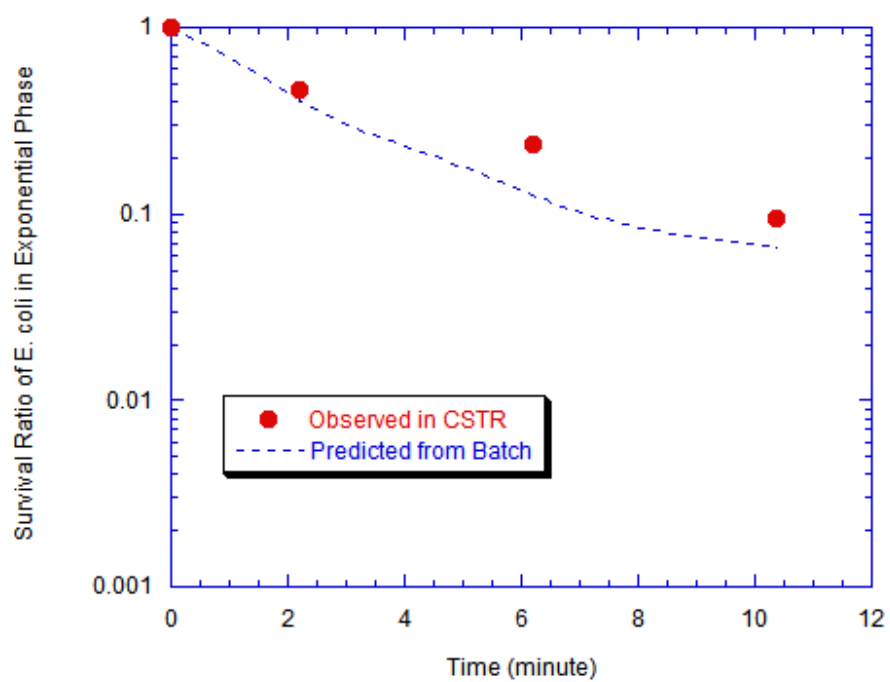


Figure 5-22 Inactivation of *E. coli* in Exponential Phase Using Monochloramine ($N_0 = 10^3$ CFU/mL, $C = 0.75$ mg/L)

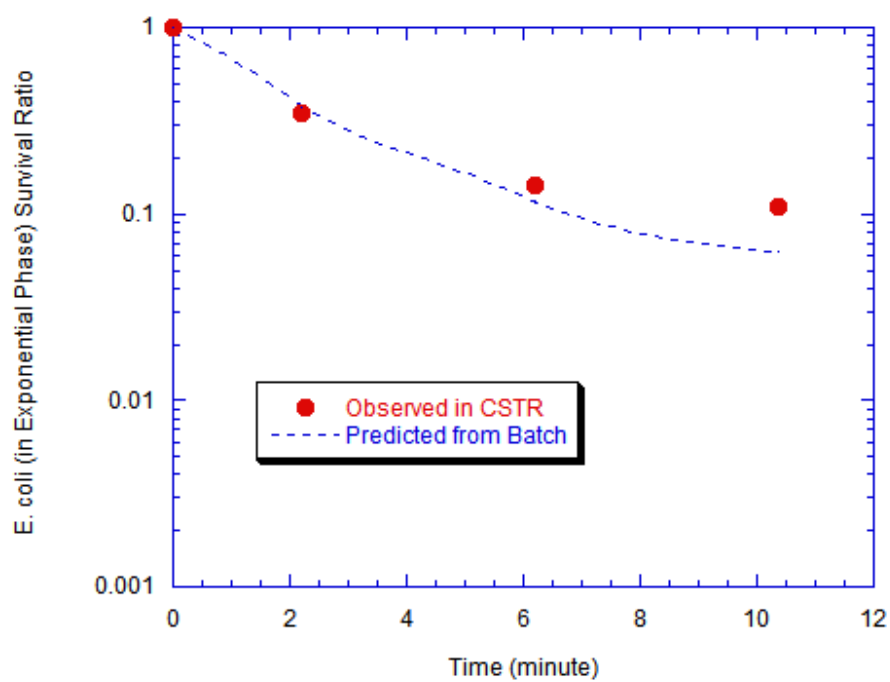


Figure 5-23 Inactivation of *E. coli* in Exponential Phase Using Monochloramine ($N_0 = 10^3$ CFU/mL, $C = 0.75$ mg/L)

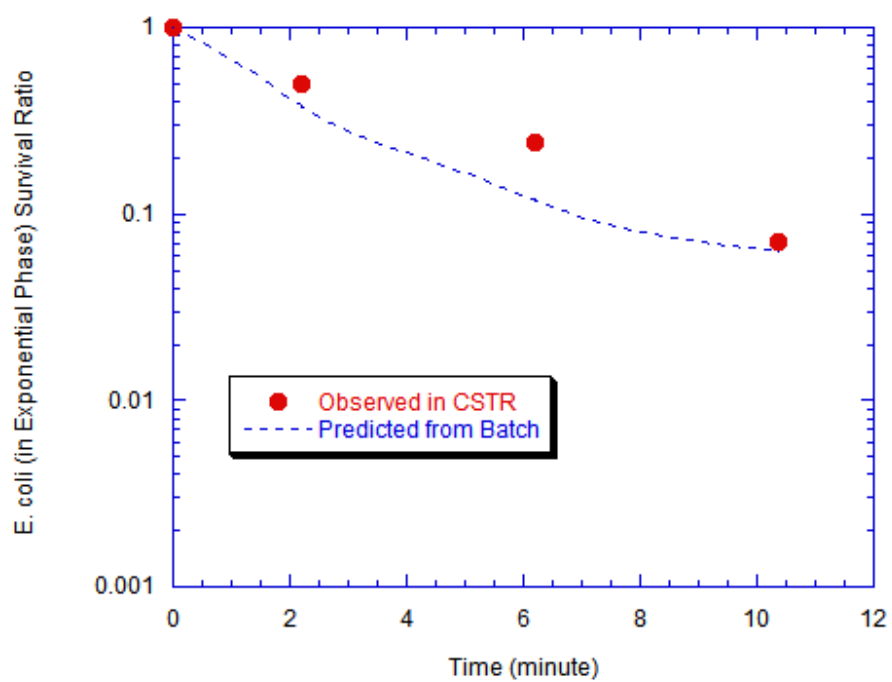


Figure 5-24 Inactivation of *E. coli* in Exponential Phase Using Monochloramine ($N_0 = 10^4$ CFU/mL, $C = 0.75$ mg/L)

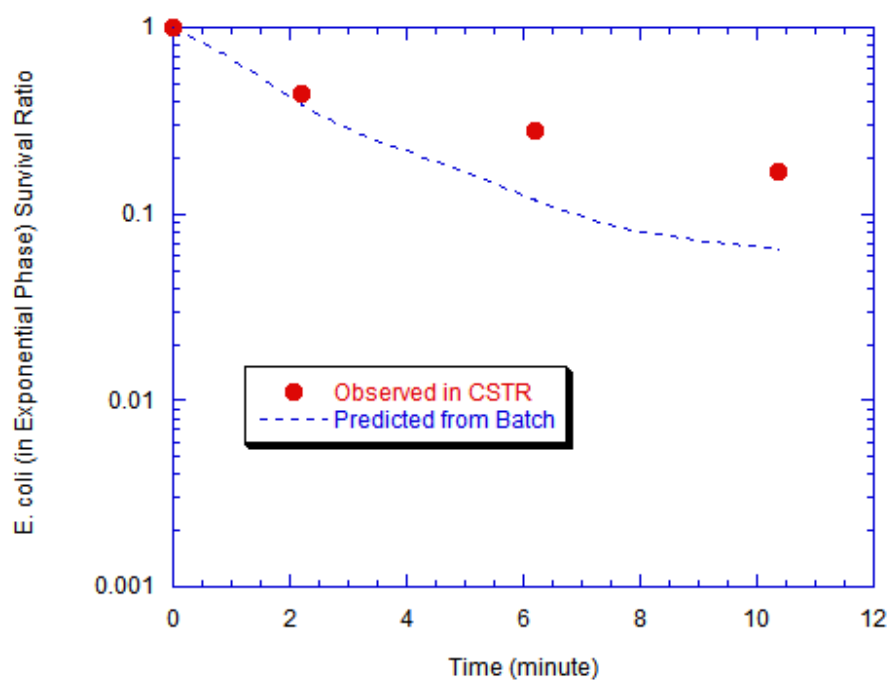


Figure 5-25 Inactivation of *E. coli* in Exponential Phase Using Monochloramine ($N_0 = 10^5$ CFU/mL, $C = 0.75$ mg/L)

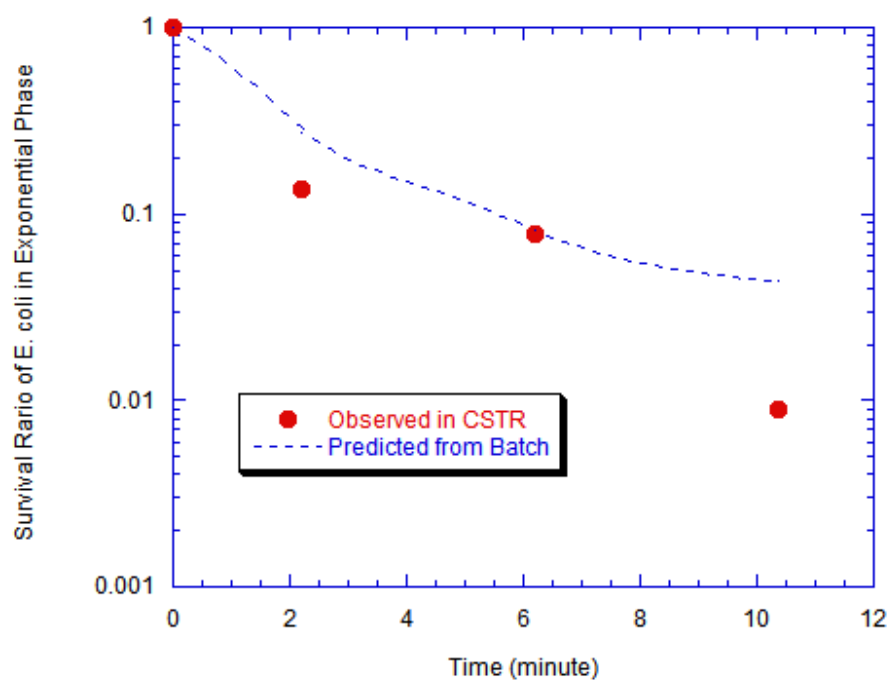


Figure 5-26 Inactivation of *E. coli* in Exponential Phase Using Monochloramine ($N_0 = 10^3$ CFU/mL, $C = 1.0$ mg/L)

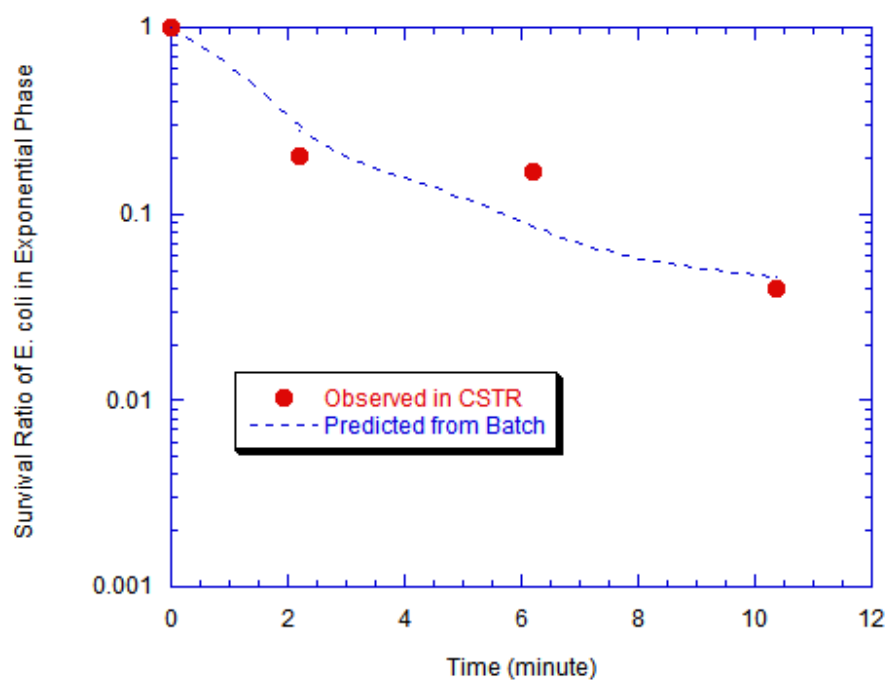


Figure 5-27 Inactivation of *E. coli* in Exponential Phase Using Monochloramine ($N_0 = 10^4$ CFU/mL, $C = 1.0$ mg/L)

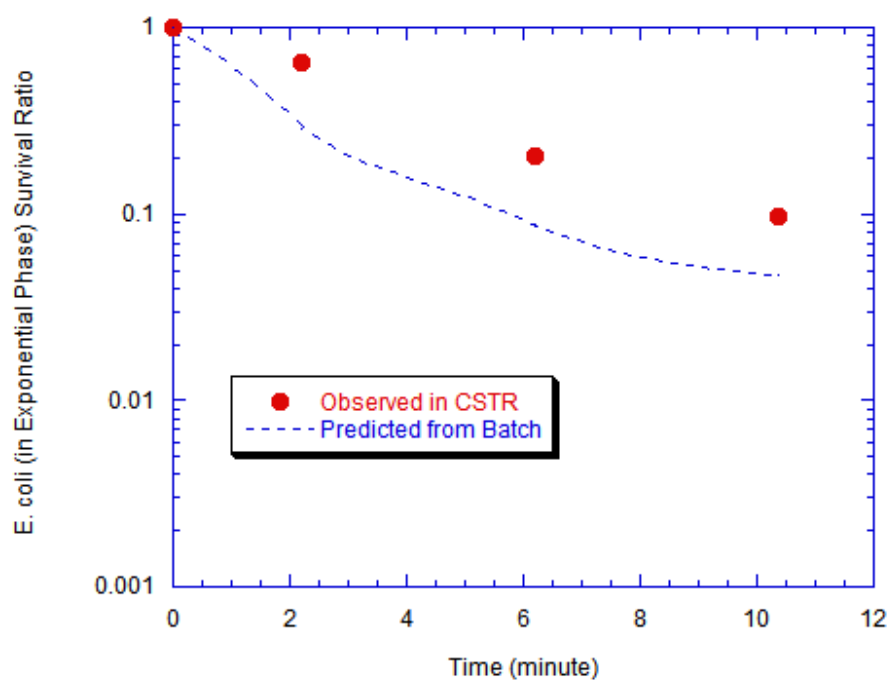


Figure 5-28 Inactivation of *E. coli* in Exponential Phase Using Monochloramine ($N_0 = 10^5$ CFU/mL, $C = 1.0$ mg/L)

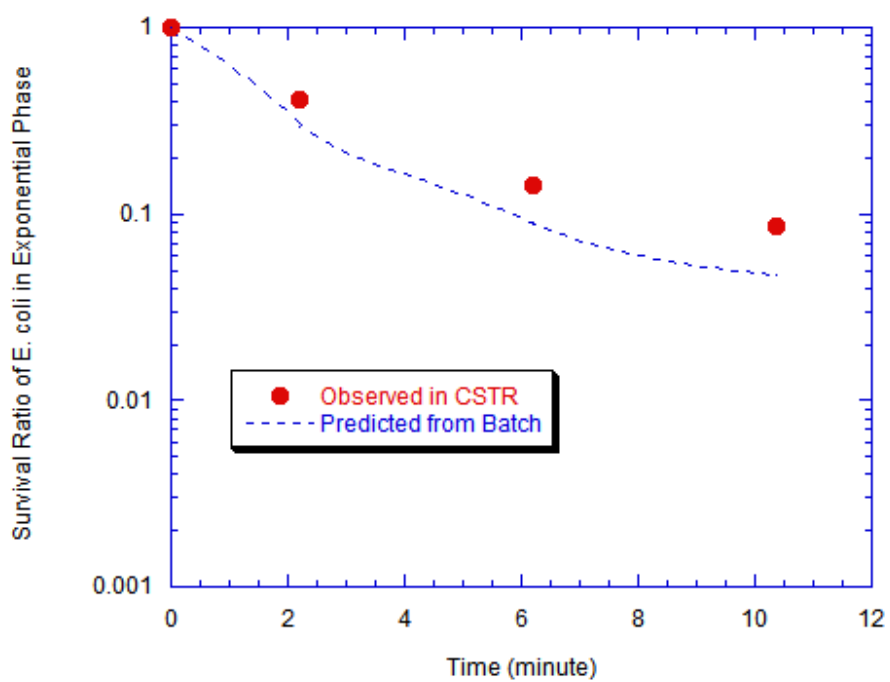


Figure 5-29 Inactivation of *E. coli* in Exponential Phase Using Monochloramine ($N_0 = 10^5$ CFU/mL, $C = 1.0$ mg/L)

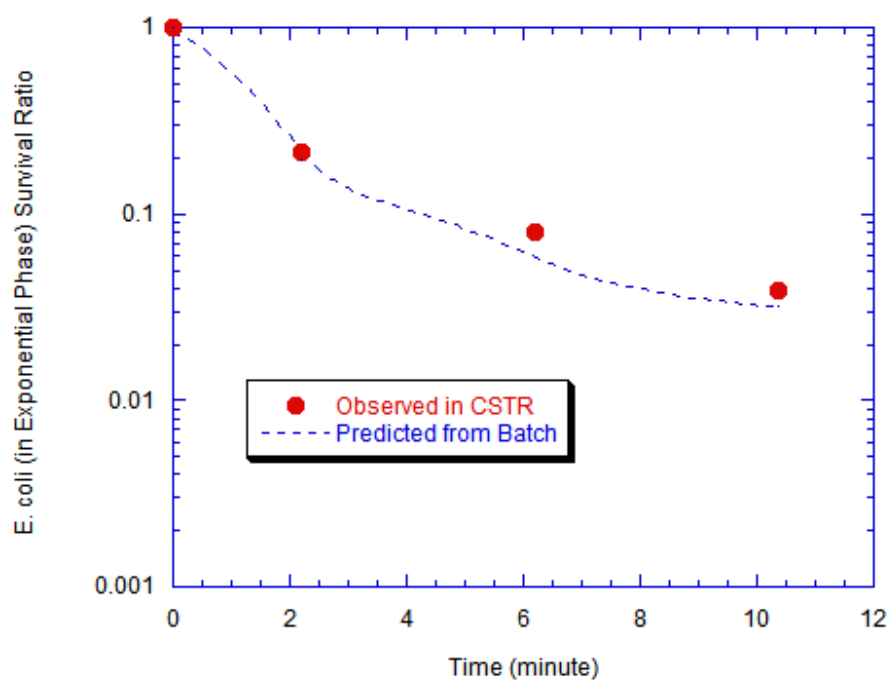


Figure 5-30 Inactivation of *E. coli* in Exponential Phase Using Monochloramine ($N_0 = 10^3$ CFU/mL, $C = 1.5$ mg/L)

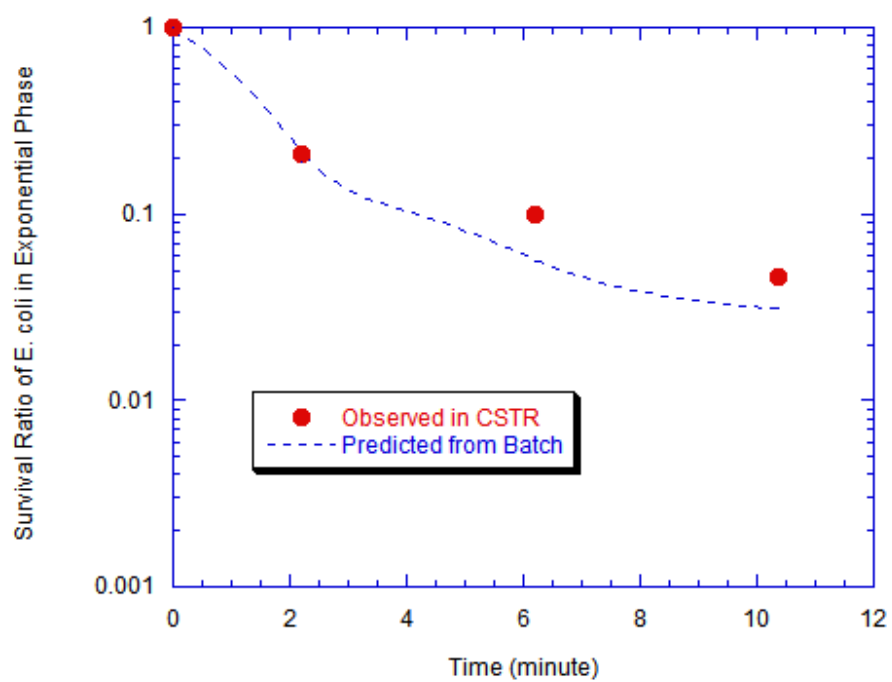


Figure 5-31 Inactivation of *E. coli* in Exponential Phase Using Monochloramine ($N_0 = 10^4$ CFU/mL, $C = 1.5$ mg/L)

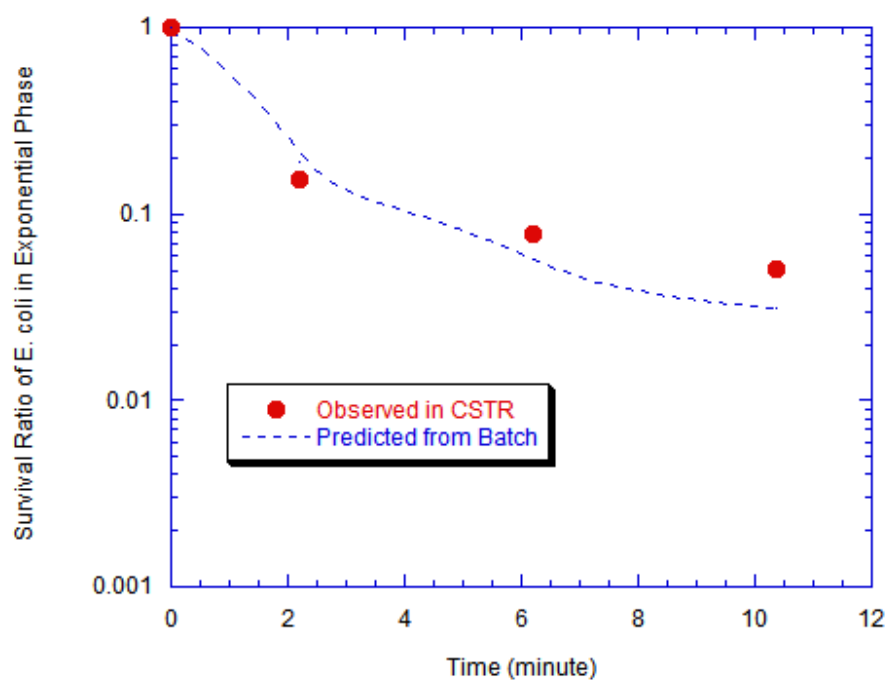


Figure 5-32 Inactivation of *E. coli* in Exponential Phase Using Monochloramine ($N_0 = 10^4$ CFU/mL, $C = 1.5$ mg/L)

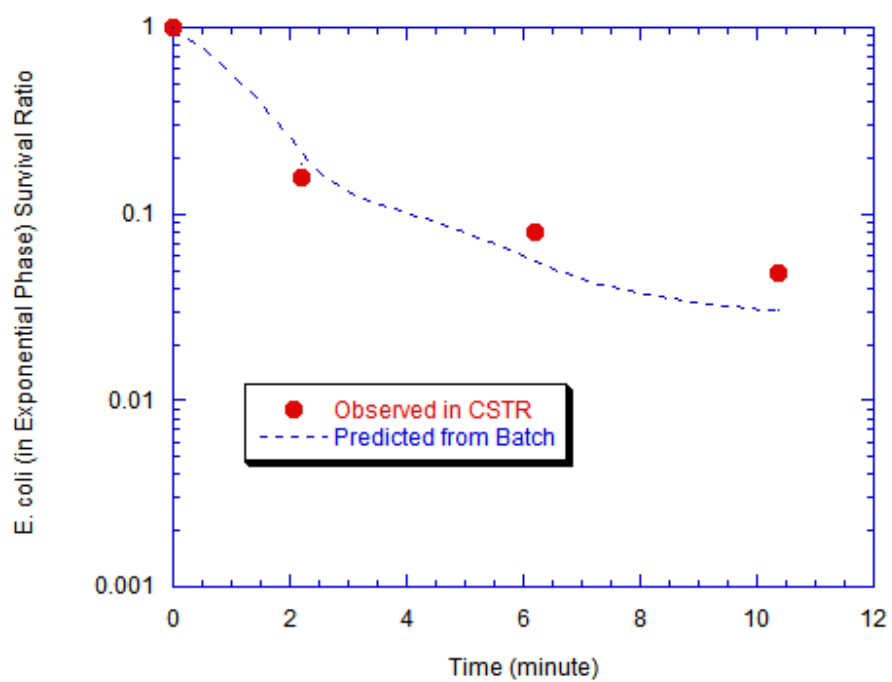


Figure 5-33 Inactivation of *E. coli* in Exponential Phase Using Monochloramine ($N_0 = 10^5$ CFU/mL, $C = 1.5$ mg/L)

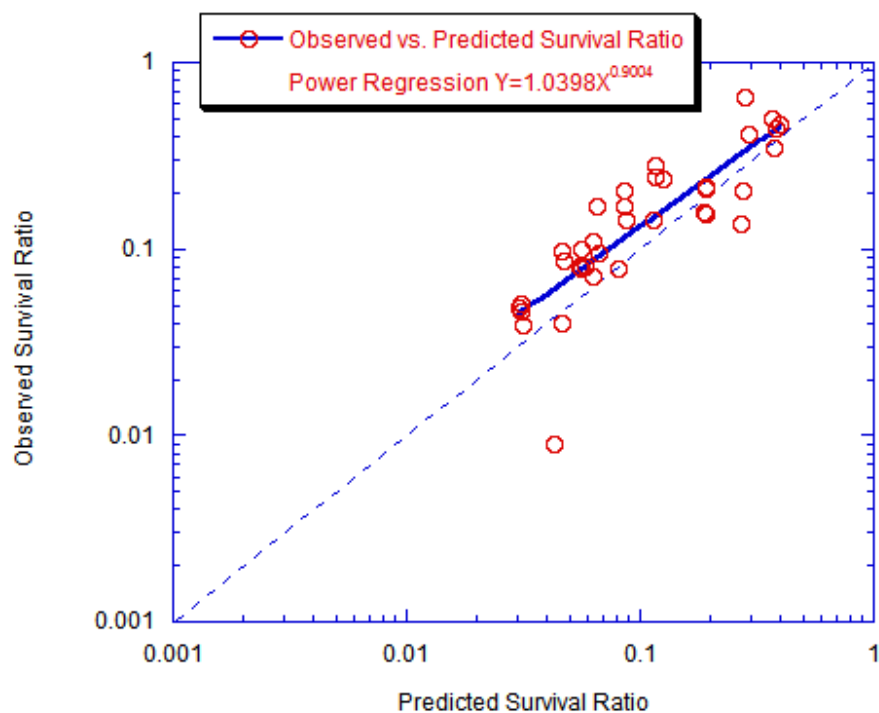


Figure 5-34 Overall Comparison of Observed vs. Predicted Survival Ratio
(Inactivation of *E. coli* in Exponential Phase Using Monochloramine)

5.3.2.3 Linear Regression between Observed and Predicted Data

The results from linear regression were shown in Table 5-7 between observed survival ratios (-ln units) and predicted survival ratios (-ln units) for five models. Using t-test with a significance level of 5%, the hypothesis of slope to be unity ($P = 0.2184$) could not be rejected; but the hypothesis of intercept to be zero ($P=0.0425$) was rejected.

Table 5-7 Linear Regression of Observation and Prediction (MEE)

Model	Linear Regression Equation	R^2
Chick	$SR_{observed} = 1.3129 \times SR_{predicted} - 0.2908$	0.7130
Chick-Watson	$SR_{observed} = 1.3415 \times SR_{predicted} - 0.3179$	0.6945
Hom	$SR_{observed} = 0.9004 \times SR_{predicted} - 0.0390$	0.6998
Power Law	$SR_{observed} = 1.3311 \times SR_{predicted} - 0.3151$	0.7026
Hom Power Law	$SR_{observed} = 0.8895 \times SR_{predicted} - 0.0276$	0.7154

Note: SR is $-\ln(\text{Survival Ratio})$

5.3.2.4 Paired t-test between CSTR Observation and Batch Prediction

A paired t-test was utilized to examine the hypothesis that the observed survival ratios (ln units) were statistically equal to predicted survival ratios (ln units) for *E. coli* in exponential phase. With a significance level of 5%, all of the models' prediction failed paired t-test (Table 5-8).

Table 5-8 Paired t-test Comparison between Observed and Predicted Survival Ratio (ln units) for *E. coli* in Exponential Phase

Model	Probability ($\alpha = 5\%$)
Chick	0.00361
Chick-Watson	0.00279
Hom	0.00232
Power Law	0.00354
Hom Power Law	0.00112

5.3.3 Inactivation of *B. subtilis* Vegetative Cells in Exponential Phase Using Monochloramine

5.3.3.1 Batch Kinetics

Table 5-9 gives the values of best-fit parameters of the Hom model which is the best-fit model used for expressing the kinetics of monochloramine disinfection on *B. subtilis* vegetative cells in exponential phase in batch system (Kaymak 2003).

Table 5-9 Batch Best-fit Model and Parameters for Exponential Phase *B. subtilis* Vegetative Cells Inactivation by Monochloramine

Best-fit Model	Best-fit Parameters		
	$k' \text{ (min}^{-1}\text{)}$	n	m
Hom	0.8031	0.2009	0.5414

5.3.3.2 CSTR Disinfection and Batch Predictions

The equation to predict CSTR performance from batch Hom kinetics was derived as

$$\left(\frac{N}{N_0}\right)_{\text{predicted}} = 1 - m(k' C^n)^{\frac{1}{m}} \theta \left(\frac{N}{N_0}\right)_{\text{predicted}} \left[-\ln\left(\frac{N}{N_0}\right)_{\text{predicted}} \right]^{\left(1 - \frac{1}{m}\right)} \quad 5-2$$

The separate comparison between the observed survival ratio and the predicted survival ratio for each disinfection experiment on *B. subtilis* vegetative cells are displayed from Figure 5-35 to Figure 5-46. The overall comparison is shown in Figure 5-47.

The comparison data points distributed mostly below the diagonal. The power regression line (linear regression line if the survival ratio being expressed in logarithm units) of comparison data is parallel to while under the diagonal, which means the over-prediction of survival ratio in CSTR from batch system. The differences between observed survival ratio (in ln units) and predicted survival ratio (in ln units) have a mean of -1.229 and a standard deviation of 0.833.

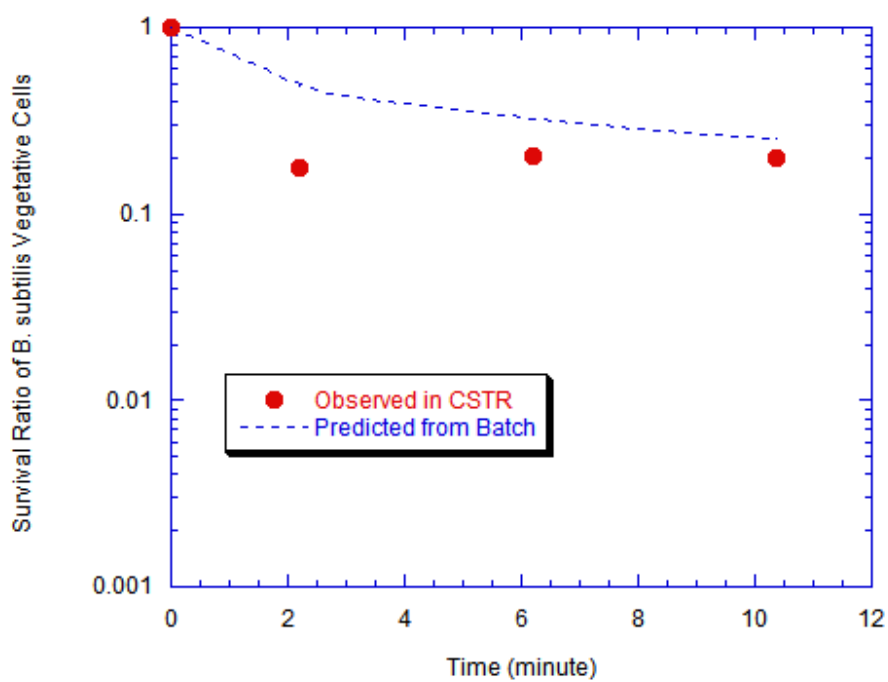


Figure 5-35 Inactivation of *B. Subtilis* Vegetative Cells in Exponential Phase
Using Monochloramine ($N_0 = 10^3$ CFU/mL, $C = 1.0$ mg/L)

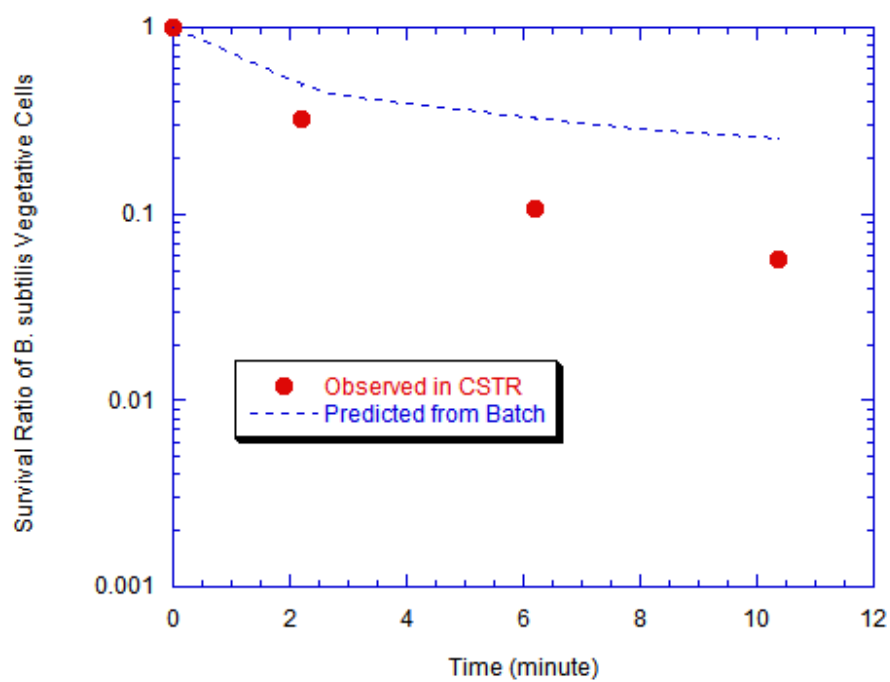


Figure 5-36 Inactivation of *B. Subtilis* Vegetative Cells in Exponential Phase
Using Monochloramine ($N_0 = 10^3$ CFU/mL, $C = 1.0$ mg/L)

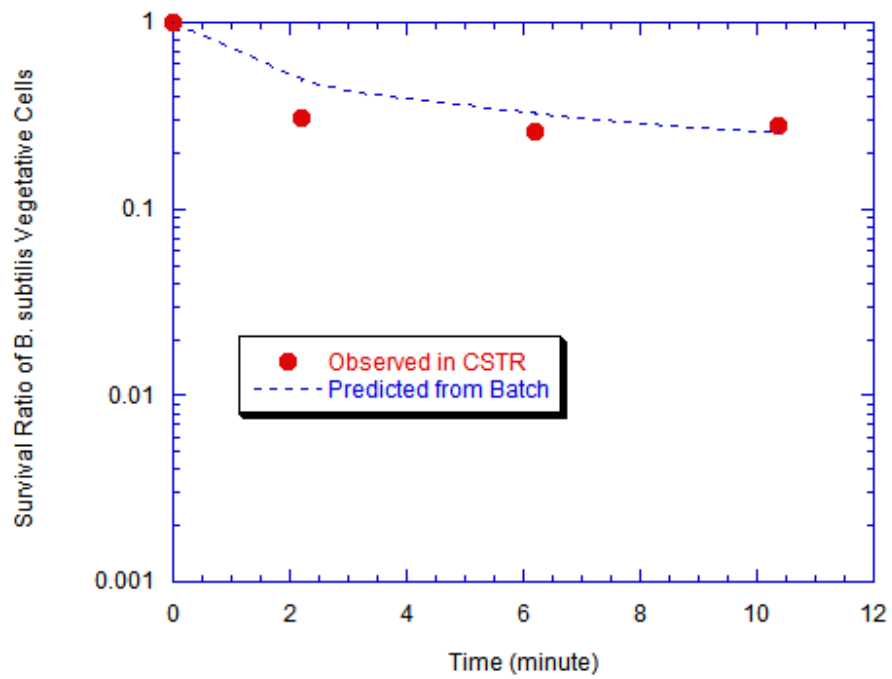


Figure 5-37 Inactivation of *B. Subtilis* Vegetative Cells in Exponential Phase
Using Monochloramine ($N_0 = 10^3$ CFU/mL, $C = 1.0$ mg/L)

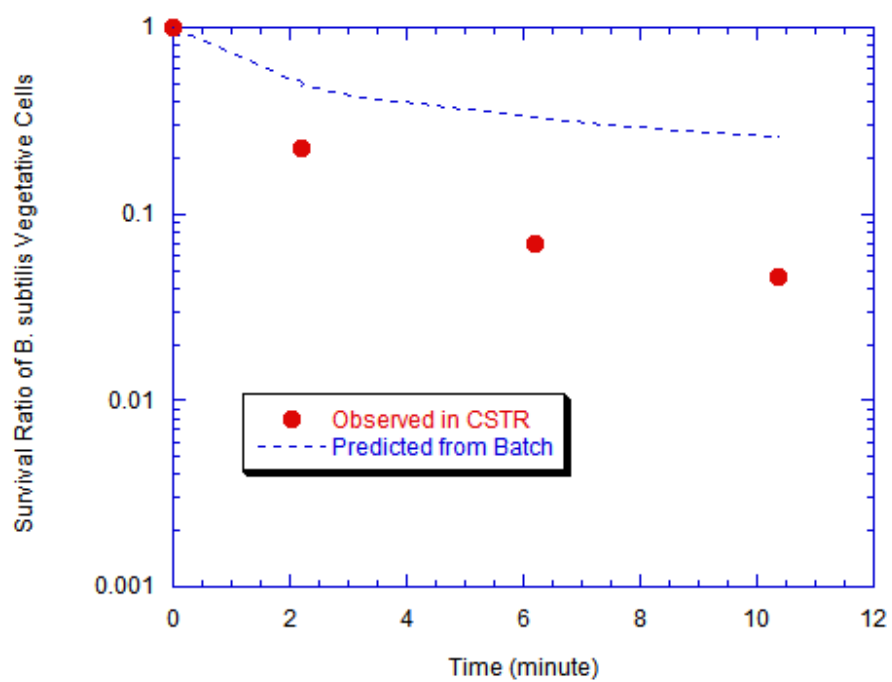


Figure 5-38 Inactivation of *B. Subtilis* Vegetative Cells in Exponential Phase
Using Monochloramine ($N_0 = 10^4$ CFU/mL, $C = 1.0$ mg/L)

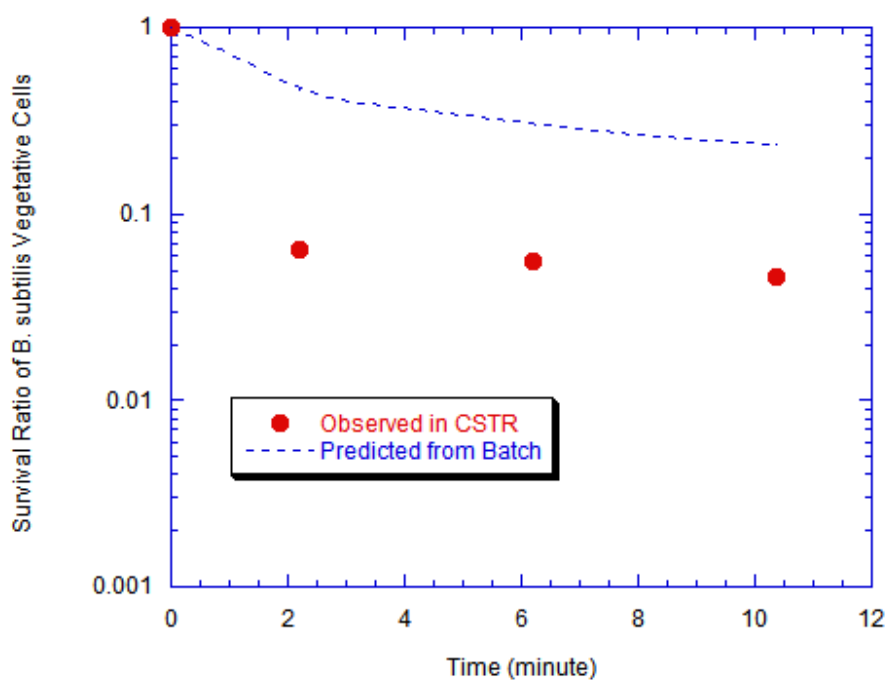


Figure 5-39 Inactivation of *B. Subtilis* Vegetative Cells in Exponential Phase
Using Monochloramine ($N_0 = 10^3$ CFU/mL, $C = 1.5$ mg/L)

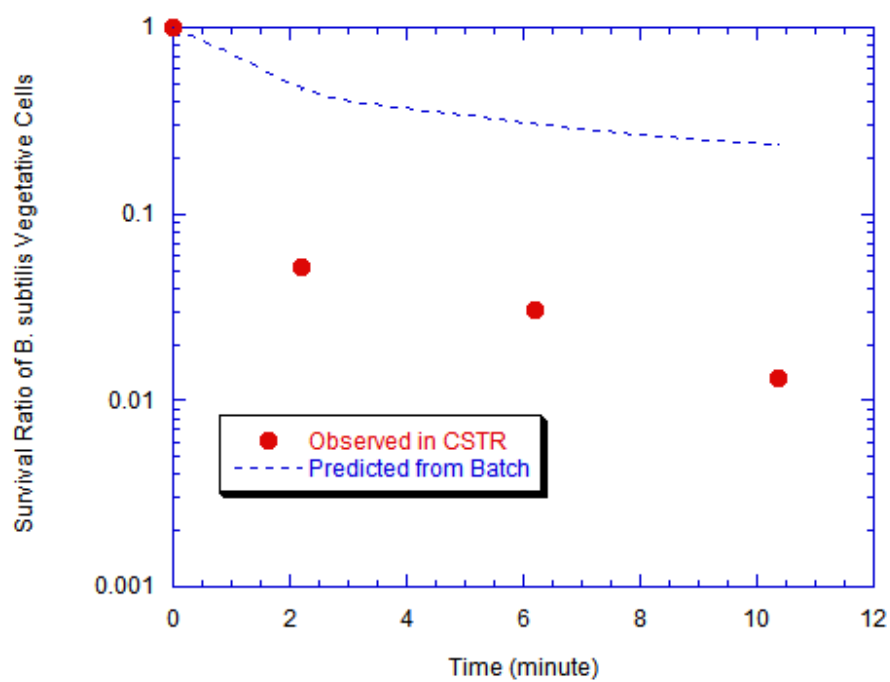


Figure 5-40 Inactivation of *B. Subtilis* Vegetative Cells in Exponential Phase
Using Monochloramine ($N_0 = 10^3$ CFU/mL, $C = 1.5$ mg/L)

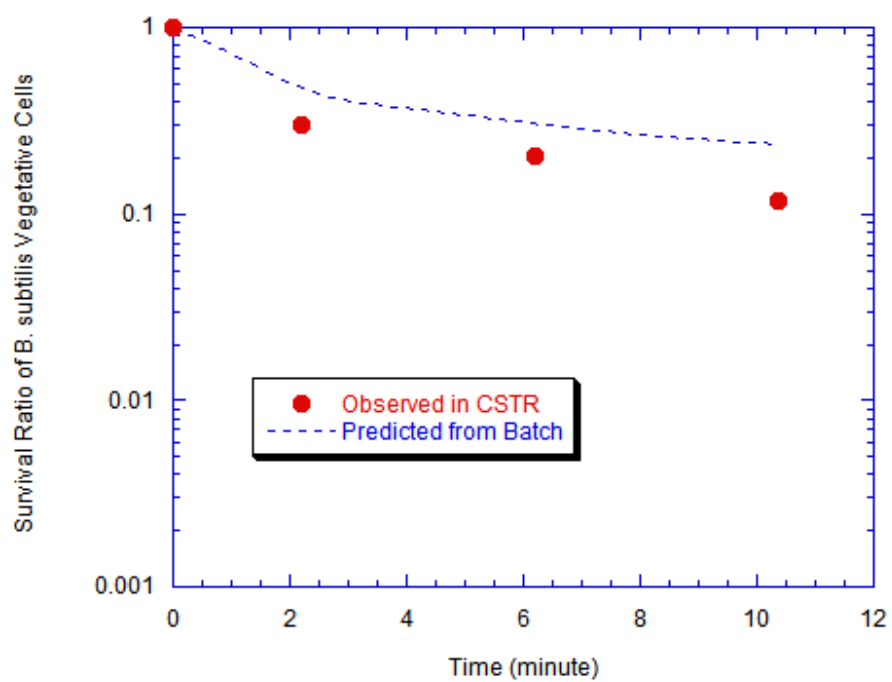


Figure 5-41 Inactivation of *B. Subtilis* Vegetative Cells in Exponential Phase
Using Monochloramine ($N_0 = 10^4$ CFU/mL, $C = 1.5$ mg/L)

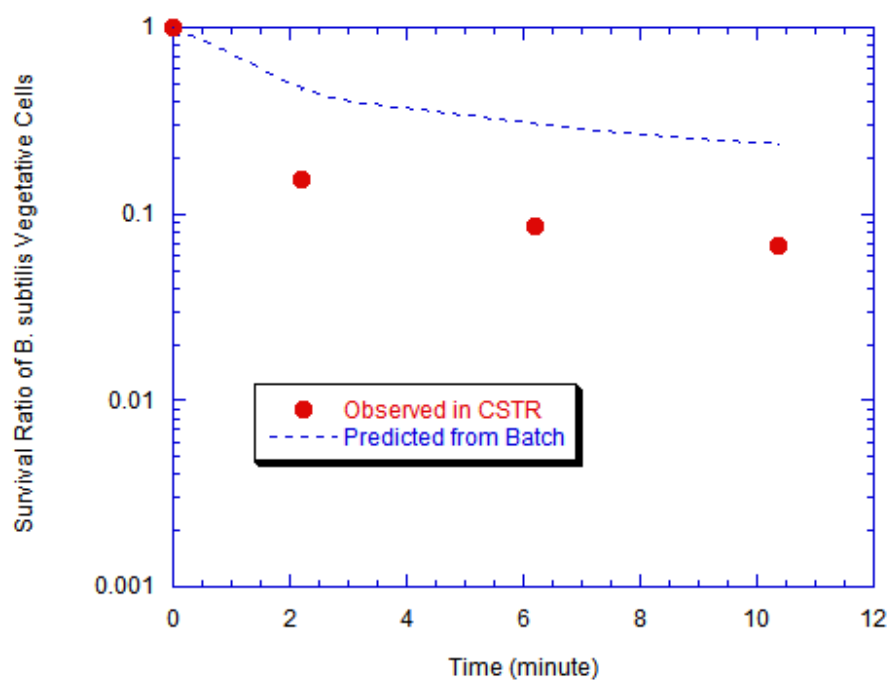


Figure 5-42 Inactivation of *B. Subtilis* Vegetative Cells in Exponential Phase
Using Monochloramine ($N_0 = 10^5$ CFU/mL, $C = 1.5$ mg/L)

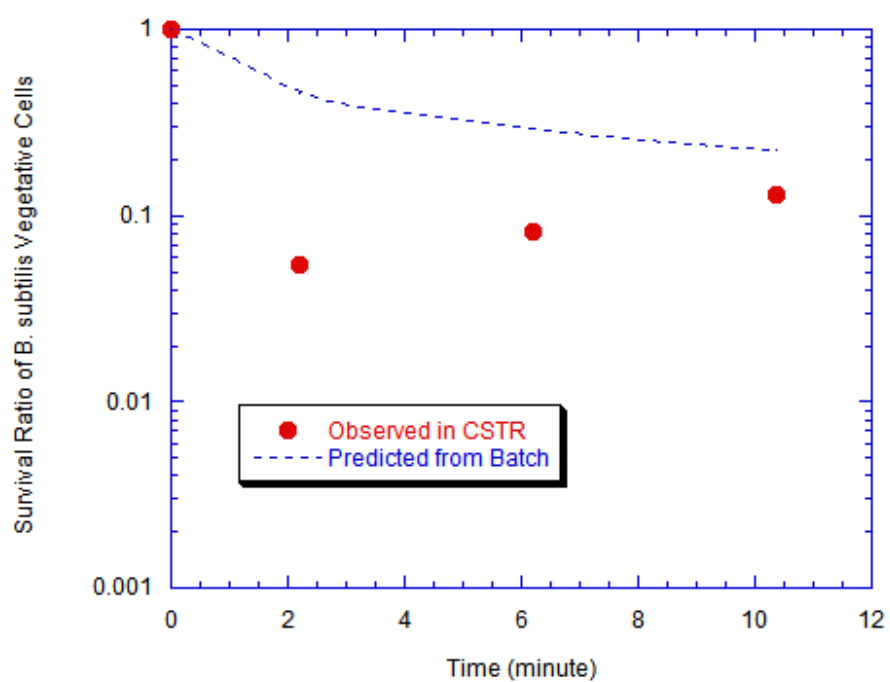


Figure 5-43 Inactivation of *B. Subtilis* Vegetative Cells in Exponential Phase
Using Monochloramine ($N_0 = 10^3$ CFU/mL, $C = 2.0$ mg/L)

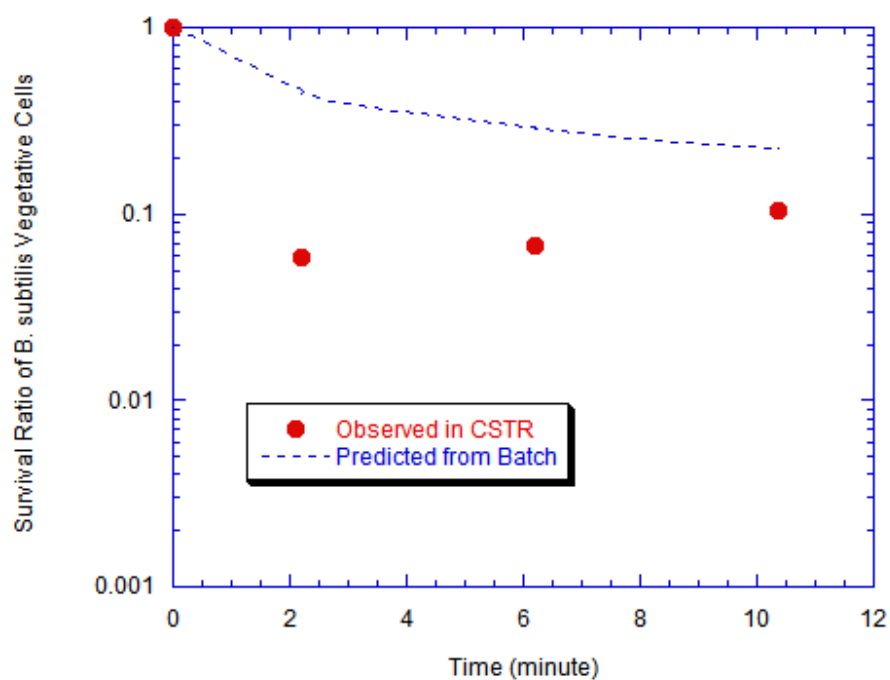


Figure 5-44 Inactivation of *B. Subtilis* Vegetative Cells in Exponential Phase
Using Monochloramine ($N_0 = 10^3$ CFU/mL, $C = 2.0$ mg/L)

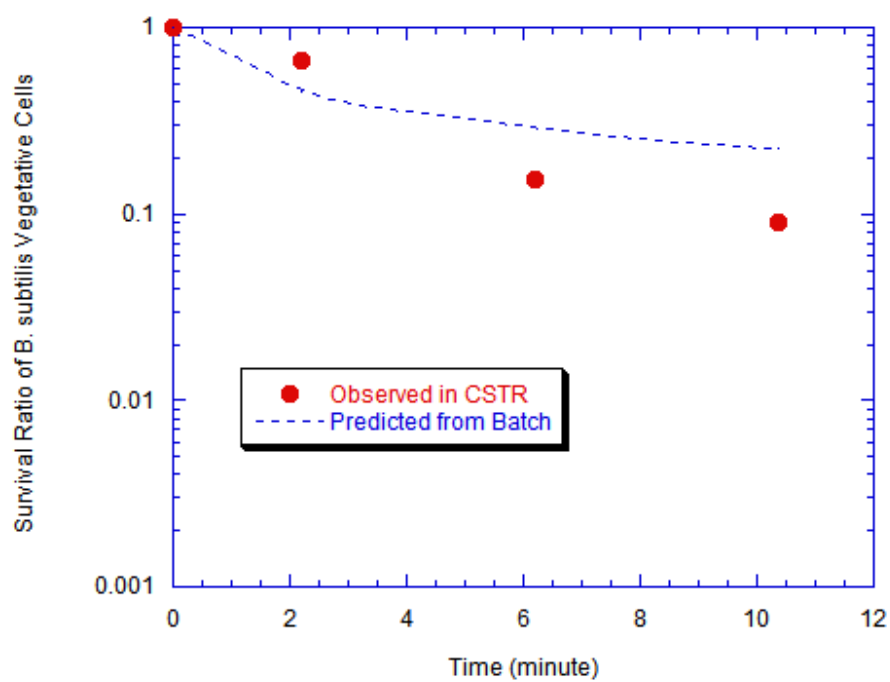


Figure 5-45 Inactivation of *B. Subtilis* Vegetative Cells in Exponential Phase
Using Monochloramine ($N_0 = 10^4$ CFU/mL, $C = 2.0$ mg/L)

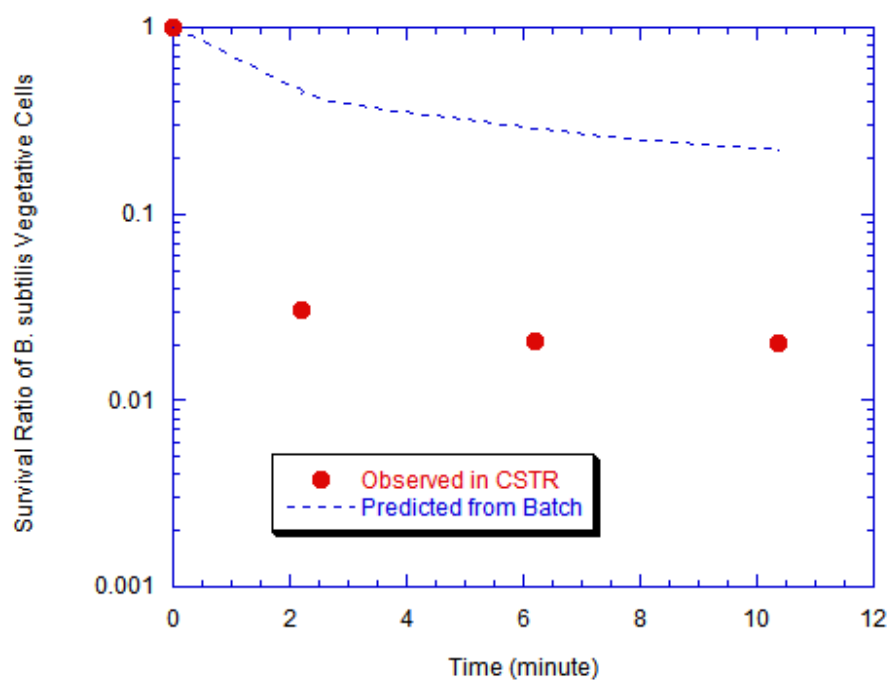


Figure 5-46 Inactivation of *B. Subtilis* Vegetative Cells in Exponential Phase
Using Monochloramine ($N_0 = 10^4$ CFU/mL, $C = 2.0$ mg/L)

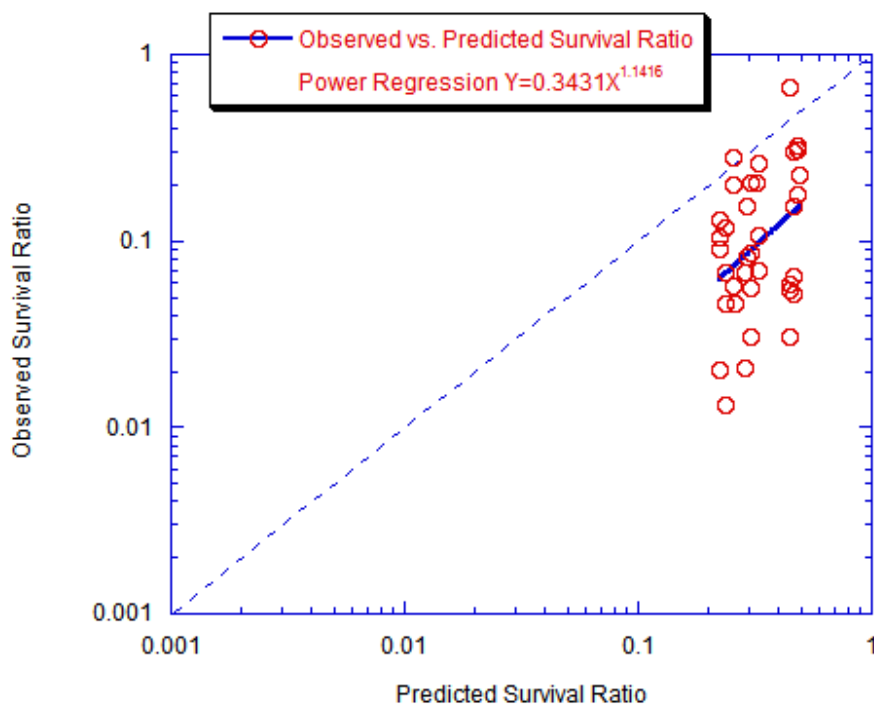


Figure 5-47 Overall Comparison of Observed vs. Predicted Survival Ratio
(Inactivation of *B. subtilis* Vegetative Cells Using Monochloramine)

5.3.3.3 Linear Regression between Observed and Predicted Data

A linear regression was performed between observed survival ratios ($-\ln$ units) and predicted survival ratios ($-\ln$ units) from Chick, Chick-Watson, Hom, Power Law, and Hom Power Law model. The regression equations and R-square values were listed in Table 5-10, where $SR_{observed}$ is *E. coli* survival ratio computed from experimental data in $-\ln$ units and $SR_{predicted}$ is *E. coli* survival ratio predicted from batch kinetics in $-\ln$ units.

Table 5-10 Linear Regression of Observation and Prediction (MBE)

Model	Linear Regression Equation	R ²
Chick	$SR_{observed} = 0.9568 \times SR_{predicted} + 1.4763$	0.1781
Chick-Watson	$SR_{observed} = 0.9907 \times SR_{predicted} + 1.5370$	0.1455
Hom	$SR_{observed} = 1.1416 \times SR_{predicted} + 1.0697$	0.1302
Power Law	$SR_{observed} = 0.6007 \times SR_{predicted} + 1.6319$	0.0974
Hom Power Law	$SR_{observed} = 1.0084 \times SR_{predicted} + 1.1812$	0.1290

Note: SR is $-\ln(\text{Survival Ratio})$

A t-test was applied on two hypotheses from the linear regressions: (1) the slope is equal to one; (2) the intercept is equal to zero. With a significance level of 5%, the hypothesis of slope one ($P = 0.5407$) could not be rejected but the hypothesis of intercept zero ($P = 0.0002$) was rejected.

5.3.3.4 Paired t-test between CSTR Observation and Batch Prediction

The paired t-test results for *B. subtilis* vegetative cells were displayed in Table 5-11. With a significance level of 5%, the hypothesis that observed survival ratios were equal to the predicted survival ratios was rejected for the five models.

Table 5-11 Paired t-test Comparison between Observed and Predicted Survival Ratio (ln units) for *B. subtilis* Vegetative Cells

Model	Probability ($\alpha = 5\%$)
Chick	1.582×10^{-12}
Chick-Watson	4.864×10^{-13}
Hom	1.862×10^{-10}
Power Law	2.336×10^{-9}
Hom Power Law	3.970×10^{-10}

5.3.4 Inactivation of *B. subtilis* Spores Using Ozone

5.3.4.1 Batch Kinetics

The Modified Multiple Target model was found to be the best-fit model to describe ozone disinfection on *B. subtilis* spores in batch system from previous study (Kaymak 2003). The values of best-fit parameters are given below in Table 5-12.

Table 5-12 Batch Best-fit Model and Parameters for *B. subtilis* Spores**Inactivation by Ozone**

Best-fit Model	Best-fit Parameters		
	k [L/(mg.min)]	n	n_c
Modified Multiple Target	1.5449	0.6992	8.4567

5.3.4.2 CSTR Disinfection and Batch Predictions

Derived from CSTR steady-state mass balance relationship and batch Modified Multiple Target model, the equation below was used to predict the *B. subtilis* spore survival ratio in a CSTR (Appendix D).

$$\left(\frac{N}{N_0}\right)_{predicted} = 1 - kn_c C^n \theta \left[1 - \left(1 - \left(\frac{N}{N_0}\right)_{predicted} \right)^{\frac{1}{n_c}} \right] \left[\left(1 - \left(\frac{N}{N_0}\right)_{predicted} \right)^{\frac{n_c-1}{n_c}} \right] \quad 5-3$$

The observed results and the predicted results for each disinfection experiment on *B. subtilis* spores are shown from Figure 5-48 to Figure 5-59. The overall comparison was displayed in Figure 5-60.

All of the comparison data points are below the diagonal which stands for the over-prediction of CSTR disinfection performance from batch kinetics. The power regression line (linear regression line with the survival ratio being expressed in logarithm units) of comparison data is parallel to the diagonal. The differences between observed survival ratio (in ln units) and predicted survival ratio (in ln units) have a mean of -0.855 and a standard deviation of 0.288.

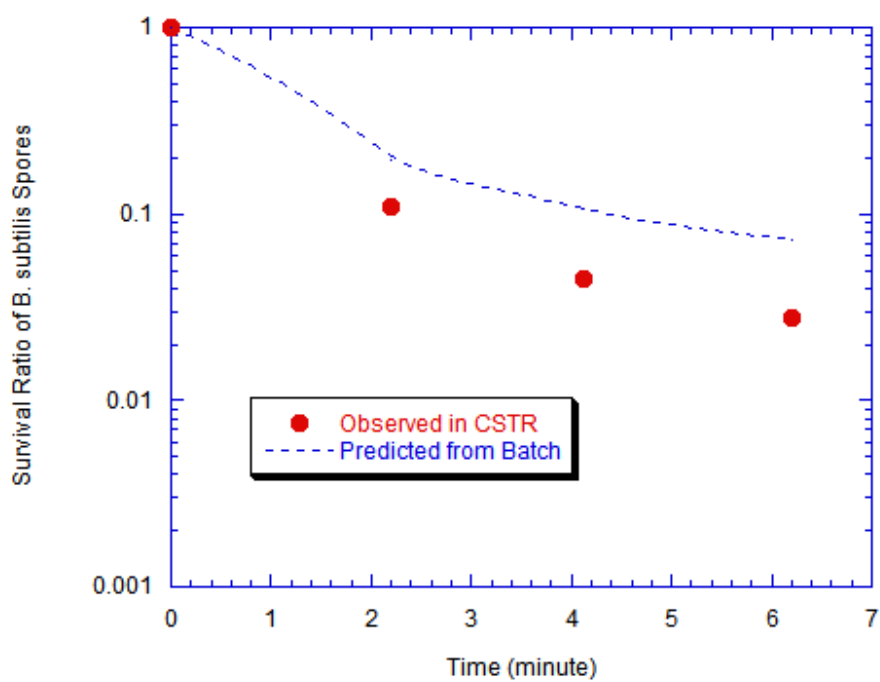


Figure 5-48 Inactivation of *B. Subtilis* Spores Using Ozone

$(N_0 = 10^3 \text{ CFU/mL}, C = 1.5 \text{ mg/L})$

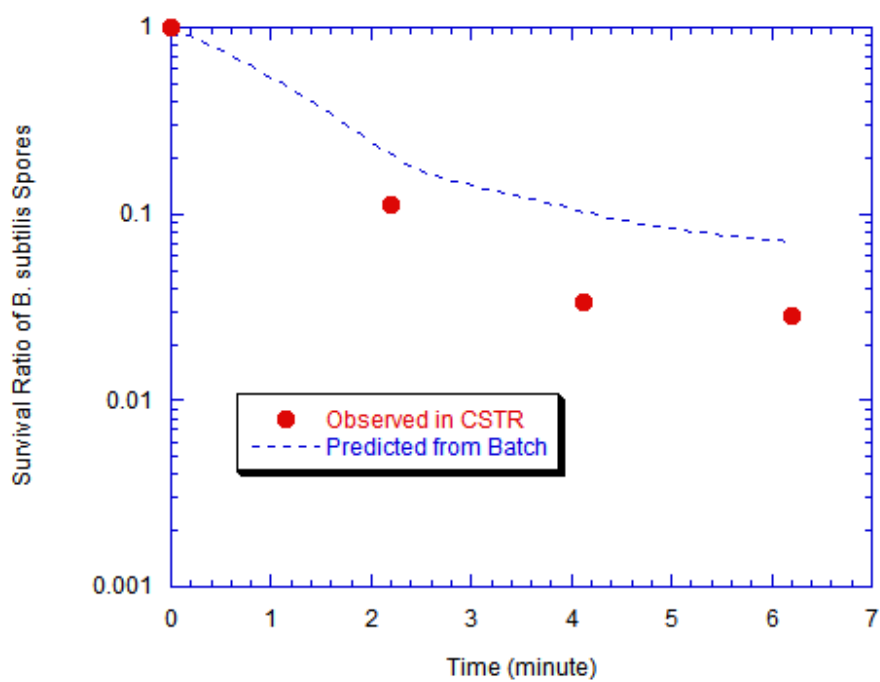


Figure 5-49 Inactivation of *B. Subtilis* Spores Using Ozone

$(N_0 = 10^4 \text{ CFU/mL}, C = 1.5 \text{ mg/L})$

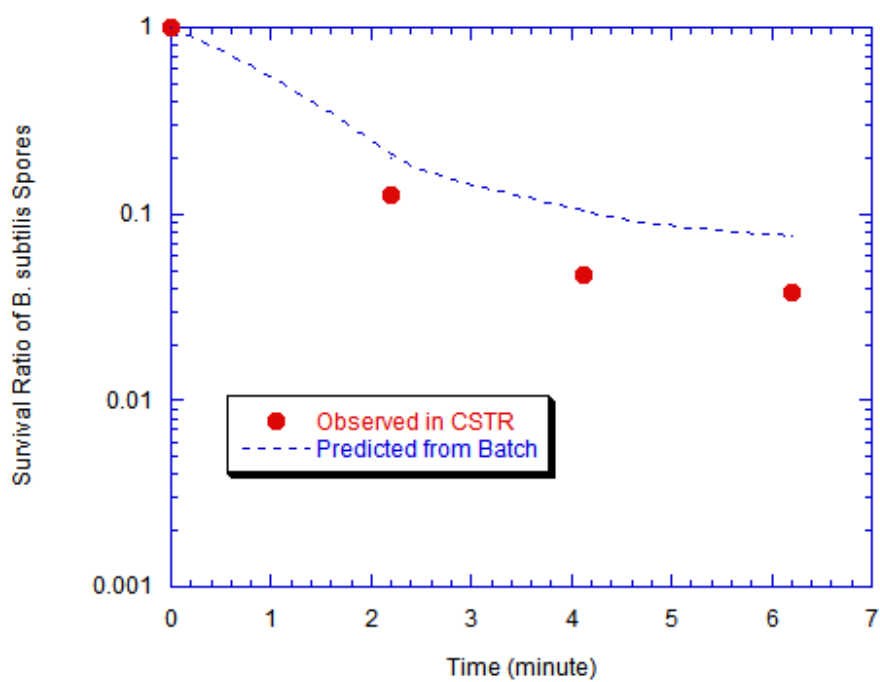


Figure 5-50 Inactivation of *B. Subtilis* Spores Using Ozone

$(N_0 = 10^5 \text{ CFU/mL}, C = 1.5 \text{ mg/L})$

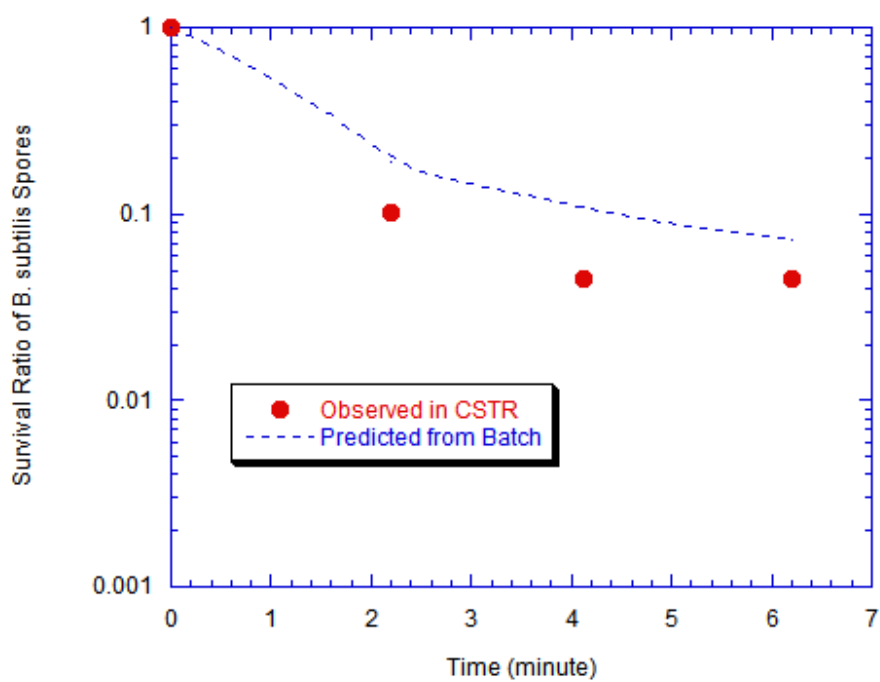


Figure 5-51 Inactivation of *B. Subtilis* Spores Using Ozone

($N_0 = 10^5$ CFU/mL, $C = 1.5$ mg/L)

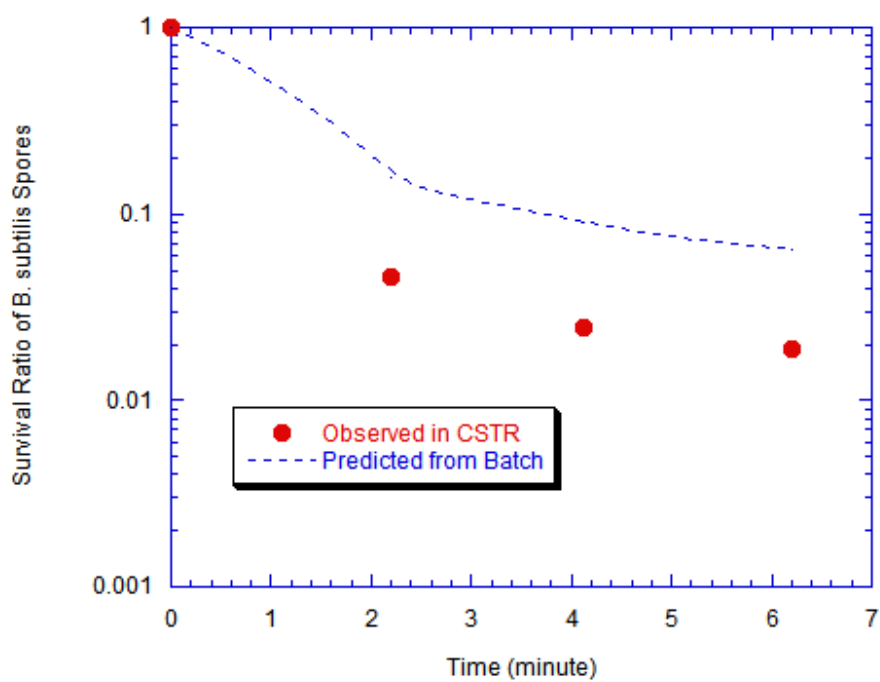


Figure 5-52 Inactivation of *B. Subtilis* Spores Using Ozone

$(N_0 = 10^3 \text{ CFU/mL}, C = 2.0 \text{ mg/L})$

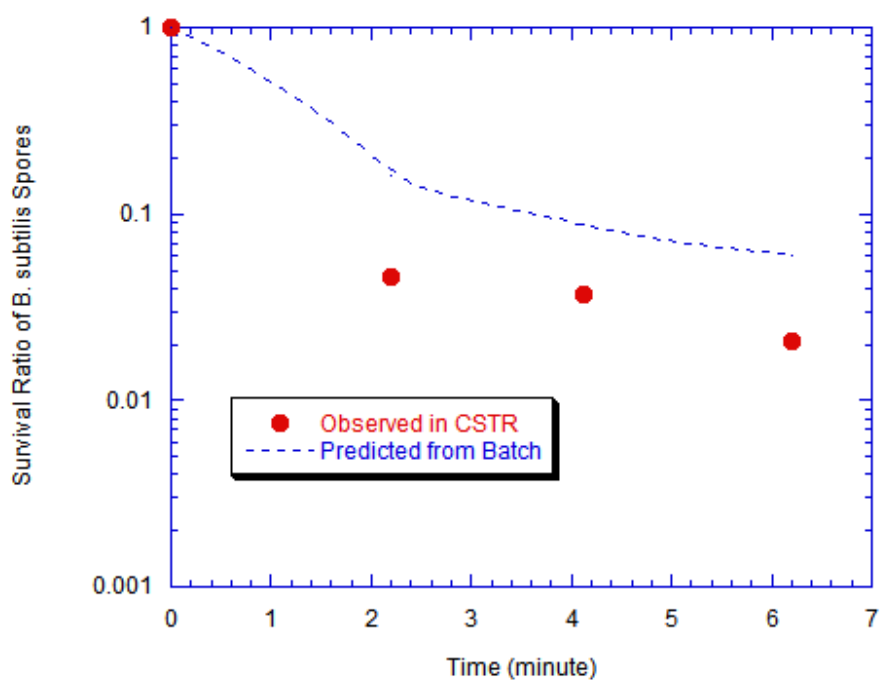


Figure 5-53 Inactivation of *B. Subtilis* Spores Using Ozone

$(N_0 = 10^3 \text{ CFU/mL}, C = 2.0 \text{ mg/L})$

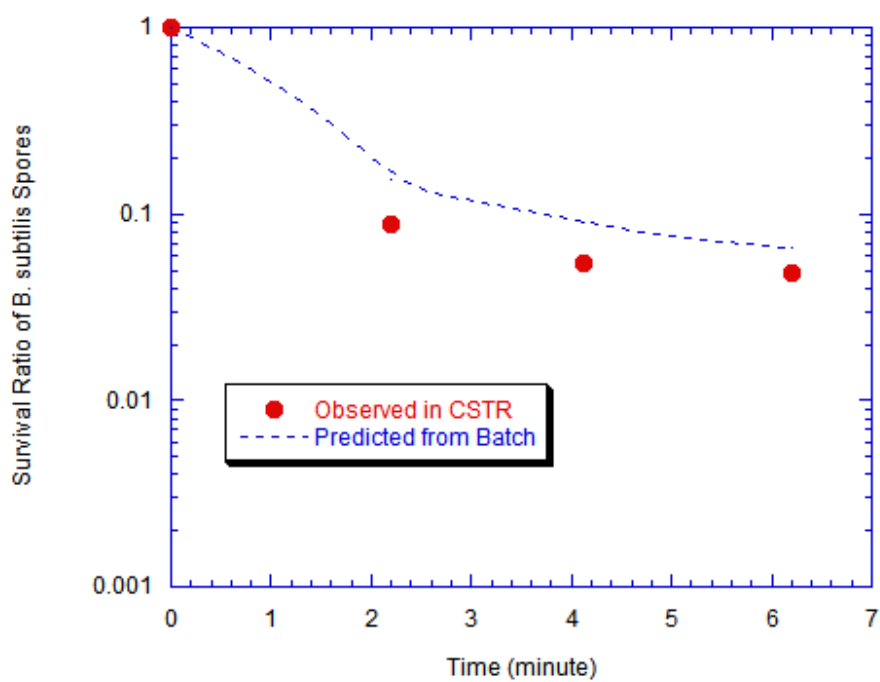


Figure 5-54 Inactivation of *B. Subtilis* Spores Using Ozone

$(N_0 = 10^4 \text{ CFU/mL}, C = 2.0 \text{ mg/L})$

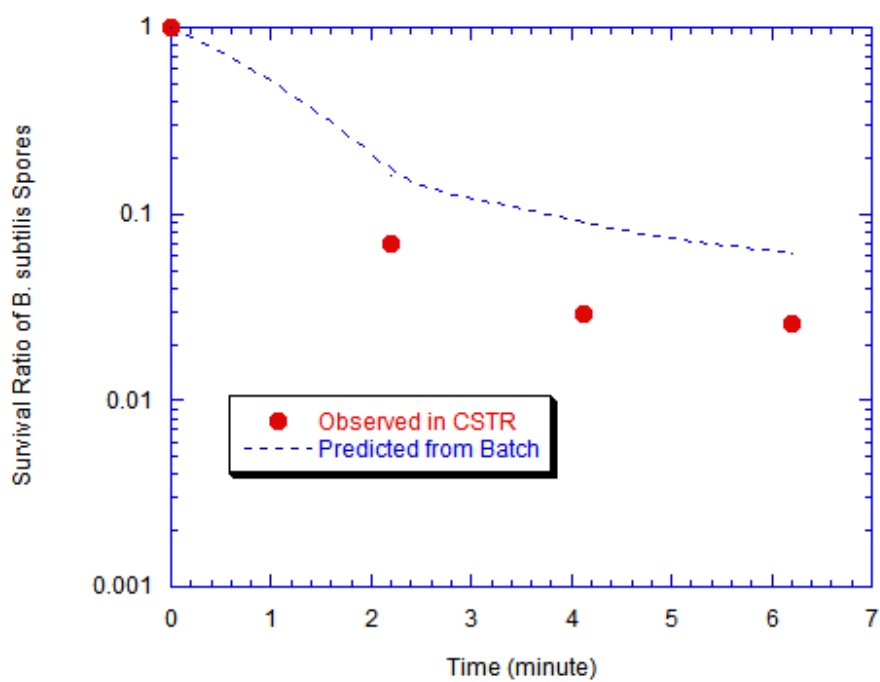


Figure 5-55 Inactivation of *B. Subtilis* Spores Using Ozone

$(N_0 = 10^5 \text{ CFU/mL}, C = 2.0 \text{ mg/L})$

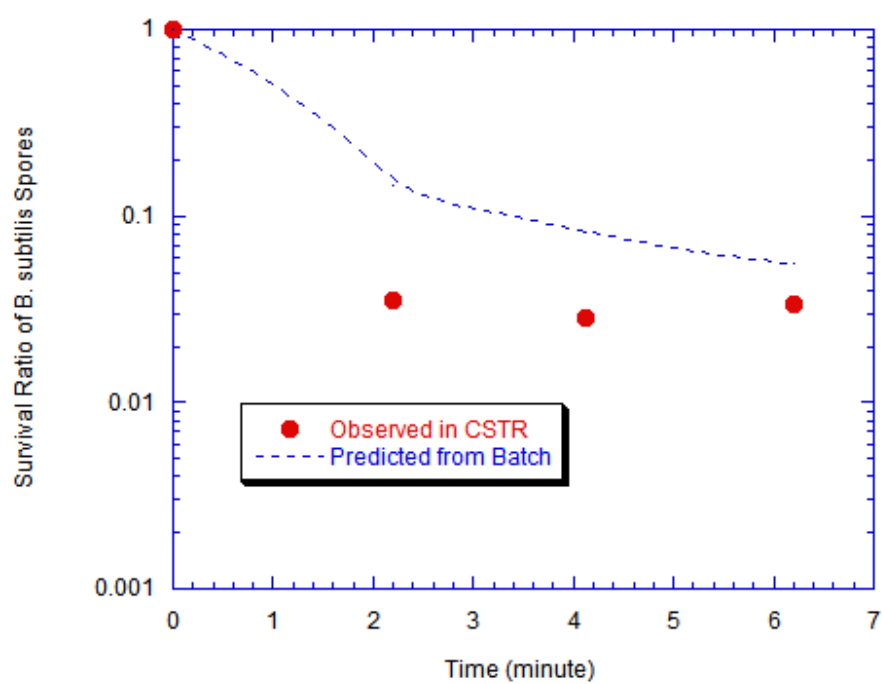


Figure 5-56 Inactivation of *B. Subtilis* Spores Using Ozone

$(N_0 = 10^3 \text{ CFU/mL}, C = 2.5 \text{ mg/L})$

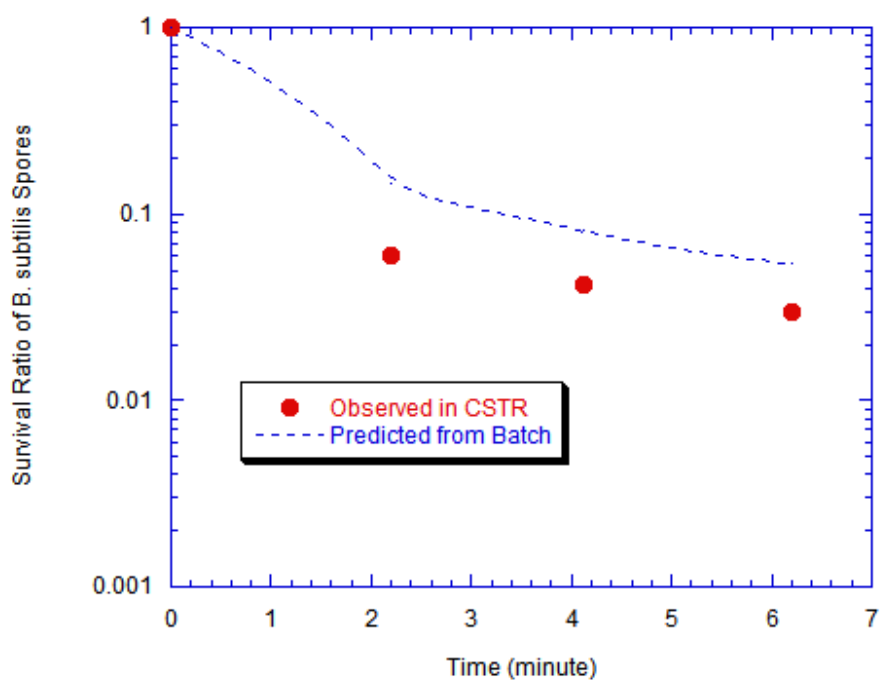


Figure 5-57 Inactivation of *B. Subtilis* Spores Using Ozone

$(N_0 = 10^4 \text{ CFU/mL}, C = 2.5 \text{ mg/L})$

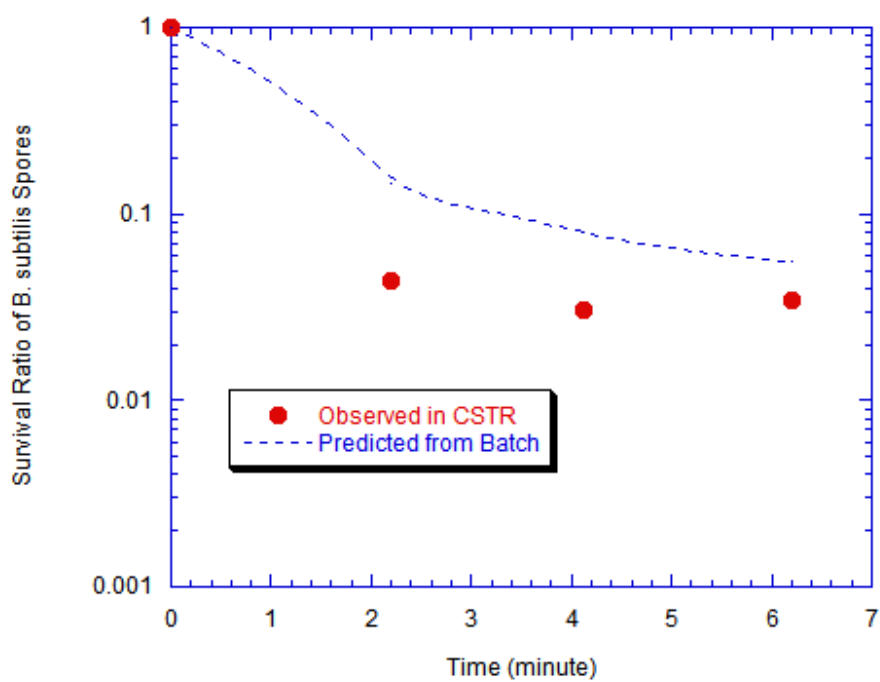


Figure 5-58 Inactivation of *B. Subtilis* Spores Using Ozone

$(N_0 = 10^4 \text{ CFU/mL}, C = 2.5 \text{ mg/L})$

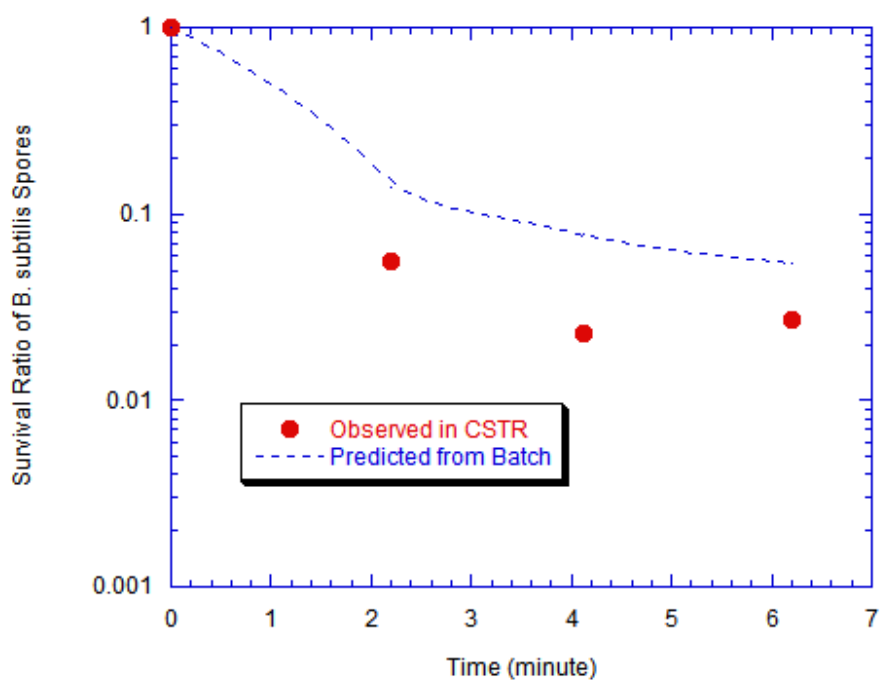


Figure 5-59 Inactivation of *B. Subtilis* Spores Using Ozone

($N_0 = 10^5$ CFU/mL, $C = 2.5$ mg/L)

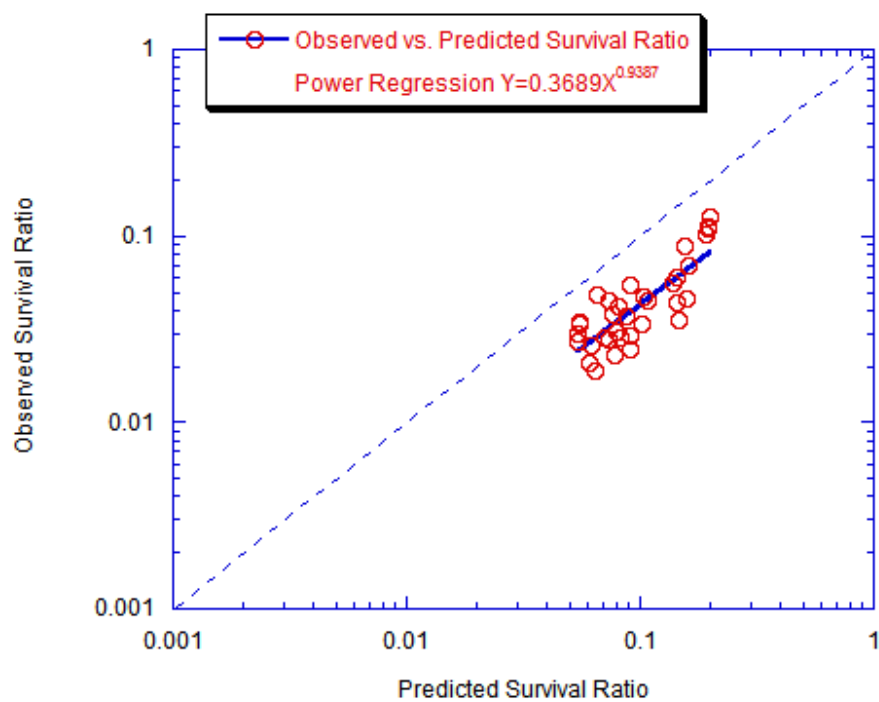


Figure 5-60 Overall Comparison of Observed vs. Predicted Survival Ratio
(Inactivation of *B. subtilis* Spores Using Ozone)

5.3.4.3 Linear Regression between Observed and Predicted Data

Expressed in negative logarithm units, the data were analyzed by the linear regression between observed survival ratios and predicted survival ratios from Chick, Chick-Watson, Hom, Power Law, Hom Power Law, and Modified Multiple Target model. Table 5-13 shows the regression results.

With a significance level of 5%, the hypothesis of slope one ($P = 0.3840$) passed t-test but intercept zero ($P = 0.00002$) failed.

Table 5-13 Linear Regression of Observation and Prediction (OBS)

Model	Linear Regression Equation	R^2
Chick	$SR_{observed} = 0.9643 \times SR_{predicted} + 0.9345$	0.6719
Chick-Watson	$SR_{observed} = 1.0566 \times SR_{predicted} + 1.2804$	0.6008
Hom	$SR_{observed} = 0.9372 \times SR_{predicted} + 1.354$	0.6231
Power Law	$SR_{observed} = 1.0298 \times SR_{predicted} + 1.3697$	0.6265
Hom Power Law	$SR_{observed} = 0.9555 \times SR_{predicted} + 1.3634$	0.6302
Modified Multiple Target	$SR_{observed} = 0.9387 \times SR_{predicted} + 0.9972$	0.6512

Note: SR is $-\ln(\text{Survival Ratio})$

5.3.4.4 Paired t-test between CSTR Observation and Batch Prediction

Table 5-14 demonstrated the results of paired t-test comparison between observed CSTR survival ratio (ln units) and predicted survival ratio (ln units) from six batch models for *B. subtilis* spores. Predictions from the six models all failed paired t-test.

Table 5-14 Paired t-test Comparison between Observed and Predicted Survival Ratio (ln units) for *B. subtilis* Spores

Model	Probability ($\alpha = 5\%$)
Chick	1.599×10^{-19}
Chick-Watson	5.408×10^{-25}
Hom	9.965×10^{-24}
Power Law	6.494×10^{-26}
Hom Power Law	1.972×10^{-24}
Modified Multiple Target	4.015×10^{-19}

5.3.5 CSTR System Correction

As previously noted, all the regression lines in the overall comparison figures (Figure 5-21, Figure 5-34, Figure 5-47 and Figure 5-60) were parallel with the diagonal, which could also be confirmed from t-tests of slope one for each series of disinfection experiments. For the hypothesis of intercept zero, disinfection on *E. coli* in stationary

phase passed t-test but disinfection in the other cases failed t-test. Deviations existed between the regression line and the diagonal. The batch equations over-predicted the survival ratio in CSTR for monochloramine inactivation on *E. coli* in stationary phase, monochloramine inactivation on *B. subtilis* vegetative cells, and ozone inactivation on *B. subtilis* spores. There was under-prediction for the survival ratio of *E. coli* in exponential phase under monochloramine disinfection in CSTR.

To determine the initial microbial density, the samples were taken from the bottom of the disinfectant reservoir and calculated according to the dilution from the reservoir to the CSTR. There might be loss or gain of bacteria quantity when bacteria suspension flows through the tubing between the reservoir and the reactor, which was not taken into consideration in previous analysis.

To check if such loss or gain of bacteria existed in the CSTR system, the blank experiments were conducted in the CSTR system. The procedures were the same as the disinfection experiments except that disinfectant solution was replaced by phosphate buffered solution. Four blank experiments were performed with one for each series.

5.3.5.1 Correction for Inactivation of *E. coli* in Stationary Phase Using Monochloramine

The blank experiment was conducted at an initial *E. coli* density level of 10^3 CFU/mL (Figure 5-61). The loss of *E. coli* in tubing was observed with an average value of 15.7%. Some bacteria could be stuck on the wall of the tubing which might be one reason of the loss. Bacteria natural die-off could be another reason.

The *E. coli* initial density in the CSTR was corrected by accounting for the loss of *E. coli* in system tubing. The observed survival ratios and predicted survival ratios were recalculated. After correction, the relationship of observed *E. coli* survival ratio versus predicted *E. coli* survival ratio was indicated in Figure 5-62. Compared to the data without correction, the power regression line is much closer to the diagonal for the data with system correction, which can also be noticed from the regression equation.

Linear regressions were reanalyzed between observed survival ratios (-ln unit) and predicted survival ratios (-ln units) from five models, as shown in Table 5-15. With a significance level of 5%, the hypotheses of both slope one ($P = 0.0509$) and intercept zero ($P = 0.8688$) passed t-test.

Table 5-15 Linear Regression II of Observation and Prediction (MES)

Model	Linear Regression Equation	R^2
Chick	$SR_{observed} = 1.3935 \times SR_{predicted} - 0.1994$	0.4982
Chick-Watson	$SR_{observed} = 1.3829 \times SR_{predicted} - 0.1725$	0.4745
Hom	$SR_{observed} = 1.079 \times SR_{predicted} + 0.2558$	0.4691
Power Law	$SR_{observed} = 1.3824 \times SR_{predicted} - 0.1812$	0.4545
Hom Power Law	$SR_{observed} = 0.9824 \times SR_{predicted} + 0.2073$	0.4044

Note: SR is $-\ln(\text{Survival Ratio})$

Paired t-test was conducted between observed survival ratio (ln units) and predicted survival ratio (ln units). With a significance level of 5%, the hypothesis of the equality between observed survival ratio (ln units) and predicted survival ratio (ln units) passed t-test ($P=0.2336$).

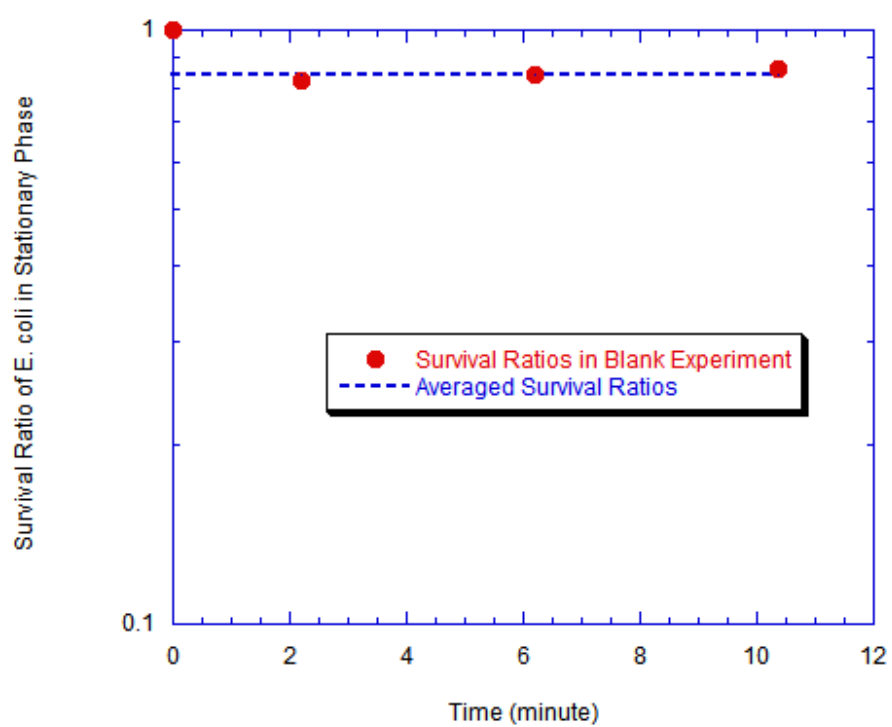


Figure 5-61 Blank Experiment of *E. coli* in Stationary Phase

$$(N_0 = 10^3 \text{ CFU/mL})$$

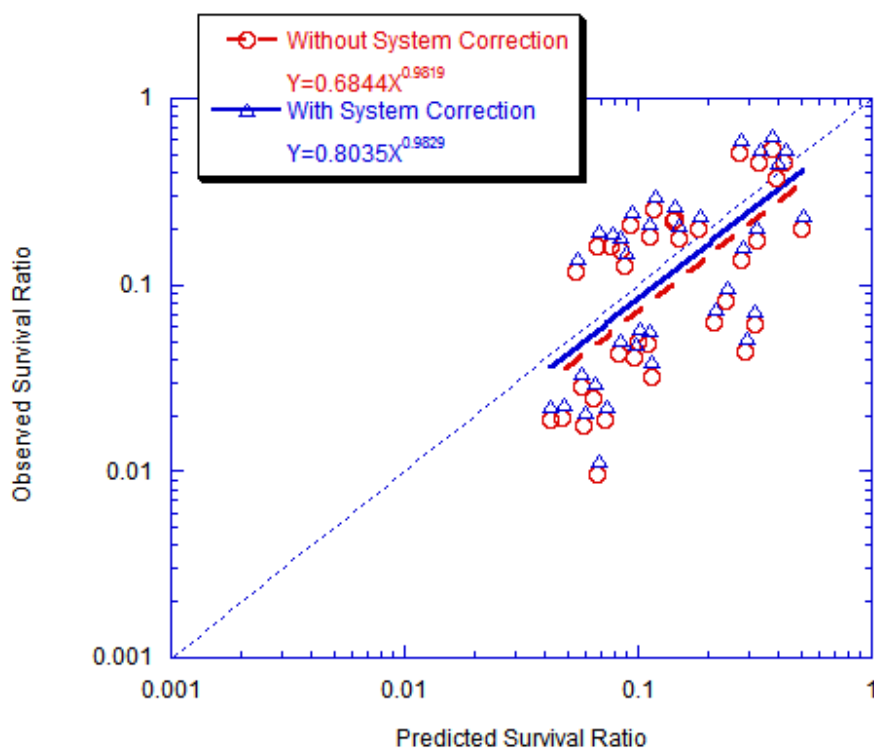


Figure 5-62 Overall Comparison of Observed vs. Predicted Survival Ratio
With and Without System Correction
(Inactivation of *E. coli* in Stationary Phase Using Monochloramine)

5.3.5.2 Correction for Inactivation of *E. coli* in Exponential Phase Using Monochloramine

The blank experiment for *E. coli* in exponential phase was also conducted at an initial *E. coli* density level of 10^3 CFU/mL (Figure 5-63). Different from *E. coli* in stationary phase, there was a gain of *E. coli* in exponential phase in tubing system with an average value of 14.0%. It seems *E. coli* in exponential phase can still grow even at low temperature (15°C).

The *E. coli* initial density in CSTR was corrected by accounting for the gain of *E. coli* in exponential phase in system tubing. The observed survival ratios and predicted survival ratios were recalculated. Compared from the regression lines and the regression equations (Figure 5-64), the new power regression line is closer to the diagonal for the data with system correction.

The linear regression results after system correction were displayed in Table 5-16 for five models. This time both hypothesis of slope one ($P = 0.1551$) and intercept zero ($P = 0.1241$) passed t-test at a significance level of 5%.

Table 5-16 Linear Regression II of Observation and Prediction (MEE)

Model	Linear Regression Equation	R ²
Chick	$SR_{observed} = 1.363 \times SR_{predicted} - 0.2456$	0.7413
Chick-Watson	$SR_{observed} = 1.3821 \times SR_{predicted} - 0.2558$	0.7164
Hom	$SR_{observed} = 0.9317 \times SR_{predicted} + 0.0216$	0.7276
Power Law	$SR_{observed} = 1.3754 \times SR_{predicted} - 0.2597$	0.727
Hom Power Law	$SR_{observed} = 0.914 \times SR_{predicted} + 0.0497$	0.7383

Note: SR is $-\ln(\text{Survival Ratio})$

From paired t-test with a significance level of 5%, the hypothesis of the equality between observed survival ratio (ln units) and predicted survival ratio (ln units) passed t-test (P=0.0885).

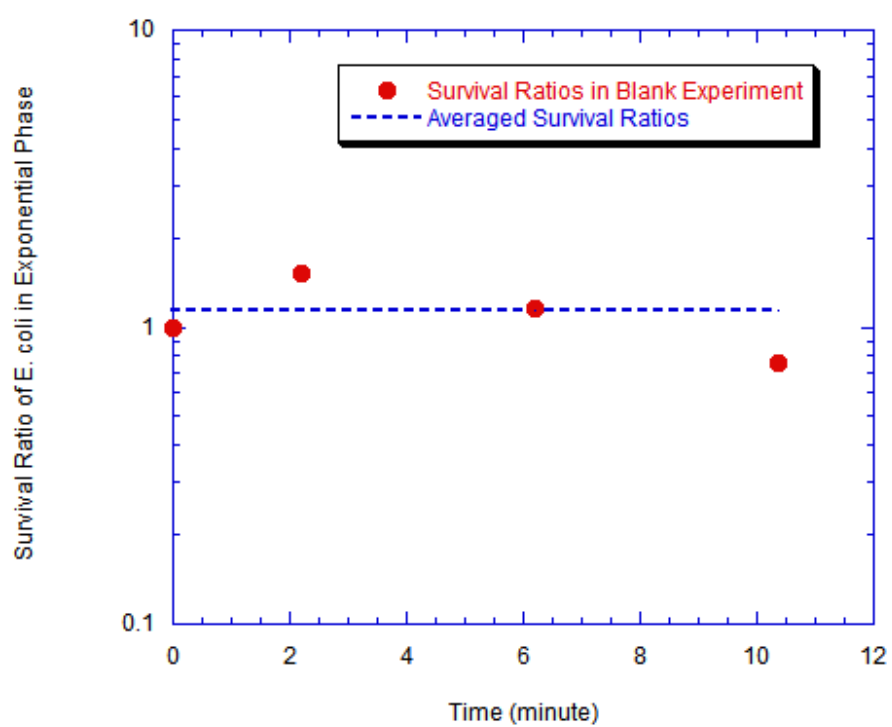


Figure 5-63 Blank Experiment of *E. coli* in Exponential Phase

$$(N_0 = 10^3 \text{ CFU/mL})$$

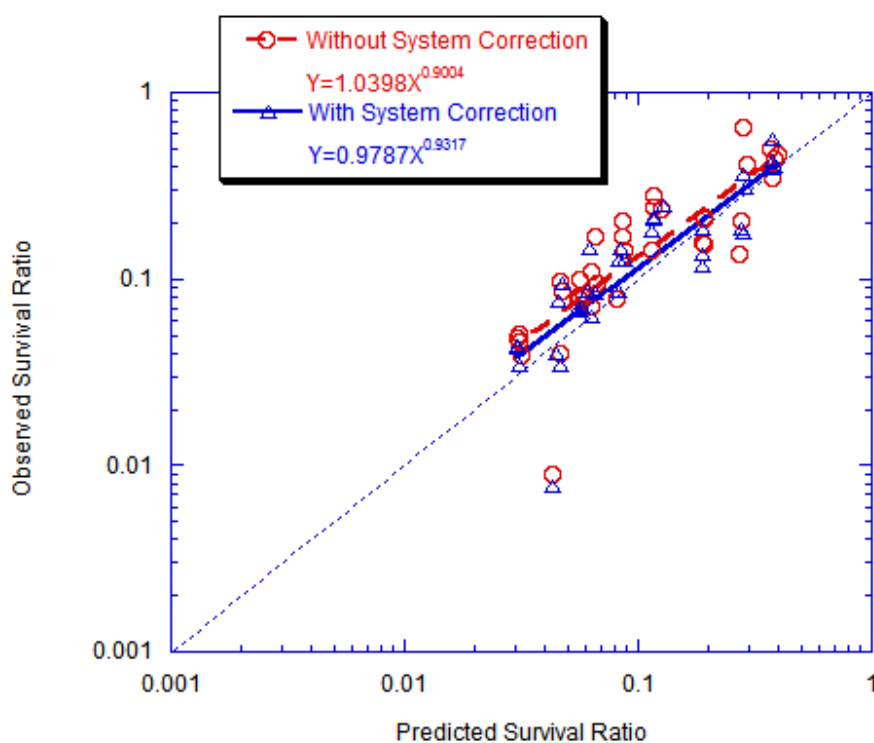


Figure 5-64 Overall Comparison of Observed vs. Predicted Survival Ratio
With and Without System Correction

(Inactivation of *E. coli* in Exponential Phase Using Monochloramine)

5.3.5.3 Correction for Inactivation of *B. subtilis* Vegetative Cells in Exponential Phase Using Monochloramine

For *B. subtilis* vegetative cells in exponential phase, the blank experiment was performed at an initial density level of 10^4 CFU/mL (Figure 5-65). The loss of *E. coli* in tubing was observed with an average value of 30.4%.

After correction of *B. subtilis* initial density and survival ratios, the relationship of observed *B. subtilis* survival ratio versus predicted *B. subtilis* survival ratio was depicted in Figure 5-66. Even though the power regression line after correction was closer to the diagonal than which without correction, there was still some certain difference from the perfect prediction.

From the results of linear regression after system correction, the hypothesis of slope one ($P = 0.2598$) passed t-test but intercept zero ($P = 0.0004$) still failed t-test at a significance level of 5%.

Table 5-17 Linear Regression II of Observation and Prediction (MBE)

Model	Linear Regression Equation	R^2
Chick	$SR_{observed} = 0.957 \times SR_{predicted} + 1.1139$	0.1782
Chick-Watson	$SR_{observed} = 0.991 \times SR_{predicted} + 1.1745$	0.1456
Hom	$SR_{observed} = 1.1419 \times SR_{predicted} + 0.7071$	0.1303
Power Law	$SR_{observed} = 0.6128 \times SR_{predicted} + 1.2873$	0.0974
Hom Power Law	$SR_{observed} = 0.5097 \times SR_{predicted} + 1.0292$	0.1995

Note: SR is $-\ln(\text{Survival Ratio})$

Using paired t-test to compare observed survival ratio (ln units) and predicted survival ratio (ln units), the hypothesis of the equality between observed survival ratio (ln units) and predicted survival ratio (ln units) was rejected ($P = 3.688 \times 10^{-7}$) with a significance level of 5%.

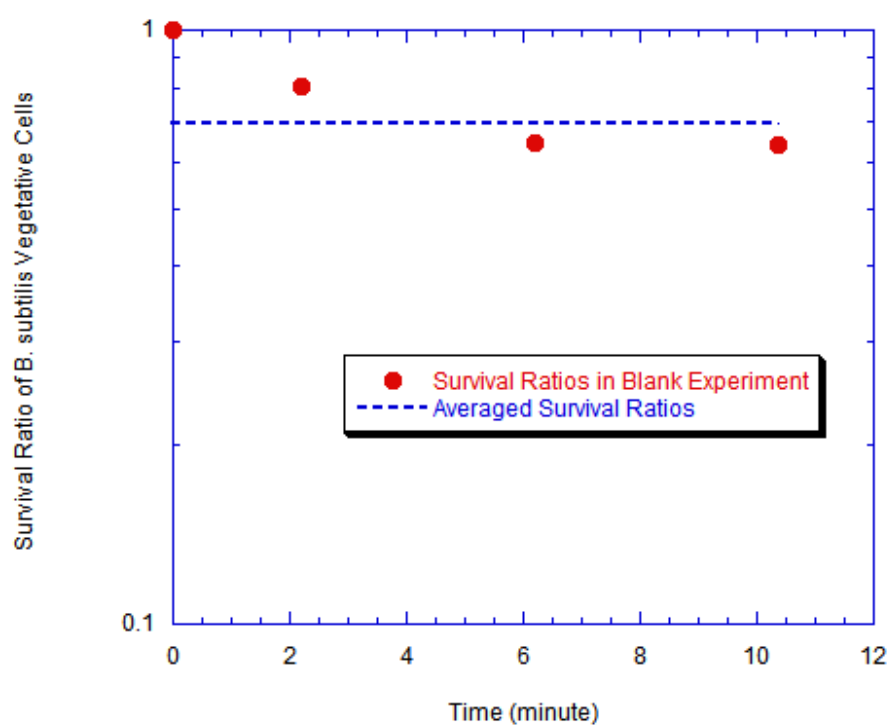


Figure 5-65 Blank Experiment of *B. subtilis* Vegetative Cells in Exponential Phase ($N_0 = 10^4$ CFU/mL)

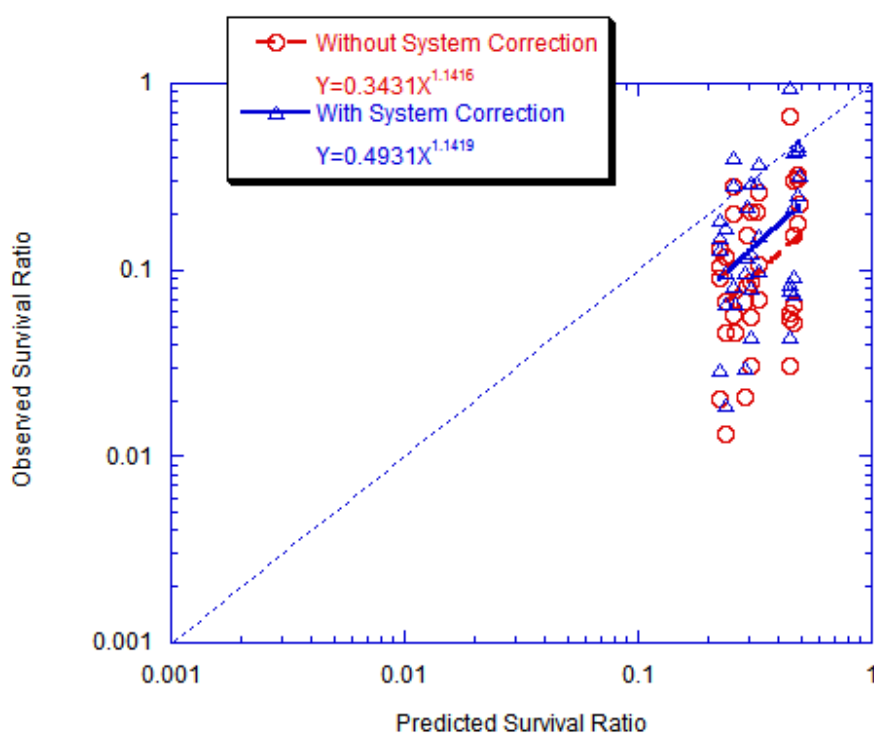


Figure 5-66 Overall Comparison of Observed vs. Predicted Survival Ratio

With and Without System Correction

(Inactivation of *B. subtilis* in Exponential Phase Using Monochloramine)

5.3.5.4 Correction for Inactivation of *B. subtilis* Spores Using Ozone

The loss of *B. subtilis* spores in the tubing system was observed at an average value of 21.5% from the blank experiment with an initial *E. coli* density level of 10^3 CFU/mL (Figure 5-67). The reasons for such loss might be bacteria attachment on the wall of tubing system.

The initial *B. subtilis* spores density in CSTR was corrected by taking consider of the loss of spores in system tubing. The observed survival ratios and predicted survival ratios were recalculated. From the comparison of observed spores survival ratio versus predicted spores survival ratio with and without system correction, as shown in Figure 5-68, the regression line with correction is closer to the diagonal then which without correction.

Using t-test and linear regression analysis (Table 5-18) for the data after system correction, the hypothesis of slope one ($P = 0.3686$) passed t-test but intercept zero ($P = 0.00007$) was rejected at a significance level of 5%.

Table 5-18 Linear Regression II of Observation and Prediction (OBS)

Model	Linear Regression Equation	R^2
Chick	$SR_{observed} = 0.9642 \times SR_{predicted} + 0.6926$	0.6718
Chick-Watson	$SR_{observed} = 1.0565 \times SR_{predicted} + 1.0385$	0.6008
Hom	$SR_{observed} = 0.9371 \times SR_{predicted} + 1.112$	0.623
Power Law	$SR_{observed} = 1.0275 \times SR_{predicted} + 1.122$	0.6266
Hom Power Law	$SR_{observed} = 0.9549 \times SR_{predicted} + 1.1195$	0.6302
Modified Multiple Target	$SR_{observed} = 0.9386 \times SR_{predicted} + 0.7553$	0.6512

Note: SR is $-\ln(\text{Survival Ratio})$

Paired t-test failed the hypothesis that observed survival ratios (ln units) were equal to the predicted survival ratios (ln units) with a significance level of 5% ($P=9.974 \times 10^{-15}$).

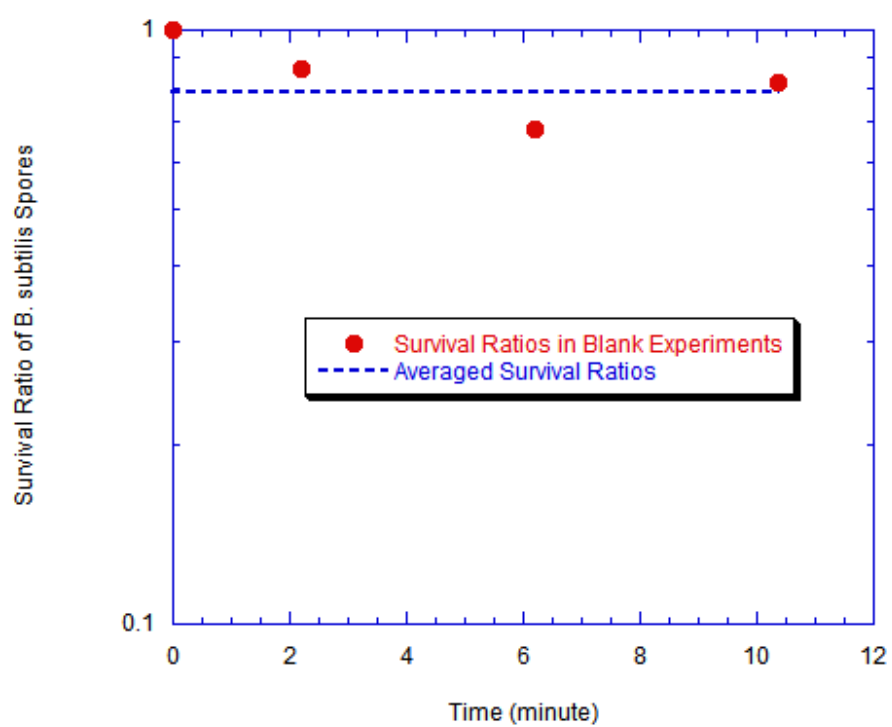


Figure 5-67 Blank Experiment of *B. subtilis* Spores ($N_0 = 10^3$ CFU/mL)

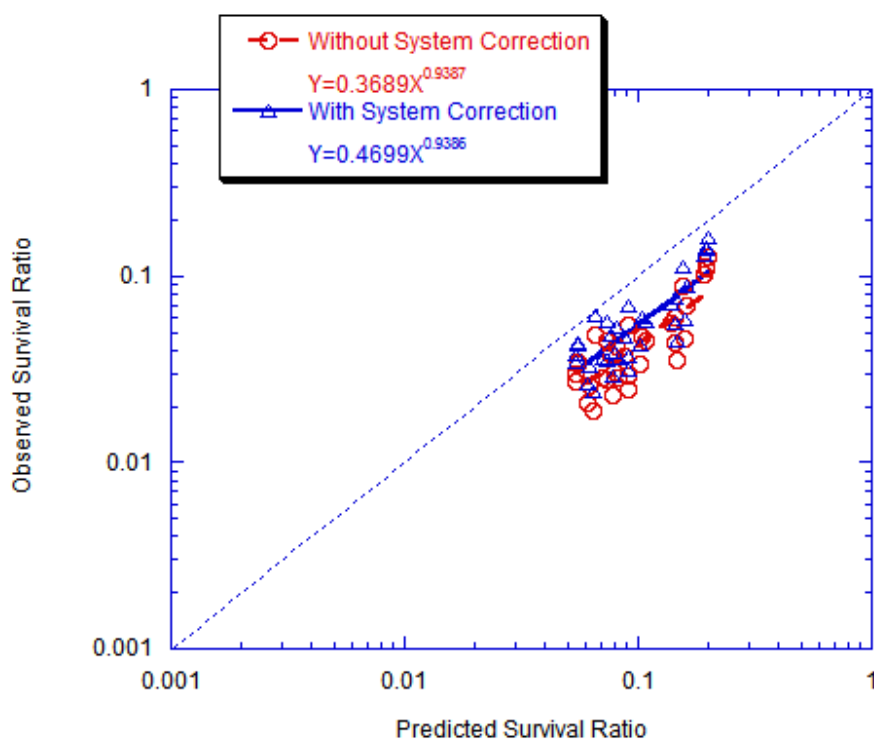


Figure 5-68 Overall Comparison of Observed vs. Predicted Survival Ratio
With and Without System Correction
(Inactivation of *B. subtilis* Spores Using Ozone)

5.3.5.5 Summary of System Correction

By performing the blank experiments in the CSTR system, the system error was corrected for the disinfection data. Loss of *E. coli* in stationary phase, gain of *E. coli* in exponential phase, loss of *B. subtilis* vegetative cells in exponential phase and loss of *B. subtilis* spores were observed in the system tubing from the reservoir to the reactor. The reason for the loss or gain might be the natural die-off or growth of bacterial or the attachment of the bacterial on the tubing wall.

After system correction on the loss/gain of bacteria in the tubing between the reservoir and the reactor, improvement was observed for the prediction of both *E. coli* disinfection and *B. subtilis* disinfection from batch system to CSTR system. For inactivation of *E. coli* in stationary phase and in exponential phase using monochloramine, *E. coli* survival ratio in the CSTR was predicted very well by the batch kinetics with system correction, according to the analysis of the overall comparison of observed and predicted survival ratio, the linear regression, and the paired t-test. For inactivation of *B. subtilis* cells and spores, the comparison did not pass the statistical analysis even though some improvement was observed from direct comparison, implicating that some differences were still existed between the observation and the prediction for *B. subtilis* disinfection. The best-fit models obtained from batch studies were not valid in the CSTR systems for *B. subtilis* disinfection. Some other factors could also contribute to the differences.

Microbial disinfection includes complex reactions between the microorganisms and the disinfectants. It can be affected by the temperature and pH of the environment,

the presence of organic matter in the external physical environment, the nature and dose of disinfectants utilized, type and growth phase of organisms being inactivated, and so on. After dissolving in water, disinfectants can produce active oxidative agents which interact with microbial cells and result in the leakage of intracellular constituents such as potassium cation, inorganic phosphate, pentoses, nucleotides and proteins. There are also some reactive intermediates or byproducts produced which alter the disinfection matrix. These organic materials may affect the disinfection process significantly. *E. coli* and *B. subtilis* are two different types of bacteria with different cell wall structure and different cell contents. During disinfection, they might produce different reactive intermediates or byproducts which can have different effects on disinfection even with the same disinfectant. Also, different cell wall structure and composition of *E. coli* and *B. subtilis* can affect the amounts and contents of the intracellular constituents leaking from their cells. Autolysis of dead cells can release organic matters to influence disinfection as well.

The difference of disinfection time between CSTR studies and batch studies might influence disinfection rate. Due to the constraints (flow rate ranges of the rotameters and size of the reservoirs) of the CSTR system, the mean residence times were limited within the range of 2.20 ~ 10.35 minutes. In batch studies, the contact time between bacteria and disinfectants were 2 ~ 10 minutes for *E. coli* in stationary phase, 1 ~ 8 minutes for *E. coli* in exponential phase, 3 ~ 45 minutes for *B. subtilis* cells, and 0.5 ~ 15 minutes for *B. subtilis* spores. The average contact times were in the same range for *E. coli* disinfection, while longer time ranges were applied to inactivate *B. subtilis* cells and spores in the batch system than in the CSTR system. This could also be one of the

reasons resulting in the consistent prediction on *E. coli* disinfection and the difference in prediction on *B. subtilis* disinfection.

The dose of disinfectants applied were in the same range for inactivation of *E. coli* and *B. subtilis* spores. For *B. subtilis* cells disinfection, the dose of monochloramine was in a somewhat higher range in the CSTR system (1 ~ 2 mg/L) than in the batch system (0.75 ~ 1.5 mg/L) due to the much shorter contact time in the CSTR studies. The non-overlapped dose ranges might bring in some differences in disinfection in the two systems and the prediction as well.

In batch inactivation of *B. subtilis* spores, ozone solution was introduced into the reactor at the beginning and ozone concentration decayed along with contact time. In CSTR disinfection, ozone solution was conducted into the reactor continuously and kept at constant dose level during the experiment. Some of the differences between the observation and the prediction might be contributed by the experimental loss of ozone in batch system even though the loss of ozone was considered to obtain batch kinetics. To eliminate this discrepancy, a semi-batch system can be utilized to perform ozone disinfection by conducting saturated ozone solution continuously into the reactor and keeping ozone dose constant in the semi-batch reactor.

5.4 The Effect of Initial Microbial Density on Disinfection in CSTR

Three factors were controlled during the disinfection experiments: initial microbial density N_0 , disinfectant dose C , and mean residence time θ . Statistical methods were applied to disinfection data with system correction to determine if these three factors had

significant effects on natural logarithm of microbial survival ratio in CSTR, especially initial microbial density N_0 .

5.4.1 Statistical Methods

For each series disinfection experiment, first the method of backwards stepwise regression was used to determine which variable might have an effect on disinfection by considering the available variables (θ , C , N_0 , and $\ln N_0$) in the regression. The variables with no significant effect on disinfection were removed by the stepwise regression. Then ANOVA was applied to consider only those variables remaining in the regression and describing those variables as continuous. The coefficient of each significant variable was computed to display the degree of the effect on disinfection in CSTR.

5.4.2 Results from Four Series Disinfection Experiments

According to backwards stepwise regression method and ANOVA test, the factors that had statistically significant effects on disinfection in CSTR are displayed in Table 5-19.

Table 5-19 Summary of Backwards Stepwise Regression and ANOVA for Disinfection Data

Experiments	Regression Coefficients					R^2
	θ	C	N_0	$\ln N_0$	Constant	
MES	-0.1510	-2.1917	4.99×10^{-6}	-0.1819	2.6023	0.7383
MEE	-0.2002	-1.3643			0.5813	0.7808
MBE		-0.7955			-0.7685	0.1461
OBS	-0.2093	-0.5360			-0.9792	0.6413

For inactivation of *E. coli* in stationary phase using monochloramine, the three factors (residence time θ , disinfection dose C , and initial microbial density $N_0/\ln N_0$) all demonstrated significant effects on disinfection.

For inactivation of *E. coli* in exponential phase using monochloramine, residence time θ and disinfection dose C showed significant effects on disinfection.

As for disinfection on *B. subtilis* vegetative cells in exponential phase by monochloramine, only monochloramine dose C could be considered to have significant effects on disinfection efficiency. Since almost all of the disinfection survival curves of *B. subtilis* cells had strong tailing off phenomena, increasing the residence time θ did not significantly improve the disinfection efficiency.

Two factors demonstrated significant effects on ozone disinfection of *B. subtilis* spores, which were residence time θ and ozone dose C .

Except for *E. coli* in stationary phase, initial microbial density $N_0/\ln N_0$ did not show significant effects on disinfection in the case of *E. coli* in exponential phase, *B. subtilis* vegetative cells, and *B. subtilis* spores.

5.4.3 Comparison of the Effects of the Initial Microbial Density on Disinfection in CSTR System and Batch System

Among six models being applied, only the Power Law model and the Hom Power Law model demonstrated the effects of initial microbial density on disinfection. From each series disinfection experiments in batch system, the best fit models were considered to be the Hom Power Law model for *E. coli* in stationary phase, the Hom model for *E. coli* in exponential phase, the Hom model for *B. subtilis* vegetative cells, and the Modified Multiple Target model for *B. subtilis* spores. So from the model expression, initial microbial density only showed effects on *E. coli* in stationary phase disinfection. Statistical analysis of batch disinfection data also gave the same results.

In the CSTR system, the same phenomenon as in the batch system was observed (Table 5-20). The CSTR gave the same results with the batch on whether initial microbial density was a significant factor on disinfection.

**Table 5-20 Effects of Initial Microbial Density on Disinfection in CSTR and
Batch System**

Experiments	Effects of Initial Microbial Density on Disinfection in Reactor	
	CSTR	Batch
MES	Yes	Yes
MEE	No	No
MBE	No	No
OBS	No	No

Chapter 6 : Summary and Conclusion

On the basis of batch disinfection experiments performed in the previous stage, lab-scale CSTR systems were set up and the disinfection experiments were conducted in the CSTR systems with the same conditions (temperature and pH) as in the batch system, to validate the batch kinetics in the CSTR system and check the effect of initial microbial density on disinfection in continuous flow system.

Two CSTR systems were used to perform disinfection experiments, one for monochloramine disinfection, and the other for ozone disinfection. By performing step input tracer tests, the residence time distribution of the reactor was obtained. The reactor was characterized as an ideal continuously stirred tank reactor and was considered to be micromixed with the segregation effects not being significant. The mean residence times determined by tanks-in-series model was applied for the following disinfection experiments.

Besides direct plot comparison, two statistical methods were used to compare the observed disinfection survival ratios in CSTR and the predicted disinfection survival ratios from batch kinetics: linear regression comparison and paired t-test comparison. Observing the change of microbial density when the microbial flow passed from the reservoir to the reactor through the tubing, the initial microbial density in the reactor was corrected systematically with an average value of 15.7% of the loss for *E. coli* in stationary phase, 14.0% of the gain for *E. coli* in exponential phase, 30.4% of the loss for *B. subtilis* cells in exponential phase, and 21.5% of the loss for *B. subtilis* spores. After system correction, linear regression and paired t-test analysis indicated that there was no

significant difference between the observed disinfection survival ratios and predicted survival ratios for *E. coli* in both stationary and exponential phase, suggesting that the batch kinetics was valid and was able to be used to predict the disinfection behavior in CSTR in the case of *E. coli* inactivation using monochloramine. For the inactivation of *B. subtilis* cells and spores, the prediction from batch kinetics over-predicted the disinfection survival ratio in both cases. The linear regression lines were parallel with the perfect prediction line but not superposed. The paired t-test comparison also rejected the adequacy of direct prediction. The differences might be caused by some other factors influencing disinfection such as the existence of reactive byproducts or intermediates, the shorter average contact time (for both *B. subtilis* cells and spores inactivation), non-overlapped disinfectant dose ranges and the way to apply ozone (for *B. subtilis* spores inactivation) utilized in CSTR studies compared with batch studies.

The initial microbial density had a significant effect on inactivation only for inactivation of *E. coli* in stationary phase using monochloramine in a CSTR. This result agreed well with the conclusion drawn from batch disinfection in which the initial microbial density also only significantly influenced the disinfection of *E. coli* in stationary phase by monochloramine. This result also agreed with the best-fit batch kinetic expression for *E. coli* in stationary phase disinfection, *i.e.*, the Hom Power Law model. For *E. coli* in exponential phase, and *B. subtilis* cells and spores, this effect was not significant either in the CSTR system or in the batch system. It was indicated that the initial microbial density is an important factor needing consideration in disinfection and this effect might be growth phase related, microorganism species related, but not reactor type related.

Chapter 7 : Engineering Significance and Future Work

This work has important engineering significance for drinking water treatment practice. It demonstrated the effect of initial *E. coli* density on disinfection in CSTR system. It indicated that the disinfection efficiency for *E. coli* in CSTR system could be predicted from batch kinetics. The prediction might also be achievable for other microorganisms with some experimental correction.

Disinfection is a complex process to inactivate the pathogenic microorganisms and is affected by many factors. Except for the commonly studied factors such as the disinfectant concentration C and the contact time T between disinfectant and microorganisms, the effect of initial microbial density N_0 has been reported to have an effect on disinfection in both batch and continuous flow system since 1970s but has not been given emphasis in EPA's regulation about disinfection (Majumdar 1973). EPA provided CT tables obtained with relatively high initial microbial density level (> 1000 No./mL) as the guidance for disinfection treatment. While in urban storm water and river water, the fecal coliforms level and *E. coli* level are usually vary over a wide range between 10^{-1} and 10^4 No./mL (Gannon and Busse 1989; Payment and Franco 1993), this is much less than the levels used in EPA studies. For certain microorganisms in certain growth phases, initial microbial density might not be an important factor for disinfection practice. In the case of *E. coli*, as shown in this study, the decrease of initial *E. coli* density results in the increase of *E. coli* survival ratio. To achieve the same fractional removal of *E. coli*, it is necessary to apply higher disinfectant dose or longer contact time at lower initial *E. coli* density level.

This study successfully predicted the disinfection efficiency of *E. coli* using monochloramine in lab-scale CSTR system from batch kinetics, suggesting that such approaches could allow small utilities to obtain disinfection credits directly from batch performance and continuous flow system characterization, thus avoiding expensive pilot studies. In the real water processes, the continuous flow system for disinfection is at the condition between ideal CSTR and ideal PFR. However, the real system usually can be simulated by a number of ideal CSTRs in series using the tanks-in-series model or by use of computational fluid dynamics (CFD) model (Greene 2003).

Future work that can be carried out following this study

In this study, *E. coli* was used as a Gram-negative bacteria and *B. subtilis* was used as a Gram-positive bacteria. Among the two bacteria and their different growth phases being chosen, the results showed that the initial microbial density played an important role only in the disinfection of *E. coli* in stationary phase. This does not mean that this effect exists in all kinds of Gram-negative bacteria in stationary phase. This also does not mean this effect is absent in other Gram-positive bacteria in different growth phases. Other Gram-negative and Gram-positive bacteria such as *Mycobacterium* and *Legionella* can be selected as the target organisms for the future studies.

The resistance of protozoan to disinfection is a major concern for water utilities. From previous studies conducted by Kaymak and Haas (2001), the initial microbial density also had a significant effect on inactivation of *Giardia muris* cysts using ozone in a batch system. This effect should be further tested in the CSTR system used in this study.

All the disinfection experiments in this study use phosphate buffered water as the water matrix. Further experiments can also be conducted using natural filtered or unfiltered water from water treatment plant which will be more close to the real water treatment process.

Various types of microorganisms coexist in the natural water. Recent studies indicated that another type of autoinducer AI-2 exists in many species of bacteria and functions as a universal signal related to cell-population density between different species (Xavier and Bassler 2003), that is, the density of one species of microorganisms might also influence the gene expression of another species of microorganisms as well as the response under disinfection. Further studies can focus on the effect of initial microbial density on disinfection in mixed populations.

The direct prediction of the behavior of *B. subtilis* cells and spores in CSTR was not successful in this study. There might be some other factors contributing to the system difference between the prediction and the observation, such as the existence of other unobserved reactants or intermediates and different contact time ranges utilized in the two systems. There is more loss of *B. subtilis* than that of *E. coli* in the tubing, which might be caused by the different attachment tendency of different organisms in the tubing and the reactor wall. Further studies can consider chemical analysis of the disinfected water and use of the data in the same contact time range in both systems for *B. subtilis* disinfection.

List of References

Anand, S. K., and Griffiths, M.W. (2003). "Quorum Sensing and Expression of Virulence in *Escherichia coli* O157:H7." international Journal of Food Microbiology **85**: 1-9.

Anmangandla, U. (1993). Nonlinear Regression Analysis of Bench-scale Microbial Disinfection Kinetics. Masters Dissertation, Drexel University.

Anotai, J. (1996). Effect of Calcium Ion on Chemistry and Disinfection Efficiency of Free Chlorine at pH 10. Drexel University.

APHA, AWWA, and WEF, American Water Works Association and Water Environment Federation (1995). Standard Methods for the Examination of Water and Wastewater, In Edited by Washington, D.C.: APHA, AWWA, WEF.

Arnold, K. W., and Kaspar, C.W. (1995). "Starvation- and Stationary-phase-induced Acid Tolerance in *Escherichia coli* O157:H7." Applied and Environmental Microbiology **61**(5): 2037-2039.

Atlas, R. M. (1995). Microorganisms in Our World, Mosby-Year Book, Inc.

Baca-DeLancey, R. R., South, M.M.T., Ding, X., and Rather, P.N. (1999). "*Escherichia coli* Genes Regulated by Cell-to-Cell Signaling." Microbiology **96**(8): 4610-4614.

Barbeau, B., Boulos, L., Desjardins, R., Coallier, J., and Prevost, M. (1999). "Examining the Use of Aerobic Spore-forming Bacteria to Assess the Efficiency of Chlorination." Water Research **33**(13): 2941-2948.

Barbeau, B., Boulos, L., Desjardins, R., Coallier, J., Prevost, M., and Duchesne, D. (1997). "A Modified Method for the Enumeration of Aerobic Spore-forming Bacteria." Canadian Journal of Microbiology **43**: 976-980.

Bassler, B. L. (1999). "How Bacteria Talk to Each Other: Regulation of Gene Expression by Quorum Sensing." Current Opinion in Microbiology **2**(6): 582-587.

Benjamin, M. M., and Datta, A.R. (1995). "Acid Tolerance of Enterohemorrhagic *Escherichia coli*." Applied and Environmental Microbiology **61**(4): 1669-1672.

Berg, J. D., Matin, A. and Roberts, P.V. (1982). "Effect of Antecedent Growth Conditions on Sensitivity of *Escherichia coli* to Chlorine Dioxide." Applied and Environmental Microbiology **44**(4): 814-819.

Bloomfield, S. F., and Arthur, M. (1994). "Mechanisms of Inactivation and Resistance of Spores to Chemical Biocides." Journal of Applied Bacteriology Symposium Supplement **76**: 91s-104s.

Bower, C. K., and Daeschel, M.A. (1999). "Resistance Responses of Microorganisms in Food Environments." International Journal of Food Microbiology **50**: 33-44.

Boyd, R. F., and Hoerl, B.G. (1991). Basic Medical Microbiology, Little, Brown and Co. (Inc.).

Cerf, O. (1977). "Tailing of Survival Curves of Bacterial Spores." Journal of Applied Bacteriology **42**: 1-19.

Chen, X., Schauder, S, Potier, N., Van Dorsselaer, A., Pelczer, I., Bassler, B.L., and Hughson, F.M. (2002). "Structural Identification of a Bacterial Quorum-Sensing Signal Containing Boron." Nature **415**(6871): 545-549.

Chesney, J. A., Eaton, J.W. and Mahoney, J.R., JR. (1996). "Bacterial Glutathione: A Sacrificial Defense against Chlorine Compounds." Journal of Bacteriology **178**(7): 2131-2135.

Chick, H. (1908). "An Investigation of the Laws of Disinfection." Journal of Hygiene **8**: 92-158.

Chiu, K., Lyn, D.A. and Blatchley III, E.R. (1999). "Integrated UV Disinfection Model Based on Particle Tracking." Journal of Environmental Engineering **125**(1): 7-16.

Clark, R. M., Read, E.J., and Hoff, J.C. (1989). "Analysis of Inactivation of *Giardia Lamblia* by Chlorine." Journal of Environmental Engineering **115**(1): 80-90.

Cloete, T. E. (2003). "Resistance Mechanisms of Bacteria to Antimicrobial Compounds." International Biodeterioration & Biodegradation **51**: 277-282.

Corona-Vasquez, B., Smuelson, A., Rennecker, J.L., and Marinas, B.J. (2002). "Inactivation of *Cryptosporidium parvum* Oocysts with Ozone and Free Chlorine." Water Research **36**(16): 4053-4063.

Crockford, A. J., Davis, G.A. and Williams, H.D. (1995). "Evidence for Cell-density-dependent Regulation of Catalase Activity in *Rhizobium leguminosarum* bv. *phaseoli*." Microbiology **141**: 843-851.

Danckwerts, P. V. (1958). "The Effect of Incomplete Mixing on Homogeneous Reactions." Chemical Engineering Science **8**: 93-102.

Datta, A. R., and Benjamin, M.M. (1999). "Cell Density Dependent Acid Sensitivity in Stationary Phase Cultures of Enterohemorrhagic *Escherichia coli* O157:H7." FEMS Microbiology Letters **181**: 289-295.

Davis, B. D., Duldecco, R., Eisen, H.N., and Ginsberg, H.S. (1990). Microbiology, J. B. Lippincott Company.

Dean, A. C. R. (1972). "Influence of Environment on the Control of Enzyme Synthesis." Journal Applied Chemical Biotechnology **22**: 245-259.

Denyer, S. P., and Stewart, G.S.A.B. (1998). "Mechanisms of Action of Disinfectants." International Biodeterioration & Biodegradation **41**: 261-268.

Driedger, A., Staub, E., Pinkernell, U., Marinas, B., Koster, W. and Gunten, U.V. (2001). "Inactivation of *Bacillus subtilis* Spores and Formation of Bromate during Ozonation." Water Research **35**(12): 2950-2960.

Driedger, A. M., Rennecker, J.L. and Marinas, B.J. (2000). "Sequential Inactivation of *Cryptosporidium parvum* Oocysts with Ozone and Free Chlorine." Water Research **34**(14): 3591-3597.

Eisenstark, A. (1998). "Bacterial Gene Products in Response to Near-ultraviolet Radiation." Mutation Research **422**: 85-95.

Facile, N., Barbeau, B., Prevost, M. and Koudjonou, B. (2000). "Evaluating Bacterial Aerobic Spores as a Surrogate for *Giardia* and *Cryptosporidium* and Inactivation by Ozone." Water Research **34**(12): 3238-3246.

Farooq, S., Engelbrecht, R.S. and Chian, E.S.K. (1977). "Influence of Temperature and U.V. Light on Disinfection with Ozone." Water Research **11**: 737-741.

Finch, G. R., Haas, C.N., Oppenheimer, J.A., Gordon, G., and Trussell, R.R. (2001). "Design Criteria for Inactivation of *Cryptosporidium* by Ozone in Drinking Water." Ozone Science & Engineering **23**: 259-284.

Flavier, A. B., Ganova-Raeva, L.M., Schell, M.A., and Denny, T.P. (1997). "Hierarchical Autoinduction in *Talstonia solanacearum*: Control of Acyl-Homoserine Lactone Production by a Novel Autoregulatory System Responsive to 3-Hydroxypalmitic Acid Methyl Ester." Journal of Bacteriology **179**(22): 7089-7097.

Foster, S. J. (1994). "The Role and Regulation of Cell Wall Structural Dynamics during Differentiation of Endospore Forming Bacteria." Journal of Appl. Bacteriol. Symp. (suppl.) **76**: 25S-39S.

Fujita, M., and Sadaie, Y. (1998). "Rapid Isolation of RNA Polymerase from Sporulating Cells of *Bacillus subtilis*." Gene **221**: 185-190.

Fuqua, W. C., Winans, S.C., and Greenberg, E.P. (1994). "Quorum Sensing in Bacteria: the LuxR-LuxI Family of Cell Density-Responsive Transcriptional Regulators." Journal of Bacteriology **176**(2): 269-275.

Gannon, J. J., and Busse, M.K. (1989). "*E. coli* and *Enterococci* Levels in Urban Stormwater, River Water and Chlorinated Treatment Plant Effluent." Water Research **23**(9): 1167-1176.

Gilbert, P., and Brown M.R.W. (1978). "Influence of Growth Rate and Nutrient-limitation on Gross Cellular Composition of *Pseudomonas aeruginosa* and Its Resistance to 3- and 4-chlorophenol." Journal of Bacteriology **133**: 1066-1072.

Gilbert, P., and Brown, M.R.W. (1980). "Cell Wall-mediated Changes in Sensitivity of *Bacillus megaterium* to Chlorhexidine and 2-phenoxyethanol, Associated with Growth Rate and Nutrient Limitation." Journal of Applied Bacteriology **48**: 223-230.

Glessner, A., Smith, R.S., Iglewski, B.H., and Robinson, J.B. (1999). "Roles of *Pseudomonas aeruginosa las* and *rhl* Quorum-Sensing Systems in Control of Twitching Motility." Journal of Bacteriology **181**(5): 1623-1629.

Gray, K. M. (1997). "Intercellular Communication and Group Behavior in Bacteria." Trends in Microbiology **5**(5): 184-188.

Greene, D. J. (2003). Numerical Simulation of Chlorine Disinfection Processes in Non-ideal Reactors, PH.D. Dissertation, Drexel University.

Gruenheid, S., and Finlay, B.B. (2000). "Crowd Control: Quorum Sensing in Pathogenic *E. coli*." Trends in Microbiology **8**(10): 442-443.

Gyurek, L. L., Li, H., Belosevic, M. and Finch, G.R. (1999). "Ozone Inactivation Kinetics of *Cryptosporidium* in Phosphate Buffer." Journal of Environmental Engineering **125**(10): 913-924.

Haas, C. N. (1988). "Micromixing and Dispersion in Chlorine Contact Chambers." Environmental Technology Letters **9**: 35-44.

Haas, C. N. (1999). Disinfection. Water Quality and Treatment-A Handbook of Community Water Supplies. R. D. Letterman, McGraw-Hill, Inc.

Haas, C. N., and Engelbrecht, R.S. (1980). "Physiological Alterations of Vegetative Microorganisms Resulting from Chlorination." Journal Water Pollution Control Federation **52**(7): 1976-1989.

Haas, C. N., and Karra, S.B. (1984). "Kinetics of Microbial Inactivation by Chlorine-I." Water Research **18**(11): 1443-1449.

Haas, C. N., Heath, M.S., Jacangelo, J., Joffe, J., Anmangandla, U., Hornberger, J.C. and Glicker, J. (1995). Development and Validation of Rational Design Methods of Disinfection, American Water Works Association.

Haas, C. N., Joffe, J., Heath, M., Jacangelo, J. and Anmangandla (1998). "Predicting Disinfection Performance in Continuous Flow Systems from Batch Disinfection Kinetics." Water Science and Technology **38**(6): 171-179.

Haas, C. N., Joffe, J., Heath, M.S. and Jacangelo, J. (1997). "Continuous Flow Residence Time Distribution Function Characterization." Journal of Environmental Engineering **123**(2): 107-114.

Hamada, A. (1995). "Chlorination and Ozonation of Contaminants in Water Environment and Role of Free Radicals." Yakugaku Zasshi **115**(10): 790-804.

Heinzel, M. (1998). "Phenomena of Biocide Resistance in Microorganisms." International Biodeterioration & Biodegradation **41**: 225-234.

Hengge-Aronis, R. (2000). The General Stress Response in *Escherichia coli*. Bacterial Stress Responses. G. Storz. Washington D.C., ASM Press.

Hengge-Aronis, R. (2002). "Signal Transduction and Regulatory Mechanisms Involved in Control of the S (RpoS) Subunit of RNA Polymerase." Microbiology and Molecular Biology Reviews **66**(3): 373-395.

Hiatt, C. W. (1964). "Kinetics of the Inactivation of Viruses." Bacteriological Reviews **28**(2): 150-163.

Holden, M., Swift, S. and Williams, P. (2000). "New Signal Molecules on the Quorum-sensing Block." Trends in Microbiology **8**(3): 101-103.

Hom, L. W. (1972). "Kinetics of Chlorine Disinfection in an Ecosystem." Journal of the Sanitary Engineering Division **98**(1): 183-193.

Huisman, G. W., and Kolter, R. (1994). "Sensing Starvation: A Homoserine Lactone-Dependent Signaling Pathway in *Escherichia coli*." Science **265**(5171): 537-539.

Hunt, N. K., and Marinas, B.J. (1997). "Kinetics of *Escherichia coli* Inactivation with Ozone." Water Research **31**(6): 1355-1362.

Hunt, N. K., and Marinas, B.J. (1999). "Inactivation of *Escherichia coli* with Ozone: Chemical and Inactivation Kinetics." Water Research **33**(11): 2633-2641.

Jarroll, E. L., Bingham, A.K., and Meyer, E.A. (1981). "Effect of Chlorine on *Giardia lamblia* Cyst Viability." Applied and Environmental Microbiology **41**(2): 483-487.

Jorgensen, F., Bally, M., Chapon-Herve, V., Michel, G., Lazdunski, A., Williams, P., and Stewart, G.S.A.B. (1999). "Rpos-dependent Stress Tolerance in *Pseudomonas aeruginosa*." Microbiology **145**(835-844).

Kaiser, D., and Losick, R. (1993). "How and Why Bacteria Talk to Each Other." Cell **73**: 873-885.

Kaymak, B. (2003). Effects of Initial Microbial Density on Disinfection Efficiency and Explanatory Mechanisms. PH.D. Dissertation, Drexel University.

Kaymak, B., and Haas, C.N. (2001). Effect of Initial Microbial Density on Disinfection Efficiency. Annual Conference of American Water Works Association, Washington, D.C.

Kobayashi, K., and Tagawa, S. (1999). "Isolation of Reductase for SoxR that Governs an Oxidative Response Regulon from *Escherichia coli*." FEBS Letters **451**: 227-230.

Kouame, Y. (1990). CSTR Microbial Inactivation by Free and Combined Chlorine, Illinois Institute of Technology.

Kouame, Y., and Haas, C.N. (1991). "Inactivation of *E. coli* by Combined Action of Free Chlorine and Monochloramine." Water Research **25**(9): 1027-1032.

Larson, M. A., and Marinas, B.J. (2003). "Inactivation of *Bacillus subtilis* Spores with Ozone and Monochloramine." Water Research **37**: 833-844.

Latifi, A., Foglino, M., Tanaka, K., Williams, P., and Lazdunski, A. (1996). "A Hierarchical Quorum-Sensing Cascade in *Pseudomonas aeruginosa* Links the Transcriptional Activators LasR and RhIR (VsmR) to Expression of the Stationary-Phase Sigma Factor RpoS." Molecular Microbiology **21**(6): 1137-1146.

Lazazzera, B. A. (2000). "Quorum Sensing and Starvation: Signals for Entry into Stationary Phase." Current Opinion in Microbiology **3**: 177-182.

Lazazzera, B. A., and Grossman, A.D. (1998). "The Ins and Outs of Peptide Signaling." Trends in Microbiology **6**(7): 288-294.

Levenspiel, O. (1999). Chemical Reaction Engineering, John Wiley & Sons, Inc., New York, NY.

Li, H., Gyurek, L.L., Finch, G.R., Smith, D.W., and Belosevic, M. (2001). "Effect of Temperature on Ozone Inactivation of *Cryptosporidium parvum* in Oxidant Demand-free Phosphate Buffer." Journal of Environmental Engineering **127**(5): 456-467.

Majumdar, S. B., Ceckler, W.H. and Sproul, O.J. (1973). "Inactivation of Poliovirus in Water by Ozonation." Journal of the Water Pollution Control Federation **45**(12): 2433-2443.

Matin, A., and Harakeh, S. (1990). Effect of Starvation on Bacterial Resistance to Disinfectants. Drinking Water Microbiology. G. A. McFeters. New York, Springer-Verlag New York Inc.

- Michels, J. J., Allain, E.J., Borchardt, S.A., Hu, P., and McCoy, W.F. (2000). "Degradation Pathway of Homoserine Lactone Bacterial Signal Molecules by Halogen Antimicrobials Identified by Liquid Chromatography with Photodiode Array and Mass Spectrometric Detection." Journal of Chromatography A **898**: 153-165.
- Morin, D., Grasland, B., Vallee-Rehel, K., Dufau, C., and Haras, D. (2003). "On-line High-performance Liquid Chromatography-mass Spectrometric Detection and Quantification of N-acylhomoserine Lactones, Quorum Sensing Signal Molecules, in the Presence of Biological Matrices." Journal of Chromatography A **1002**: 79-92.
- Motulsky, H. J., and Ransnas, L.A. (1987). "Fitting Curves to Data Using Nonlinear Regression: A Practical and Nonmathematical Review." The FASEB Journal: Official Publication of the Federation of American Societies for Experimental Biology **1**(5): 365-374.
- Nauman, E. B., and Buffham, B.A. (1983). Mixing in Continuous Flow Systems, John Wiley & Sons, Inc., New York, NY.
- Nealson, K. H., Platt, T., and Hastings, J.W. (1970). "Cellular Control of the Synthesis and Activity of the Bacterial Luminescent System." Journal of Bacteriology **104**: 313-322.
- Oktyabrsky, O. N., Smirnova, G.V. and Muzyka, N.G. (2001). "Role of Glutathione in Regulation of Hydroperoxidase I in Growing *Escherichia coli*." Free Radical Biology and Medicine **31**(2): 250-255.
- Payment, P., and Franco, E. (1993). "*Clostridium perfringens* and Somatic Coliphages as Indicators of the Efficiency of Drinking Water Treatment for Viruses and Protozoan Cysts." Applied and Environmental Microbiology **59**(8): 2418-2424.
- Pernitsky, D. J., Finch, G.R. and Huck, P.M. (1995). "Disinfection Kinetics of Heterotrophic Plate Count Bacteria in Biologically Treated Potable Water." Water Research **29**(5): 1235-1241.
- Pomposiello, P. J., and Demple, B. (2001). "Redox-operated Genetic Switches: the SoxR and OxyR Transcription Factors." Trends in Biotechnology **19**(3): 109-114.

Qasim, S. R., Motley, E.M. and Zhu, G. (2000). Water Works Engineering-Planning, Design, and Operation, Prentice Hall PTR, Prentice-Hall Inc.

Radziminski, C., Ballantyne, L., Hodson, J., Creason, R., Andrews, R.C., and Chauret, C. (2002). "Disinfection of *Bacillus subtilis* Spores with Chlorine Dioxide: A Bench-scale and Pilot-scale Study." Water Research **36**: 1629-1639.

Rennecker, J. L., Driedger, A.M., Rubin, S.A. and Marinas, B.J. (2000). "Synergy in Sequential Inactivation of *Cryptosporidium parvum* with Ozone/free Chlorine and Ozone/monochloramine." Water Research **34**(17): 4121-4130.

Rennecker, J. L., Marinas, B.J., Owens, J.H., and Rice, E.W. (1999). "Inactivation of *Cryptosporidium parvum* Oocysts with Ozone." Water Research **33**(11): 2481-2488.

Rice, E. W., Hoff, J.C., and Schaefer III, F.W. (1982). "Inactivation of *Giardia* Cysts by Chlorine." Applied and Environmental Microbiology **43**(1): 250-251.

Roustan, M., Stambolieva, Z., Duguet, J.P., Wable, O. and Mallevalle, J. (1991). "Influence of Hydrodynamics on *Giardia* Cyst Inactivation by Ozone. Study by Kinetics and by 'CT' Approach." Ozone Science and Engineering **13**(4): 451-462.

Roy, D., Chian, E.S.K. and Engelbrecht, R.S. (1981). "Kinetics of Enteroviral Inactivation by Ozone." Journal of the Environmental Engineering Division **107**(EE5): 887-901.

Rubin, A. J., Evers, D.P., Eyman, C.M., and Jarroll, E.L. (1989). "Inactivation of Gerbil-Cultured *Giardia Lamblia* Cysts by Free Chlorine." Applied and Environmental Microbiology **55**(10): 2592-2594.

Russell, A. D. (1995). "Mechanisms of Bacterial Resistance to Biocides." International Biodeterioration & Biodegradation **36**(3-4): 247-265.

Russell, A. D., Hugo, W.B. and Ayliffe, G.A.J. (1999). Principles and Practice of Disinfection, Preservation and Sterilization, Oxon, OX: Blackwell Science.

Saby, S., Leroy, P. and Block, J. (1999). "*Escherichia coli* Resistance to Chlorine and Glutathione Synthesis in Response to Oxygenation and Starvation." Applied and Environmental Microbiology **65**(12): 5600-5603.

Selleck, R. E., Saunier, B.M. and Collins, H.F. (1978). "Kinetics of Bacterial Deactivation with Chlorine." Journal of the Environmental Engineering Division **104**(EE6): 1197-1213.

Severin, B. F., Suidan, M.T. and Engelbrecht, R.S. (1983). "Kinetic Modeling of U.V. Disinfection of Water." Water Research **17**(11): 1669-1678.

Severin, B. F., Suidan, M.T. and Engelbrecht, R.S. (1984). "Series-event Kinetic Model for Chemical Disinfection." Journal of Environmental Engineering **110**(2): 430-439.

Sitnikov, D. M., Schineller, J.B. and Baldwin, T.O. (1996). "Control of Cell Division in *Escherichia coli*: Regulation of Transcription of FtsQA Involves Both RpoS and SdiA-mediated Autoinduction." Proceedings of the National Academy of Sciences of the United States of America **93**: 336-341.

Song, R., Westerhoff, P., Minear, R., and Amy, G. (1997). "Bromate Minimization during ozonation." Journal of American Water Works Association **89**(6): 69-78.

Sterkenburg, A., Vlegels, E. and Wouters, J.T.M. (1984). "Influence of Nutrient Limitation and Growth Rate on the Outer Membrane Proteins of *Klebsiella aerogenes* NCTC 418." Journal of General Microbiology **130**: 2347-2355.

Storz, G., and Imlay, J.A. (1999). "Oxidative Stress." Current Opinion in Microbiology **2**(2): 88-194.

Storz, G., Tartaglia, L.A. and Ames, B.N. (1990). "Transcriptional Regulator of Oxidative Stress-inducible Genes: Direct Activation by Oxidation." Science **248**(4952): 189-194.

Straub, T. M., Gerba, C.P., Zhou, X., Price, R. and Yahya, M.T. (1995). "Synergistic Inactivation of *Escherichia coli* and *MS-2 coliphage* by Chloramine and Curic Chloride." Water Research **29**(3): 811-818.

Surette, M. G., and Bassler, B.L. (1998). "Quorum Sensing in *Escherichia coli* and *Salmonella typhimurium*." Proceedings of the National Academy of Sciences of the United States of America **95**: 7046-7050.

Surette, M. G., Miller, M.B., and Bassler, B.L. (1999). "Quorum Sensing in *Escherichia coli*, *Salmonella typhimurium*, and *Vibrio harveyi*: A New Family of Genes Responsible for Autoinducer Production." Microbiology **96**(4): 1639-1644.

Tchobanoglous, G., and Schroeder, E.D., Ed. (1987). Water Quality, Addison-Wesley Publishing Co.

Thorne, S. H., and Williams, H.D. (1999). "Cell Density-dependent Starvation Survival of *Rhizobium leguminosarum* bv. *phaseoli*: Identification of the Role of an N-Acyl homoserine Lactone in Adaptation to Stationary Survival." Journal of Bacteriology **181**(3): 981-990.

Tosa, K., Hirata, T. and Taguchi, K. (1995). "Chloramine-induced Injury of Enterotoxigenic *Escherichia coli*." Water Science and Technology **31**(5-6): 135-139.

Trussell, R., and Chao, J. (1977). "Rational Design of Chlorine Contact Facilities." Journal of the Water Pollution Control Federal **49**(5): 659-667.

USEPA (1989). "Filtration and Disinfection; Turbidity, *Giardia Lamblia*, Viruses, *Legionella*, and Heterotrophic Bacteria. Final Rule." Federal Register **54**(124): 27486-27541.

USEPA (1991). Guidance Manual for Compliance with the Filtration and Disinfection Requirements for Public Water Systems Using Surface Water Sources, Science and Technology Branch, Criteria and Standards Division Office of Drinking Water, USEPA, Washington, D.C.

USEPA (1998a). "Stage 1 Disinfectants and Disinfection Byproducts Rule (Stage 1 DBPR)." Federal Register **63**(241): 69390-69476.

USEPA (1998b). "National Primary Drinking Water Regulations: Interim Enhanced Surface Water Treatment; Final Rule." Federal Register **63**(241): 69478-69521.

USEPA (1999). "Wasterwater Technology Fact Sheet: Ozone Disinfection." **EPA 832-F-99-063**.

Utsumi, H., Hakoda, M., Shimbara, S., Nagaoka, H., Chung and Y., Hamada, A. (1994). "Active Oxygen Species Generated during Chlorination and Ozonation." Water Science and Technology **30**(9): 91-99.

Venkobachar, C., Iyengar, L. and Rao, A.V.S.P. (1977). "Mechanism of Disinfection: Effect of Chlorine on Cell Membrane Functions." Water Research **11**: 727-729.

Venkobachar, C., Iyengar, L., and Rao, A.V.S.P. (1975). "Mechanism of Disinfection." Water Research **9**: 119-124.

Walker, M. W., Kinter, M.T., Roberts, R.J. and Spitz, D.R. (1995). "Nitric Oxide-induced Cytotoxicity: Involvement of Cellular Resistance to Oxidative Stress and the Role of Glutathione in Protection." Pediatric Research **37**(1): 41-49.

Watson, H. E. (1908). "A Note on the Variation of the Rate of Disinfection with Change in the Concentration of the Disinfectant." J. Hygiene **8**: 536-542.

Westerterp, K. R., Swaaij, W.P.M.v. and Beenackers, A.A.C.M. (1984). Chemical Reactor Design and Operation, John Wiley & Sons Ltd.

White, G. C. (1999). Handbook of Chlorination and Alternative Disinfectants, John Wiley & Sons, Inc.

Whiteley, M., Parsek, M.R. and Greenberg, E.P. (2000). "Regulation of Quorum Sensing by RpoS in *Pseudomonas aeruginosa*." Journal of Bacteriology **182**(15): 4356-4360.

Xavier, K. B., and Bassler, B.L. (2003). "LuxS Quorum Sensing: More than Just a Numbers Game." Current Opinion in Microbiology **6**: 191-197.

Xiong, R., Xie, G., Edmondson, A.E. and Sheard, M.A. (1999). "A Mathematical Model for Bacterial Inactivation." International Journal of Food Microbiology **46**: 45-55.

Yamada, M., Talukder, A.A. and Nitta, T. (1999). "Characterization of the SsnA Gene, Which is Involved in the Decline of Cell Viability at the Beginning of Stationary Phase in *Escherichia coli*." Journal of Bacteriology **181**(6): 1838-1846.

Zambrano, M. M., and Kolter, R. (1996). "GASping for Life in Stationary Phase." Cell **86**: 181-184.

Zhou, H., and Smith, D.W. (1994). "Kinetics of Ozone Disinfection in Completely Mixed System." Journal of Environmental Engineering **120**(4): 841-858.

Zwietering, T. H. (1959). "The Degree of Mixing in Continuous Flow Systems." Chemical Engineering Science **11**(1): 1-15.

Appendix A: Derivation of Segregation Number Calculation

- (1) Determination of the efficiency of the Labo Stirrer from given specification

From the instruction manual for the Labo Stirrer (Model LR400C), the maximum torque of $0.245 N \cdot m$ was given at 1200 rpm for a O.D. 60mm stirring propeller.

$$\begin{aligned} T_{\max} &= 0.245 N \cdot m \\ n &= 1200 \text{rpm} = 20 \text{rps} \\ d &= 0.06 \text{m} \end{aligned}$$

The Renolds number is

$$\begin{aligned} N_R &= \frac{n \rho d^2}{\mu} \\ &= \frac{(20 \text{rps}) \times (999.1 \text{kg/m}^3) \times (0.06 \text{m})^2}{(1.14 \times 10^{-3} \text{N} \cdot \text{s/m}^2)} \\ &= 6.31 \times 10^4 \end{aligned}$$

From the mixing power function curve for standard tank configuration (Tchobanoglous and Schroeder 1987), power number is

$$N_p = \phi = 6$$

The power requirement:

$$\begin{aligned} P &= N_p \rho n^3 d^5 \\ &= 6 \times (999.1 \text{kg/m}^3) \times (20 \text{rps})^3 \times (0.06 \text{m})^5 \\ &= 37.29 \text{W} \end{aligned}$$

The corresponding torque needed:

$$T = \frac{P}{2\pi n} = \frac{(37.29W)}{2\pi \times (20rps)} = 0.297N-m$$

From the Lab Stirrer manual, the giving torque T is $0.245N-m$ for the standard blades ($d = 0.006m$) at 1200 rpm .

The efficiency of the stirrer is

$$\eta = \frac{0.245}{0.297} \times 100\% = 82.49\%$$

- (2) Determination of the segregation number calculation under experimental condition

$$n = 1000rpm = 16.67rps$$

$$d = 0.028m$$

The Renolds number is

$$\begin{aligned} N_R &= \frac{n\rho d^2}{\mu} \\ &= \frac{(16.67rps) \times (999.1kg/m^3) \times (0.028m)^2}{(1.14 \times 10^{-3} N-s/m^2)} \\ &= 1.15 \times 10^4 \end{aligned}$$

From the mixing power function curve for standard tank configuration (Tchobanoglous and Schroeder 1987), power number is

$$N_p = \phi = 6$$

The power requirement:

$$\begin{aligned} P &= N_p \rho n^3 d^5 \\ &= 6 \times (999.1 \text{ kg/m}^3) \times (16.67 \text{ rps})^3 \times (0.028 \text{ m})^5 \\ &= 0.478 \text{ W} \end{aligned}$$

The corresponding torque needed:

$$T = \frac{P}{2\pi n} = \frac{(0.478 \text{ W})}{2\pi \times (16.67 \text{ rps})} = 4.57 \times 10^{-3} \text{ N-m}$$

The power needed to be imparted to the water by mixer:

$$P' = P\eta = 0.478 \times 82.49\% = 0.394 \text{ W}$$

The power dissipated per unit mass of water is:

$$\varepsilon = \frac{P'}{V\rho} = \frac{(0.394 \text{ W})}{(500 \times 10^{-6} \text{ m}^3) \times (999.1 \text{ kg/m}^3)} = 0.789 \text{ W/kg}$$

The segregation number is

$$\begin{aligned}
S_g &= \frac{\mu^{1.5}}{4\pi^2 \rho^{1.5} \varepsilon^{0.5} D \theta} \\
&= \frac{(1.14 \times 10^{-3} \text{ N-s/m}^2)^{1.5}}{4\pi^2 \times (999.1 \text{ kg/m}^3)^{1.5} \times (0.789 \text{ W/kg})^{0.5} \times (10^{-9} \text{ m}^2/\text{s}) \theta} \\
&= \frac{0.035}{\theta}
\end{aligned}$$

Appendix B: Derivation of the Hom Power Law Model for CSTR Prediction

CSTR steady state mass balance relation

$$\left(\frac{N}{N_0}\right)_{\text{predicted in CSTR}} = 1 + \frac{r_{\text{batch}} \theta}{N_0}$$

Inactivation rate expression of the Hom Power Law in batch system

$$r = \frac{dN}{dt} = -mk' C^n t^{m-1} N^x$$

In continuous flow system it can also be expressed as

$$r = -mk' C^n N^x \left\{ \frac{\left[\left(\frac{N}{N_0} \right)^{(1-x)} - 1 \right] N_0^{(1-x)}}{(x-1)k' C^n} \right\}^{\left(1-\frac{1}{m}\right)}$$

Substitute the above expression into CSTR mass balance relation

$$\left(\frac{N}{N_0}\right)_{\text{predicted}} = 1 - mk' C^n \theta \left(\frac{N}{N_0}\right)_{\text{predicted}}^x N_0^{x-1} \left\{ \frac{\left[\left(\frac{N}{N_0} \right)_{\text{predicted}}^{1-x} - 1 \right] N_0^{1-x}}{(x-1)k' C^n} \right\}^{\left(1-\frac{1}{m}\right)}$$

Appendix C: Derivation of the Hom Model for CSTR Prediction

CSTR steady state mass balance relation

$$\left(\frac{N}{N_0} \right)_{\text{predicted in CSTR}} = 1 + \frac{r_{\text{batch}} \theta}{N_0}$$

Inactivation rate expression of the Hom model in batch system

$$r = \frac{dN}{dt} = -mk' C^n t^{m-1} N$$

In continuous flow system, it can also be expressed as (Haas 1995)

$$r = -mN(k' C^n)^{\frac{1}{m}} \left[-\ln \left(\frac{N}{N_0} \right) \right]^{\left(1 - \frac{1}{m} \right)}$$

Substitute the above expression into CSTR mass balance relation

$$\left(\frac{N}{N_0} \right)_{\text{predicted}} = 1 - m(k' C^n)^{\frac{1}{m}} \theta \left(\frac{N}{N_0} \right)_{\text{predicted}} \left[-\ln \left(\frac{N}{N_0} \right)_{\text{predicted}} \right]^{\left(1 - \frac{1}{m} \right)}$$

Appendix D: Derivation of the Modified Multiple Target Model

for CSTR Prediction

CSTR steady state mass balance relation

$$\left(\frac{N}{N_0} \right)_{\text{predicted in CSTR}} = 1 + \frac{r_{\text{batch}} \theta}{N_0}$$

The batch Modified Multiple Target Model

$$\frac{N}{N_0} = 1 - \left(1 - e^{-kC^n t} \right)^{n_c}$$

The inactivation rate expression can be derived as

$$\begin{aligned} N &= N_0 - N_0 \left(1 - e^{-kC^n t} \right)^{n_c} \\ r &= \frac{dN}{dt} = -N_0 \left[n_c \left(1 - e^{-kC^n t} \right)^{(n_c - 1)} \right] \left[-e^{-kC^n t} \right] \left[-kC^n \right] \\ &= -kn_c C^n N_0 e^{-kC^n t} \left(1 - e^{-kC^n t} \right)^{(n_c - 1)} \end{aligned}$$

and

$$\left(1 - e^{-kC^n t} \right)^{n_c} = 1 - \frac{N}{N_0}$$

$$1 - e^{-kC^n t} = \left(1 - \frac{N}{N_0} \right)^{\frac{1}{n_c}}$$

$$e^{-kC^n t} = 1 - \left(1 - \frac{N}{N_0}\right)^{\frac{1}{n_c}}$$

Substitute the above two equations and the inactivation rate expression into CSTR

mass balance equation

$$\frac{N}{N_0} = 1 + \frac{r\theta}{N_0} = 1 - kn_c C^n \theta \left[1 - \left(1 - \frac{N}{N_0}\right)^{\frac{1}{n_c}} \right] \left[\left(1 - \frac{N}{N_0}\right)^{\frac{n_c-1}{n_c}} \right]$$

Appendix E: Matlab Program

This Matlab program was written to predict the survival ratios in a continuously stirred tank reactor based on the batch kinetics. It includes three matlab function files (CSTRSSMB.m, CSTRPREDN.m, and DATAINPUT.m) and six batch inactivation models (the simplified Chick-Watson model, the Chick-Watson model, the Hom model, the Power Law model, the Hom Power Law Model, and the Modified Multiple Target model).

CSTRSSMM.m file is used to describe the steady-state mass balance in the CSTR for different kinetic models. CSTRPREDN.m is used to compute the predicted microbial density in the CSTR. DATAINPUT.m is used to input the values of experimental data and the best-fit model parameters to obtain the predicted survival ratios in the CSTR.

This Matlab program was written by using Matlab 5.2 (The MathWorks, Inc.) and can be applied on both Mackintosh and PC platforms.

CSTRSSMB.m

```

function mb=CSTRSSMB(pred_N,params,theta,C,N0,model)
% steady-state mass balance equation for disinfection reaction in CSTR

switch model
case 'chick'
    k=params(1);
    r=-k*C.*pred_N;
case 'chick-watson'
    k=params(1);
    n=params(2);
    r=-k*C.^n.*pred_N;
case 'hom'
    k=params(1);
    n=params(2);
    m=params(3);
    r=-m*pred_N.*(k*C.^n).^(1/m).*(-log(pred_N/N0)).^(1-1/m);
case 'power-law'
    k=params(1);
    n=params(2);
    x=params(3);
    r=-k*(C.^n).*(pred_N.^x);
case 'hom power-law'
    k=params(1);
    n=params(2);
    m=params(3);
    x=params(4);
    r=-m*k*C.^n.*pred_N.^x.*(((pred_N/N0).^(1-x)-1).*N0.^(1-x))./((x-1)*k*C.^n)).^(1-1/m);
case 'modified multiple target'
    k=params(1);
    n=params(2);
    nc=params(3);
    r=-k*nc*C.^n.*N0.*(1-(1-pred_N/N0).^(1/nc)).*(1-pred_N/N0).^((nc-1)/nc);
otherwise
    disp('INPUT MODEL ERROR!')
    return
end
mb=(N0-pred_N)./theta+r;

```

CSTRPREDN.m

```

function pred_N=CSTRPREDN(params,theta,C,N0,model)
% computes the predicted microbial density pred_N in CSTR

switch model
case 'chick'
    k=params(1);
    pred_N=N0./(1+k*C.*theta);
case 'chick-watson'
    k=params(1);
    n=params(2);
    pred_N=N0./(1+k*C.^n.*theta);
case 'hom'
    k=params(1);
    n=params(2);
    m=params(3);
    for p=1:length(N0)
        pred_N(p)=fzero('CSTRSSMB',[N0(p)-1,1],[[],[]],params,theta(p),C(p),N0(p),model);
    end
    pred_N=pred_N';
case 'power-law'
    k=params(1);
    n=params(2);
    x=params(3);
    for p=1:length(N0)
        pred_N(p)=fzero('CSTRSSMB',[N0(p)-1,1],[[],[]],params,theta(p),C(p),N0(p),model);
    end
    pred_N=pred_N';
case 'hom power-law'
    k=params(1);
    n=params(2);
    m=params(3);
    x=params(4);
    for p=1:length(N0)
        pred_N(p)=fzero('CSTRSSMB',[N0(p)-1,1],[[],[]],params,theta(p),C(p),N0(p),model);
    end
    pred_N=pred_N';
case 'modified multiple target'
    k=params(1);
    n=params(2);
    nc=params(3);
    for p=1:length(N0)

```

```
    pred_N(p)=fzero('CSTRSSMB',[N0(p)-1,1],[[],[],params,theta(p),C(p),N0(p),model);  
end  
    pred_N=pred_N';  
otherwise  
    disp('INPUT MODEL ERROR!')  
    return  
end
```

DATAINPUT.m

```

clear all
format short g

data=[];
theta=data(:,1);
C=data(:,2);
N0=data(:,3);
N=data(:,4);
model='hom power-law'; %input the fitting model name

switch model
case 'chick'
    params=[0.7829];
case 'chick-watson'
    params=[0.7823 0.8999];
case 'hom'
    params=[0.1827 1.5843 1.7735];
case 'power-law'
    params=[0.6729 0.8569 1.0206];
case 'hom power-law'
    params=[0.004832 2.4737 2.9479 1.218];
otherwise
    disp('INPUT MODEL ERROR!')
    return
end

pred_N=CSTRPREDN(params,theta,C,N0,model);
obs_SR=N./N0;
pred_SR=pred_N./N0;
result=[pred_N obs_SR pred_SR];

disp(' ')
disp('    pred_N    obs. SR    pred. SR')
disp('-----')
disp(result)

```

Appendix F: Experimental Data

Tracer Test Data

Residence Time: $\theta = 2 \text{ minute}$

Flow Rate: $Q_1 = Q_2 = 125 \text{ ml/min}$

Original Conductivity: $C_0 = 5395 \text{ umhos/cm}$

Date of Experiments: 3/15/2002

Sampling time $t \text{ (min)}$	Specific Conductivity $C \text{ (umhos/cm)}$
0	9.61
0.333	836.5
0.667	1495
1.000	2035
1.333	2515
1.667	2910
2.000	3260
2.333	3570
2.667	3810
3.000	4035
3.333	4225
3.667	4385
4.000	4520
4.333	4645
4.667	4745
5.000	4835
5.333	4910
5.667	4980
6.000	5040
7.000	5165
8.000	5245
9.000	5300
10.000	5335
11.000	5355
12.000	5370

Residence Time: $\theta = 4 \text{ minute}$

Flow Rate: $Q_1 = Q_2 = 62.5 \text{ ml/min}$

Original Conductivity: $C_0 = 5392.5 \text{ umhos/cm}$

Date of Experiments: 3/15/2002

Sampling time $t \text{ (min)}$	Specific Conductivity $C \text{ (umhos/cm)}$
0	11.09
0.5	659.5
1	1200
1.5	1695
2	2115
2.5	2500
3	2815
3.5	3120
4	3380
4.5	3605
5	3795
5.5	3975
6	4130
6.5	4270
7	4395
7.5	4505
8	4600
8.5	4690
9	4765
9.5	4835
10	4895
10.5	4955
11	5000
11.5	5050
12	5080
14	5205
16	5280
18	5320
20	5350
22	5370
24	5380

Residence Time: $\theta = 6 \text{ minute}$

Flow Rate: $Q_1 = Q_2 = 41.7 \text{ ml/min}$

Original Conductivity: $C_0 = 5605 \text{ umhos/cm}$

Date of Experiments: 3/14/2002

Sampling time $t \text{ (min)}$	Specific Conductivity $C \text{ (umhos/cm)}$
0	8.565
1	904
2	1635
3	2190
4	2700
5	3140
6	3500
7	3795
8	4060
9	4290
10	4470
11	4635
12	4780
13	4895
14	5000
15	5090
16	5170
17	5235
18	5285
21	5405
24	5480
27	5535
30	5565
33	5580
36	5590

Residence Time: $\theta = 10 \text{ minute}$

Flow Rate: $Q_1 = Q_2 = 25 \text{ ml/min}$

Original Conductivity: $C_0 = 5360 \text{ umhos/cm}$

Date of Experiments: 3/14/2002

Sampling time $t \text{ (min)}$	Specific Conductivity $C \text{ (umhos/cm)}$
0	9.375
2	983
4	1765
6	2400
8	2900
10	3340
12	3705
14	3990
16	4235
18	4445
20	4615
22	4750
24	4865
26	4950
28	5030
30	5095
35	5195
40	5255
45	5300
50	5325
55	5340
60	5355

CSTR Disinfection Data without System Correction

Species and Growth Phase of Bacteria: *E. coli* in stationary phase

Disinfectant: monochloramine

Temperature: 15°C

pH: 7

Date of Experiment	Residence Time θ (min)	Disinfectant Residual C (mg/L)	Initial Microbial Density N_0 (CFU/mL)	Microbial Density after Disinfection N (CFU/mL)
6/26/2002	2.20	0.752	963	190
6/26/2002	6.20	0.760	1193	240
6/26/2002	10.35	0.748	928	170
6/18/2002	2.20	1.009	1685	636
6/18/2002	6.20	0.992	1443	322
6/18/2002	10.35	1.004	1363	209
5/30/2002	2.20	1.527	1823	245
5/30/2002	6.20	1.505	2085	84
5/30/2002	10.35	1.527	1852	52
6/19/2002	2.20	1.524	1221	54
6/19/2002	6.20	1.516	1196	59
6/19/2002	10.35	1.498	1493	26
5/21/2002	2.20	0.772	10272	4605
5/21/2002	6.20	0.768	15617	2779
5/21/2002	10.35	0.768	16762	2099
4/17/2002	2.20	1.034	29125	1785
4/17/2002	6.20	1.029	19503	631
4/17/2002	10.35	1.019	19937	190
5/14/2002	2.20	1.056	16884	2943
5/14/2002	6.20	1.056	21886	1048
5/14/2002	10.35	1.056	24747	614
5/16/2002	2.20	1.518	16033	1308
5/16/2002	6.20	1.527	13463	581
5/16/2002	10.35	1.518	21038	404
4/12/2002	2.20	0.770	74444	39806
4/12/2002	6.20	0.700	86027	19119
4/12/2002	10.35	0.780	80640	12963

5/09/2002	2.20	0.768	407407	185519
5/09/2002	6.20	0.776	351852	89756
5/09/2002	10.35	0.799	343434	55722
5/07/2002	2.20	1.021	234007	118785
5/07/2002	6.20	1.056	205387	43434
5/07/2002	10.35	1.043	262626	30697
6/21/2002	2.20	1.511	77244	4815
6/21/2002	6.20	1.480	110277	2099
6/21/2002	10.35	1.502	106783	2222

Species and Growth Phase of Bacteria: *E. coli* in exponential phase

Disinfectant: monochloramine

Temperature: 15°C

pH: 7

Date of Experiment	Residence Time θ (min)	Disinfectant Residual C (mg/L)	Initial Microbial Density N_0 (CFU/mL)	Microbial Density after Disinfection N (CFU/mL)
8/24/2002	2.20	0.717	561	259
8/24/2002	6.20	0.717	527	125
8/24/2002	10.35	0.732	571	54
9/25/2002	2.20	0.773	3384	1178
9/25/2002	6.20	0.773	4360	626
9/25/2002	10.35	0.777	3956	431
8/17/2002	2.20	1.071	1318	177
8/17/2002	6.20	1.071	868	67
8/17/2002	10.35	1.092	784	7
9/05/2002	2.20	1.478	3215	687
9/05/2002	6.20	1.454	3586	286
9/05/2002	10.35	1.459	3114	121
8/15/2002	2.20	0.780	10000	4946
8/15/2002	6.20	0.764	10387	2529
8/15/2002	10.35	0.768	13300	953
8/29/2002	2.20	1.039	33502	6801
8/29/2002	6.20	1.024	39057	6532
8/29/2002	10.35	1.029	39226	1552
8/20/2002	2.20	1.488	10943	2313
8/20/2002	6.20	1.502	9848	976
8/20/2002	10.35	1.493	9377	428
8/22/2002	2.20	1.498	23857	3670
8/22/2002	6.20	1.493	26693	2102
8/22/2002	10.35	1.478	23190	1168
9/18/2002	2.20	0.757	198653	88215
9/18/2002	6.20	0.761	180135	50842
9/18/2002	10.35	0.749	215488	36027
9/06/2002	2.20	1.024	323232	209428
9/06/2002	6.20	1.010	437710	89899
9/06/2002	10.35	1.019	385522	37710
9/10/2002	2.20	0.990	299663	124579

9/10/2002	6.20	0.990	324916	46465
9/10/2002	10.35	1.007	326599	28283
9/19/2002	2.20	1.523	102102	15916
9/19/2002	6.20	1.527	119953	9643
9/19/2002	10.35	1.527	118285	5772

Species and Growth Phase of Bacteria: *B. subtilis* cells in exponential phase

Disinfectant: monochloramine

Temperature: 15°C

pH: 7

Date of Experiment	Residence Time θ (min)	Disinfectant Residual C (mg/L)	Initial Microbial Density N_0 (CFU/mL)	Microbial Density after Disinfection N (CFU/mL)
12/09/2002	2.20	1.054	3906	1256
12/09/2002	6.20	1.040	4192	451
12/09/2002	10.35	1.040	4091	236
12/12/2002	2.20	1.092	1602	284
12/12/2002	6.20	1.054	534	110
12/12/2002	10.35	1.064	717	143
1/04/2003	2.20	1.029	2436	751
1/04/2003	6.20	1.046	1785	460
1/04/2003	10.35	0.998	1919	537
12/13/2002	2.20	1.559	1093	56
12/13/2002	6.20	1.573	696	21
12/13/2002	10.35	1.535	452	6
12/19/2002	2.20	1.573	1401	90
12/19/2002	6.20	1.550	1301	73
12/19/2002	10.35	1.592	934	43
12/18/2002	2.20	1.969	716	39
12/18/2002	6.20	1.946	480	39
12/18/2002	10.35	1.983	317	41
1/07/2003	2.20	2.127	1263	74
1/07/2003	6.20	2.102	1001	67
1/07/2003	10.35	2.000	717	75
12/11/2002	2.20	0.941	8175	1845
12/11/2002	6.20	0.964	6523	454
12/11/2002	10.35	0.941	2469	113
12/03/2002	2.20	1.526	10060	3050
12/03/2002	6.20	1.564	7140	1471
12/03/2002	10.35	1.531	5556	657
11/27/2002	2.20	1.973	45741	30370
11/27/2002	6.20	2.031	49444	7630
11/27/2002	10.35	2.069	49074	4407
12/10/2002	2.20	2.113	29630	909

12/10/2002	6.20	2.145	27441	572
12/10/2002	10.35	2.138	21717	438
12/01/2002	2.20	1.545	67677	10303
12/01/2002	6.20	1.545	52525	4545
12/01/2002	10.35	1.498	44949	3064

Species and Growth Phase of Bacteria: *B. subtilis* spores

Disinfectant: ozone

Temperature: 15°C

pH: 8

Date of Experiment	Residence Time θ (min)	Disinfectant Residual C (mg/L)	Initial Microbial Density N_0 (CFU/mL)	Microbial Density after Disinfection N (CFU/mL)
3/06/2003	2.20	1.513	1648	182
3/06/2003	4.11	1.577	1722	77
3/06/2003	6.20	1.566	1894	53
3/02/2003	2.20	2.106	1605	74
3/02/2003	4.11	2.032	1630	40
3/02/2003	6.20	1.873	1747	33
3/10/2003	2.20	2.085	1732	80
3/10/2003	4.11	2.148	1755	65
3/10/2003	6.20	2.074	1830	38
3/17/2003	2.20	2.402	1393	49
3/17/2003	4.11	2.339	1346	38
3/17/2003	6.20	2.360	1193	40
3/14/2003	2.20	1.492	19186	2169
3/14/2003	4.11	1.683	16850	567
3/14/2003	6.20	1.640	19853	567
3/03/2003	2.20	2.190	6940	617
3/03/2003	4.11	2.032	6690	360
3/03/2003	6.20	1.831	6006	290
3/18/2003	2.20	2.444	15666	941
3/18/2003	4.11	2.413	12896	534
3/18/2003	6.20	2.455	14281	430
3/21/2003	2.20	2.413	14264	621
3/21/2003	4.11	2.466	14264	440
3/21/2003	6.20	2.370	14298	487
3/25/2003	2.20	1.450	97097	12246
3/25/2003	4.11	1.661	100267	4738
3/25/2003	6.20	1.460	90757	3403
3/26/2003	2.20	1.566	116617	11778
3/26/2003	4.11	1.545	108775	4872
3/26/2003	6.20	1.556	116617	5239
3/31/2003	2.20	2.032	85419	5873

3/31/2003	4.11	2.042	118952	3437
3/31/2003	6.20	2.000	105606	2736
3/20/2003	2.20	2.614	99600	5539
3/20/2003	4.11	2.593	98265	2269
3/20/2003	6.20	2.413	105272	2836

System Correction Data

Inactivation of *E. coli* in Stationary Phase Using Monochloramine

Date of Experiment	Residence Time θ (min)	Microbial Density in the Reservoir N_1 (CFU/mL)	Microbial Density in the Reactor N_2 (CFU/mL)
5/27/2003	2.20	7441	3070
5/27/2003	6.20	7608	3203
5/27/2003	10.35	6507	2803

Inactivation of *E. coli* in Exponential Phase Using Monochloramine

Date of Experiment	Residence Time θ (min)	Microbial Density in the Reservoir N_1 (CFU/mL)	Microbial Density in the Reactor N_2 (CFU/mL)
5/31/2003	2.20	6039	4571
5/31/2003	6.20	4571	2636
5/31/2003	10.35	3103	1168

Inactivation of *B. subtilis* Cells in Exponential Phase Using Monochloramine

Date of Experiment	Residence Time θ (min)	Microbial Density in the Reservoir N_1 (CFU/mL)	Microbial Density in the Reactor N_2 (CFU/mL)
6/02/2003	2.20	97306	39057
6/02/2003	6.20	98316	31650
6/02/2003	10.35	98653	31650

Inactivation of *B. subtilis* Spores Using Ozone

Date of Experiment	Residence Time θ (min)	Microbial Density in the Reservoir N_1 (CFU/mL)	Microbial Density in the Reactor N_2 (CFU/mL)
6/05/2003	2.20	4738	2035
6/05/2003	4.11	4905	1668
6/05/2003	6.20	4338	1768

Vita

Lijie Li

Birth Date: October 1st, 1972

Birth Place: Baoji, P.R.China

Education

1999-2004 PhD in Environmental Engineering, Drexel University, U.S.A.

1996-1999 M.S. in Fermentation Engineering, Wuxi University of Light
Industry, P.R. China

1989-1993 B.S. in Food Engineering, Sichuan University, P.R.China

Professional Experience

1999-2004 Graduate Research Assistant, Drexel University, U.S.A.

1996-1999 Graduate Research Assistant, Wuxi University of Light Industry,
P.R. China

1993-1996 Assistant Engineer, SuLandLink Feed & Aquatic Co., P.R.China

